

REPORT DOCUMENTATION PAGE

Form Approved
OMB No. 0704-0188

Public reporting burden for this collection of information is estimated to average 1 hour per response, including the time for reviewing instructions, searching existing data sources, gathering and maintaining the data needed, and completing and reviewing the collection of information. Send comments regarding this burden estimate or any other aspect of this collection of information, including suggestions for reducing this burden, to Washington Headquarters Services, Directorate for Information Operations and Reports, 1215 Jefferson Davis Highway, Suite 1204, Arlington, VA 22202-4302, and to the Office of Management and Budget, Paperwork Reduction Project (0704-0188), Washington, DC 20503.

1. AGENCY USE ONLY (Leave blank)

2. REPORT DATE

Nov 16, 95

3. REPORT TYPE AND DATES COVERED

Final Sep 92 - Sep 95

4. TITLE AND SUBTITLE

Vortex Breakdown over Unsteady Wings
and its Control

5. FUNDING NUMBERS

F49620 -
92-5-0532

6. AUTHOR(S)

Ismet Gursul

7. PERFORMING ORGANIZATION NAME(S) AND ADDRESS(ES)

University of Cincinnati

8. PERFORMING ORGANIZATION
REPORT NUMBER

9. SPONSORING/MONITORING AGENCY NAME(S) AND ADDRESS(ES)

AIR FORCE OFFICE OF SCIENTIFIC RESEARCH
DIRECTORATE OF AEROSPACE SCIENCES
BOLLING AFB, DC 20332-6448

10. SPONSORING/MONITORING
AGENCY REPORT NUMBER

F49620
92-5-0532

11. SUPPLEMENTARY NOTES

12a. DISTRIBUTION/AVAILABILITY STATEMENT

APPROVED FOR PUBLIC RELEASE
DISTRIBUTION IS UNLIMITED

12b. DISTRIBUTION CODE

19960221 006

13. ABSTRACT (Maximum 200 words)

Control of vortex breakdown continues to be of vital importance because the breakdown may have a considerable effect on aircraft performance, such as the effect on the time-averaged lift force (Lee and Ho, 1990). Breakdown is also important because of the unsteady nature of flow downstream of vortex breakdown. The unsteadiness may affect the stability of the aircraft and also cause buffeting. The objectives of this work are to understand the physics of unsteady flow phenomena in vortex breakdown region, and to develop techniques for active (feedback) and passive (open loop) control of vortex breakdown over steady and unsteady delta wings.

14. SUBJECT TERMS

15. NUMBER OF PAGES

596

16. PRICE CODE

17. SECURITY CLASSIFICATION
OF REPORT

UNCLASSIFIED

18. SECURITY CLASSIFICATION
OF THIS PAGE

UNCLASSIFIED

19. SECURITY CLASSIFICATION
OF ABSTRACT

UNCLASSIFIED

20. LIMITATION OF ABSTRACT

**VORTEX BREAKDOWN OVER UNSTEADY WINGS
AND ITS CONTROL**

FINAL TECHNICAL REPORT

Grant No: F49620-92-J-0532

Period Covered: 9/30/92-9/30/95

Prepared for

Air Force Office of Scientific Research
110 Duncan Avenue, Suite B115
Bolling Air Force Base, DC 20332-0001

Prepared by

Ismet Gursul
Assistant Professor
University of Cincinnati
Department of Mechanical, Industrial and Nuclear Engineering
Cincinnati, OH 45221-0072

Approved for public release
distribution unlimited

AFSC
30-12
and 15

TABLE OF CONTENTS

1. INTRODUCTION

2. EXPERIMENTAL FACILITIES

3. RESULTS

3.1. Unsteady Flow Phenomena in Vortex Breakdown Region

3.2. Time Scales of Vortex Breakdown

3.3. Active (Feedback) Control of Vortex Breakdown

3.4. Vortex Breakdown over a Pitching Delta Wing

3.5. Control of Vortex Breakdown with Leading-Edge Flaps

3.6. Control of Vortex Breakdown with Variable Sweep

4. CONCLUSIONS

REFERENCES

Appendix A: "Unsteady Flow Phenomena over Delta Wings at High Angle of Attack", *AIAA Journal*, vol. 32, no. 2, February 1994, pp. 225-231.

Appendix B: "On Fluctuations of Vortex Breakdown Location", *Physics of Fluids*, vol. 7, no.1, January 1995, pp. 229-231.

Appendix C: "Active Control of Vortex Breakdown over a Delta Wing", *AIAA Journal*, Volume 33, No 9, 1995, pp.1743-1745.

Appendix D: "Vortex Breakdown over a Pitching Delta Wing", *Journal of Fluids and Structures*, vol. 9, 1995, pp. 571-583.

Appendix E: "Control of Vortex Breakdown with Leading-Edge Devices", AIAA 95-0676, 33rd Aerospace Sciences Meeting and Exhibit, January 9-12, 1995, Reno, NV.

1. INTRODUCTION

Control of vortex breakdown continues to be of vital importance because the breakdown may have a considerable effect on aircraft performance, such as the effect on the time-averaged lift force (Lee and Ho, 1990). Breakdown is also important because of the unsteady nature of flow downstream of vortex breakdown. The unsteadiness may affect the stability of the aircraft and also cause buffeting. The objectives of this work are to understand the physics of unsteady flow phenomena in vortex breakdown region, and to develop techniques for active (feedback) and passive (open loop) control of vortex breakdown over steady and unsteady delta wings.

The control problem is particularly important for unsteady delta wings as well as for unsteady free stream (LeMay et al., 1990; Gursul and Ho, 1994). The vortex breakdown may appear on the wing even if no breakdown is observed in the steady case (Gursul and Ho, 1993). The time-dependent nature of breakdown location may affect unsteady loading on the wing. One of the objectives of this work is to study the possibility of controlling the breakdown in unsteady flows.

It is well known that there are two important parameters which determine the breakdown location: *swirl angle* and *external pressure gradient* outside the vortex core. The principle of any control method is to alter either or both of these parameters. Blowing and suction in the tangential direction along a rounded leading-edge (Wood et al., 1990; Gu et al., 1993) and suction applied around the vortex axis (Werle, 1960; Parmenter and Rockwell, 1990) were shown to delay breakdown. The former is believed to be due to a change in the strength and location of the leading-edge vortices. This is achieved by affecting the location of separation on the rounded leading-edge. Direct control of the separation point modifies the vortex properties such that a reduction in the swirl angle is achieved. The purpose of applying suction around the vortex axis is to reduce the local adverse pressure gradient, which is achieved by accelerating the axial flow along the core.

Since all of the vorticity of the leading-edge vortices originates from the separation point along the leading-edge, leading-edge devices are particularly attractive tools that can be used to influence the strength and structure of these vortices. For example, leading-edge flaps are known to be capable of controlling the circulation and location of the leading-edge

vortices (Spedding et al., 1987; Karagounis et al., 1989; Cheng et al., 1988). These studies concentrated primarily on the effect of leading-edge flaps at low angle of attack where vortex breakdown was not observed over the wing. Recently, the effect of vortex cavity flaps at high angles of attack has been reported (Schaeller et al., 1994). One of the purposes of this work is to explore the effect of leading-edge flaps on vortex breakdown phenomena. The stationary as well as oscillating flaps may provide further insight into the possibility of control of vortex breakdown. We also studied vortex breakdown over a delta wing with variable sweep angle since this method allows a direct control of circulation of leading-edge vortex. Again, periodic variations of sweep angle was studied with the control of vortex breakdown in mind. Application of this technique in unsteady flows was demonstrated for a pitching delta wing.

2. EXPERIMENTAL FACILITIES

Experiments were carried out in a wind tunnel and a water channel, both with a cross-sectional area of 61 cm by 61 cm. The first model delta wing (see Figure 1) was only used in wind tunnel testing. It had a sweep angle of 70° . It was made of 3/4 in. (19 mm) thick Plexiglas and had a chord length of $c=14$ in. (356 mm). The surface was flat whereas the leading edges were beveled at 45° on the windward side. On the lee surface grooves were made for purposes of pressure measurements. The grooves were covered by aluminum plates on which pressure taps of 1 mm diameter and a depth of 2 mm were located. The plates were flush mounted to the surface so that no interference of flow would be introduced. Unsteady pressure measurement locations in the streamwise direction were along the centerline and along the ray $y/s=0.5$ from the apex. Additional pressure taps for mean pressure measurements were located in the spanwise direction at $x/c=0.6$ and $x/c=0.8$. All unused taps were sealed by tape during the experiment. The Reynolds number was varied from 127,000 to 254,000, although most of the results are for $Re=254,000$. At the largest angle of attack, the blockage ratio was 0.08.

The other two model delta wings, one with variable sweep angle and one with leading-edge flaps, are shown in Figures 2 and 3, respectively. For both models, the base

model has a sweep angle of $\Lambda=70^\circ$. The chord lengths are $c=254$ mm and 268 mm for the model with flaps and the variable sweep delta wing, respectively. The Reynolds number was around $Re=50,000$ for the water channel experiments. The flap angle δ (measured from the upper surface) could be varied up to 180° . For the variable sweep delta wing, the range of sweep angle was from $\Lambda=60^\circ$ to $\Lambda=70^\circ$. The base plate of the models was made of Plexiglas and the thin plates were made of stainless steel. The motion of the flaps was guided with gears and joints which were connected to a ring. The flaps were opened by rotating this ring. The rotation of the ring was achieved by pulling a cable which was attached to the ring. For the variable sweep delta wing, the two plates were used to change the sweep angle. The motion of the plates was guided with a cable-pulley-pin system. The wing was opened by pulling the cable. For both models, a spring assured the closing of the wing or flaps when the tension on the cable was released. A bicycle brake cable whose sheath was fixed near the trailing-edge and outside the water channel was attached to a drum which was driven by a DC motor position control system (see Figure 4). A sine wave from a function generator was used to drive the DC motor position control system. A potentiometer was used to monitor the variation of the flap angle or sweep angle. This flexible system allowed the use of flaps or variable sweep even for a pitching motion of the delta wings.

The experiments were conducted both for stationary and pitching delta wings. The pitching mechanism was similar to the one used by LeMay et al (1990). A displacement transducer was used to monitor the variation of the angle of attack. A variable speed DC motor and a speed controller were used to drive the pitching mechanism. For the combined motion of pitching and harmonic variations of sweep angle, the input signal to the DC motor position control system was obtained by applying a phase shift to the displacement transducer signal from the pitching mechanism. This provided the desired phase angle between angle of attack $\alpha(t)$ and sweep angle $\Lambda(t)$.

Flow visualization of vortex breakdown was done by injecting fluid with food coloring dye near the apex of the models. The flow visualization was videotaped for further analysis. The velocity was measured with a single component laser Doppler velocimetry

(LDV) system. The measurement uncertainties for breakdown location (x/c) and mean velocity were estimated as 0.4% and 1%, respectively. Ensemble-averaging technique was applied to the velocity signals in the case of periodic variations of flap angle or sweep angle. Typically, 100 cycles were averaged in order to obtain the phase-averaged velocity. The standard deviation from the phase-averaged value was also calculated.

3. RESULTS

3.1. Unsteady Flow Phenomena in Vortex Breakdown Region

In the wind tunnel experiments with the first model delta wing, coherent pressure fluctuations have been detected on the upper wing surface as the angle of attack increases and breakdown location moves over the wing as shown in Figure 5. The time traces shown in the figure were taken at a location close to trailing-edge ($x/c=0.93$) and approximately underneath the leading-edge vortex ($y/s=0.5$). At the smallest angle of attack $\alpha=15^\circ$, there is no breakdown over the wing. At larger angles of attack, the breakdown moves over the wing causing increased pressure fluctuations.

Simultaneous pressure measurements at two locations in the spanwise direction indicated that the disturbances rotate in the same direction as the leading-edge vortex (see Figure 6). Moreover, simultaneous hot-wire measurements at two points which are at either side of the vortex axis showed that there existed a phase angle of approximately 180 deg. between the signals (Figure 7). This implies that the disturbances are helical waves with azimuthal wavenumber $n=1$, if the instability is presented as $\exp\{i(\alpha x + n\phi - \omega t)\}$. It was shown that this type of unsteady flow is a result of the instability of the time-averaged swirling flow with a wake-like axial profile (Garg and Leibovich, 1979; Gursul, 1994), as is found in breakdown regions, and is observed in other swirling flows as well.

Measurements showed that the dominant frequency detected from the pressure fluctuations on the upper surface is not constant, but vary with the streamwise distance. Other main parameters of the instability such as the wavelength and phase speed were determined for a large range of angle of attack (Gursul, 1994, see Appendix A).

3.2. Time Scales of Vortex Breakdown

It has been observed in several experiments that vortex breakdown location is not steady and exhibits fluctuations in the streamwise direction (Lowson, 1964; Garg and Leibovich, 1979; Payne et al., 1988; Thompson et al., 1991). One possible source is the hydrodynamic instability of the "breakdown wake" (i.e., the flow in the wake of the vortex breakdown) where wake-like axial velocity profiles are observed. The quasi-periodic nature of the flow in the wake of breakdown may interact with the breakdown process through upstream influence. It has not been possible to determine, from the previous experiments, the role of the helical mode instability in the unsteady nature of breakdown location.

We carried out flow visualization and laser Doppler velocimetry (LDV) measurements in the water channel. The results (see Figure 8) indicated that the fluctuations of vortex breakdown location occur at much lower frequencies than the frequency of the hydrodynamic instability of the flow in the wake of breakdown. It is thus suggested that the helical mode instability does not influence the unsteady nature of breakdown location (Gursul and Yang, 1995, see Appendix B).

In order to understand the nature of the organized fluctuations, simultaneous flow visualization of the two leading edge vortices was performed for $\Lambda=70^\circ$ and $\alpha=37^\circ$. The cross-spectrum of the fluctuations for the two breakdowns (the left and right vortices) is shown in Figure 9. It is obvious that both breakdowns oscillate at the same frequency and the phase angle between them is approximately 180° . In other words, there is an antisymmetric motion of breakdown locations for left and right vortices. There is clearly an interaction between the opposite leading-edge vortices. However, the exact nature of this interaction is not known.

As a summary, the spectrum of unsteady flow phenomena over delta wings as a function of dimensionless frequency is shown in Figure 10. In this graph, the range of the dominant frequency of the oscillations of breakdown location was obtained from the flow visualization for different angles of attack. The range of the helical mode instability was available from the previous experiments (Gursul, 1994). The frequency range for the Kelvin-Helmholtz instability of the shear layer separated from the leading-edge was

estimated from the experiments and numerical simulations (Gad-el-Hak and Blackwelder, 1987; Gordnier and Visbal, 1994). When compared with the frequency of the helical mode instability, the frequency range of the spectrum of breakdown location for a stationary delta wing is much closer to the frequency range of typical aerodynamic maneuvers (up to $fc/U_\infty \approx 0.03$). The response of breakdown location and possible coupling between the wing motion and breakdown location in this frequency range is very important.

3.3. Active (Feedback) Control of Vortex Breakdown

The pressure fluctuations induced by the helical mode instability of vortex breakdown can be used to control the vortex breakdown location. As shown in Figure 5, with the increasing angle of attack as the breakdown moves toward the apex, the amplitude of pressure fluctuations increases. Hence the rms value of pressure was chosen as the control variable. The basic idea of the breakdown control is to alter the circulation of the leading-edge vortex as the control variable varies. This has been achieved with the model delta wing with variable sweep. A feedback control loop was used to control the amplitude of pressure fluctuations at a single point on a delta wing. The block diagram of the feedback control system is shown in Figure 11. Further information is available in the published article (Gursul et al., 1995, see Appendix C).

First, the active control experiments were conducted for a stationary delta wing at angle of attack $\alpha = 23$ deg. (see Figure 12). Initially the sweep angle was set to $\Lambda = 60$ deg. For this value of sweep angle, the vortex breakdown location is over the wing and closer to the apex. Once the control loop is activated, it varies the sweep angle dynamically until the amplitude of pressure fluctuations are below a threshold value (or until the breakdown location moves downstream of trailing edge). In figure 12, the plots of pressure fluctuation, feedback voltage, and sweep angle are shown. Around $t = 5$ seconds, the feedback control was turned on. It is seen that the sweep angle increases and becomes nearly constant around

$\Lambda=68.5$ deg. after a small overshoot. This new sweep angle corresponds to a case where the breakdown location is downstream of the wing. The decrease in pressure fluctuations and feedback voltage accompany the variation of sweep angle.

The active control experiments for the pitching delta wing were conducted in a similar way. As the delta wing was pitched periodically between 15 deg and 23 deg, the initial sweep angle was set to 60 deg. For this range of angle of attack, the vortex breakdown is over the wing during the whole cycle. The plots of angle of attack, pressure fluctuations, feedback voltage and sweep angle are shown in Figure 13. When the control loop is turned on suddenly, the sweep angle increases and becomes nearly constant around a new value for which the breakdown location is downstream of the wing.

6.4. Vortex Breakdown over a Pitching Delta Wing.

Several experimental studies of vortex breakdown over pitching delta wings have shown that there is a phase shift between the motion of the wing and the movement of breakdown location (LeMay et al., 1990; Wolffelt, 1987; Woodgate, 1971; Atta and Rockwell, 1990). The phase delay mainly depends on the reduced frequency $k=\omega c/2U_\infty$ (LeMay et al. 1990) and can be as large as 180° . Nevertheless, the physics of this phase lag is not well understood.

It has been suggested that delta wing vortex breakdown in unsteady free stream is driven by the external pressure gradient (Gursul and Ho, 1994). Likewise, the observed phase delay of the breakdown location for pitching delta wing may be related to the variations of the adverse pressure gradient on the wing surface. In order to test this hypothesis, unsteady pressure on a pitching delta wing was measured and correlated with the movement of the breakdown location.

It was shown earlier that vortex breakdown flowfields over delta wings show helical-mode instability which produces coherent pressure fluctuations on the suction surface. With increasing angle of attack, the amplitude of the pressure fluctuations due to the signature of breakdown increases. When the delta wing is pitched sinusoidally (between 29° and 39°), the instantaneous pressure signature of the breakdown varies as the

breakdown location moves back and forth in the streamwise direction (Figure 14). It is evident that the maximum fluctuation level due to the breakdown occurs not at the maximum angle of attack, but later, at a smaller angle of attack as the wing pitches down. In order to quantify the phase delay, the phase-averaging technique was applied to the pressure signal, i.e.

$$C_p = \langle C_p \rangle + C_p'$$

where the $\langle C_p \rangle$ is the phase-averaged pressure coefficient. The standard deviation from the phase-averaged value,

$$C_{p, sd}' = \sqrt{\langle (C_p')^2 \rangle}$$

was calculated as a function of angle of attack. The variation of the standard deviation shown in Figure 15 reveals hysteresis loops. The loops become wider with increasing reduced frequency, which is an indication of increasing phase delays.

In order to investigate the possible relationship between the pressure field and the dynamic character of breakdown location, pressure measurements were carried out along the centerline ($y/s=0$) and $y/s=0.5$. For the leading-edge vortex, the pressure gradient on the suction surface of the wing acts as the external pressure gradient. However, interpretation of the pressure along the $y/s=0.5$ is not straightforward, since the measurement locations are approximately underneath the vortex. Whether the unsteady variation of pressure is the end result of the vortex breakdown remains uncertain. On the other hand, along the centerline $y/s=0$, the effects of vortex on pressure are negligible. This is verified by a simple test. A control cylinder with diameter $d/c=0.047$ was placed at $x/c=0.92$, $z/c=0.37$ (for $\alpha=29^\circ$) which caused a premature breakdown. The mean pressure coefficient along the spanwise direction at $x/c=0.80$ for the cases with and without the cylinder shows that there is a large reduction in the induced pressure underneath the vortex due to the breakdown, whereas the effects are minimum at the centerline (Figure 16).

For the pitching motion, the variation of the phase-averaged pressure along the centerline as a function of time is shown in Figure 17 for two different values of reduced frequency. The angle of attack varies as

$$\alpha = 34^\circ - 5^\circ \cos \omega t.$$

The pressure along the centerline varies in magnitude as a function of time. For the smaller reduced frequency ($k=0.19$), the maximum pressure (suction) occurs when the angle of attack is closer to the maximum angle of attack; however, there exists a time delay. For $k=0.35$, this phase delay is larger. The pressure field for a pitching wing seems to be delayed in time compared to the quasi-steady case. This phase delay is close to that of the breakdown location obtained from pressure fluctuations (i.e., from the variation of the standard deviation shown in Figure 15). Thus, there exists a definite relationship between the pressure field on the wing and the location of the vortex breakdown.

The Fourier analysis of the phase averaged signal showed that most of the energy was concentrated at the fundamental frequency. The phase angle between the angle of attack α and $\langle -C_p \rangle$ was calculated at each measurement station and plotted in Figure 18. The phase delay increases with increasing reduced frequency. At large reduced frequencies, there is also considerable variation of the phase angle in the streamwise direction. However, it should be kept in mind that the amplitude of the pressure variations becomes smaller toward the trailing-edge where the largest phase angles are observed.

The variation of phase lag between the wing motion and $\langle -C_p \rangle$ is shown as a function of reduced frequency in Figures 19. Also shown are the phase lags obtained from the pressure fluctuations in addition to those determined by flow visualization for a similar model. It is evident that there exists a definite relationship between the pressure field on the wing surface and the location of the vortex breakdown.

In conclusion, variation of the phase-averaged pressure along the wing centerline as a function of time shows that there is a phase delay between the wing motion and the pressure field. This phase delay is close to the phase delay of the movement of breakdown location. The phase delay of pressure increases with increasing reduced frequency and is not sensitive to Reynolds number variation. Similar phase lags of pressure were found for smaller angle-of-attack range for which the breakdown is absent. This confirms that the observed time delays in breakdown location is related to the variation of the external pressure gradient generated by the wing. Further information can be found in the published journal article (Gursul and Yang, 1995, see Appendix D).

3.5. Control of Vortex Breakdown with Leading-edge Flaps

The location of vortex breakdown as a function of the flap angle δ is shown in Figure 20 for several values of angle of attack. At low angles of attack ($\alpha=16^\circ$ and $\alpha=20^\circ$), as the flap angle decreases from 180° , the breakdown location moves toward the trailing-edge. This effect is similar to that of increasing sweep angle (or decreasing aspect ratio). The breakdown location suddenly moves in far wake as it approaches the trailing-edge. At larger angles of attack ($\alpha=25^\circ$ and $\alpha=30^\circ$), the breakdown location does not change much initially as the flap angle decreases from 180° , but it moves rapidly toward the trailing-edge. At the largest angle of attack ($\alpha=35^\circ$), the breakdown location moves downstream first, with decreasing flap angle, and then upstream for $\delta < 65^\circ$.

Obviously, the effect of flaps on vortex breakdown strongly depends on the angle of attack. If one considers the response of vortex breakdown, for example $x_{bd}/c > 0.40$, there is a clear difference between the variations of breakdown location with flap angle at $\alpha=16^\circ$, 20° and $\alpha=25^\circ$, 30° . The slopes of the variations are very different. In order to gain further insight, detailed flow structures were studied for $\alpha=20^\circ$ and 25° .

A variety of flow patterns were observed depending on flap angle and angle of attack. As an example, constant levels of the mean axial velocity in a cross plane upstream of breakdown ($x/c=0.40$) are shown for two flap angles and for no flaps in Figure 21. The presence of the flaps produces an adverse pressure gradient in the spanwise direction and increases the size of the separated flow region on the upper surface of the wing. This also causes a marked change in the structure of the leading-edge vortices. For $\delta=60^\circ$, the core of the leading-edge vortex is much larger compared to that of the wing with no flaps. For $\delta=100^\circ$, much larger axial velocities are observed in the core. This also implies larger pressure drop at the core, which in turn is a result of the larger swirl velocities. Outside of the flaps, either high speed regions or flow reversal (due to the separated flow) are observed depending on flap angle and angle of attack.

Variation of swirl velocity was also investigated by traversing across the vortex core. The maximum swirl velocity is shown in Figure 22 as a function of the flap angle.

The arrows on the figure indicate the flap angle at which breakdown is at the trailing-edge of the wing. It seems that the vortex breakdown appears on the wing when the swirl level reaches a certain value. For $\alpha=20^\circ$, the swirl level does not change much with the flap angle δ when the breakdown is over the wing. On the other hand, for $\alpha=25^\circ$, the swirl level increases rapidly with the flap angle (when the breakdown is over the wing), explaining the sensitivity of breakdown location with respect to the variations in the flap angle.

In addition to the changes in the swirl level (or strength of the vortex), the location of the vortex core (in the cross plane) exhibits variations with the flap angle. The location of the vortex core was obtained from the velocity measurements (not shown here), which suggested that the existence of the flap may affect the pressure gradient outside of the vortex core. For example, for $\alpha=20^\circ$, there is a gradual variation of breakdown location with the flap angle, although the swirl level does not change much in the same range. This implies that the external pressure gradient for the vortex core is affected by the changes in the geometry of the wing.

Experiments with oscillating flaps were also conducted. The variation of vortex breakdown location for harmonic variations of flap angle between 60° and 180° is shown in Figure 23 together with that of the steady flap angles. The reduced frequency is $k=\omega c/2U_\infty=0.4$, where ω is the radial frequency and U_∞ is the free stream velocity. The variation of breakdown location reveals a hysteresis loop. This is an indication of a time lag response, which is similar to the response of a pitching delta wing.

In conclusion, it was shown that the effect of flaps and sensitivity of breakdown location strongly depends on angle of attack. Velocity measurements showed that, with the varying flap angle, large changes take place in the vortex core diameter and location, in axial and swirl velocity profiles, and in the secondary vortex structure. In general, with the increasing flap angle, larger swirl velocities are observed. The variation of maximum swirl velocity seems to be correlated with the variations of breakdown location as the flap angle is varied. In addition, experiments with oscillating flaps showed that there exists a hysteresis loop in the variation of breakdown location. This indicated a time-lag response similar to that of a pitching delta wing.

3.6. Control of Vortex Breakdown with Variable Sweep

In static experiments, the location of vortex breakdown moves toward the apex with decreasing sweep angle (or aspect ratio), as known from a number of experiments with different aspect ratio wings. Therefore, in the steady case, the location of breakdown shows a monotonic variation with the sweep angle, as opposed to the variation with the flap angle. The variation of breakdown location was studied for harmonic variations of sweep angle, i.e.

$$\Lambda = \Lambda_0 + \Lambda_1 \sin \omega t$$

The variations of the ensemble-averaged breakdown location are shown in Figure 24 for $\Lambda_0 = 65^\circ$ and $\Lambda_1 = 2.5^\circ$ for different values of the reduced frequency, which show hysteresis loops. The loops become narrower with increasing reduced frequency. Actually, at very large reduced frequency ($k=2.0$ and $k=4.0$ (not shown here)), the ensemble-averaged breakdown location is almost constant. The phase lag of vortex breakdown location with respect to that of the quasi-steady case was found by plotting the time history of breakdown location. This is shown in Figure 25. It seems that the phase lag reaches a maximum at $k=0.4$ and then decreases. This time-lag behavior seems to be an inherent response of breakdown location in unsteady flows, regardless of the type of motion.

In order to understand the phase lag of vortex breakdown, phase-averaged velocity measurements were carried out in a cross plane (at $x/c=0.5$) upstream of breakdown location for a reduced frequency of $k=0.4$. It should be noted that the flow field of the leading-edge vortex develops very gradually before vortex breakdown. Indeed, the velocity changes drastically only in a small neighborhood of the breakdown location. It is also known that the swirl level of the leading edge vortex does not vary much in the streamwise direction. Therefore, these measurements give a good indication of the upstream conditions before breakdown. Contours of constant phase-averaged axial velocity are shown at different sweep angles for $\Lambda_0 = 66^\circ$ and $\Lambda_1 = 3^\circ$ in Figure 26. Also shown are the mean velocity contours in the steady case for the minimum sweep angle $\Lambda = 63^\circ$ and the maximum sweep angle $\Lambda = 69^\circ$. As the sweep angle varies dynamically, the location of the vortex core

(defined as the location at which the phase-averaged axial velocity is maximum) varies mostly in the spanwise direction. Note that the axial velocity contours are very similar for the dynamic and static cases. Also the two flow fields for the mean sweep angle $\Lambda_0=66^\circ$ (for increasing and decreasing sweep angle) are not very different from each other. All these suggest that the structure of leading edge vortex is not affected much by the unsteadiness and is approximately quasi-steady. Nevertheless, there is a small phase lag in the development of the vortical flow. This is evident from the contours of constant standard deviation from the phase-averaged velocity shown in Figure 27. It should be noted that the shape of the contours of the standard deviation (or rms velocity fluctuations in the steady case) is related to the main vortex as well as the shear layer and secondary separation region.

The variations of the main parameters are summarized in Figure 28. The variation of sweep angle and ensemble-averaged breakdown location with time are shown at the top of Figure 28 for one cycle of the motion. In the middle of the figure, the location of the vortex core in the dynamic and static cases are shown. Note that the phase lag of the core location (with respect to the quasi-steady case) is small compared to the larger phase lag of breakdown location with respect to the sweep angle variations. In order to get a good indication of the strength of the vortex, the circulation around a fixed contour (see inset in Figure 28) was calculated from the phase-averaged velocity measurements. Although this contour covers the main vortex and most of the secondary vortex and shear layer, it is a reasonable indicator for the strength of the main vortex. Moreover, if it is assumed that conical flow exists, the circulation increases linearly with the streamwise distance from the apex. In this case, the measured circulation at a fixed streamwise distance is related to the rate of increase of the circulation along the streamwise direction (or the rate at which vorticity is fed into the leading-edge vortex). Note that the phase lag of the circulation (with respect to the quasi-steady case) is also small (bottom of Figure 28). In conclusion, the unsteady effects on the vortex core location and strength are not very strong. Therefore, the large phase lag of breakdown location cannot be explained with the variations in the upstream conditions since the location and strength of the vortex exhibit smaller phase lags.

This suggests that the variations of the *external pressure gradient* (which is one of the two control parameters for breakdown, the *swirl level* being the other one) should be responsible for the large phase lag of vortex breakdown location.

Perturbations applied at the leading-edge by varying sweep angle dynamically around a mean value may provide an effective way for breakdown control in unsteady flows. In order to demonstrate this, a pitching motion of the delta wing was considered, i.e.

$$\alpha = \alpha_0 + \alpha_1 \sin \omega t$$

The well known hysteresis loop for the location of the vortex breakdown is shown in Figure 29 for $\alpha_0 = 25^\circ$ and $\alpha_1 = 5^\circ$. Now, the perturbations of the sweep angle with the same frequency as pitching, but with a phase angle are considered, i.e.

$$\alpha = \alpha_0 + \alpha_1 \sin \omega t$$

$$\Lambda = \Lambda_0 + \Lambda_1 \sin (\omega t + \Phi)$$

The variation of breakdown location for three different values of the phase angle Φ is shown in Figure 30. The phase angle Φ was varied over a range of 360° , and the maximum and minimum values of breakdown location during a cycle was documented. The results are shown in Figure 31. It appears that for $\Phi = 0^\circ$, the breakdown location is approximately constant and the average location has moved downstream. (The dashed lines indicate the maximum and minimum location for the pitching motion only at the average sweep angle Λ_0). The perturbations of sweep angle not only decrease the amplitude of the variations of breakdown location, but also move the average location downstream.

The results for a different set of parameters ($\Lambda_0 = 66^\circ$, $\Lambda_1 = 3^\circ$, $\alpha_0 = 20^\circ$ and $\alpha_1 = 5^\circ$) are shown in Figure 32. In this case, the amplitude of the variations decreases considerably at an optimum phase angle around 35° . However, the average location does not change much. Experiments for a different range of angle of attack and sweep angle, as well as reduced frequency, showed that the optimum phase angle is somewhere between 0° and 35° . A simple explanation of the optimum phase angle, based on the time-lag response of breakdown location (with respect to the variations in $\alpha(t)$ and $\Lambda(t)$), is possible. As a first approximation, the response of vortex breakdown location to harmonic variations of angle of attack ($\alpha = \alpha_0 + \alpha_1 \sin \omega t$, for constant sweep angle $\Lambda = \Lambda_0$) will be in the form of $x_{bd} = x_0 + x_1$

$\sin(\omega t + \pi - \phi_\alpha)$, where ϕ_α is the phase lag with respect to the quasi-steady case. Since, in the quasi-steady case, the vortex breakdown location moves toward apex with increasing angle of attack, there is a phase angle of π in the expression of x_{bd} . Similarly, the response of vortex breakdown location to harmonic variations of sweep angle ($\Lambda = \Lambda_0 + \Lambda_1 \sin(\omega t + \Phi)$, for constant angle of attack $\alpha = \alpha_0$) will be in the form of $x_{bd} = x_0 + x_1 \sin(\omega t + \Phi - \phi_\Lambda)$, where ϕ_Λ is the phase lag with respect to the quasi-steady case. Since it is desired to cancel the variations of breakdown location due to $\alpha(t)$ with the variations due to $\Lambda(t)$, the arguments of these two responses should be out of phase, i.e. $(\omega t + \Phi - \phi_\Lambda) + \pi = (\omega t + \pi - \phi_\alpha)$, which yields $\Phi = \phi_\Lambda - \phi_\alpha$. For the case shown in Figure 32, the phase lags ϕ_Λ and ϕ_α were found by plotting the time history of breakdown location, which yielded $\phi_\Lambda = 85^\circ$ and $\phi_\alpha = 40^\circ$. Therefore, Φ is predicted as $\Phi = \phi_\Lambda - \phi_\alpha = 45^\circ$, which is close to the experimental results shown in Figure 32. Although this simple model provided a reasonable prediction for the optimum phase angle between $\alpha(t)$ and $\Lambda(t)$, detailed flow field information is necessary for further understanding.

In summary, harmonic variations of sweep angle were studied for a delta wing with variable sweep. The variation of vortex breakdown location showed hysteresis loops and phase lag which depend on the reduced frequency. However, measurements of the phase-averaged axial velocity in a cross flow plane upstream of breakdown location showed no major unsteady effects in the development of the flow field. The larger time lag of vortex breakdown location cannot be explained with the variations in the upstream conditions since the location and strength of the vortex exhibit smaller phase lags. This suggests that the *external pressure gradient* plays a major role in the dynamic response of breakdown location. Use of variable sweep for breakdown control was demonstrated for a pitching delta wing. Oscillations of sweep angle with the same frequency as pitching, but with a phase angle were considered. It was shown that, at an optimum phase angle, the perturbations of sweep angle decrease the amplitude of the variations of breakdown location. In some cases, it was also observed that the average breakdown location moved downstream.

CONCLUSIONS

Coherent pressure fluctuations observed on delta wings are due to the first helical mode instability of the swirling flows. Characteristics of this instability was studied in detail.

The fluctuations of vortex breakdown location occur at much lower frequencies than the frequency of the hydrodynamic instability of the flow in the wake of breakdown. It is thus suggested that the helical mode instability does not influence the unsteady nature of breakdown location. The source of the fluctuations was identified as the interaction between the opposite leading-edge vortices.

A feedback control loop was used to control vortex breakdown location. For this purpose, the amplitude of pressure fluctuations was chosen as the control variable. It was demonstrated that it is feasible to use a variable sweep angle mechanism as a means of controlling the vortex breakdown location by influencing the circulation of the leading edge vortex.

Unsteady pressure measurements were carried out on a pitching delta wing in order to study the effects of pressure gradient on the phase lag between the wing motion and the movement of breakdown location. The results indicate that the observed time lag of breakdown location is strongly linked to the external pressure gradient generated by the wing.

Effect of leading-edge devices on vortex breakdown was investigated. Stationary as well as oscillating leading-edge flaps were shown to alter the structure of the leading-edge vortices, and consequently the location of vortex breakdown. Also, periodic variations of the sweep angle were used to control the breakdown location for a pitching delta wing.

REFERENCES

Atta, R. and Rockwell, D., "Leading-edge vortices due to low Reynolds number flow past a pitching delta wing," AIAA Journal, Vol. 28, pp. 995-1004, 1990.

Cheng, H.K., Edwards, R.H., Jia, Z.X. and Lee, C.J., "Vortex-Dominated Slender-Wing Problems Studied by a Point-Vortex Method", AIAA-88-3744, 1988.

Gad-el-Hak, M. and Blackwelder, R F, "Control of the discrete vortices from a delta wing", AIAA Journal, vol. 25, No. 5, September 1987, pp. 1042-1049.

Garg, A. K. and Leibovich, S., "Spectral characteristics of vortex breakdown flowfields," Physics of Fluids, Vol. 22, 2053, 1979.

Gordnier, R. and Visbal, M. R., "Unsteady vortex structure over a delta wing," Journal of Aircraft, Vol. 31, 243, 1994

Gu, W., Robinson, O. and Rockwell, D., "Control of Vortices on a Delta Wing by Leading-Edge Injection", AIAA Journal, vol. 31, no. 7, July 1993, pp. 1177-1186.

Gursul, I. "Unsteady Flow Phenomena over Delta Wings at High Angle of Attack", *AIAA Journal*, vol. 32, no. 2, February 1994, pp. 225-231.

Gursul, I. and Ho, C-M. "Vortex Breakdown over Delta Wings in Unsteady Freestream", *AIAA Journal*, vol. 32, no. 2, February 1994, pp. 433-436.

Gursul, I. and Ho, C-M., "Vortex Breakdown over Delta Wings in Unsteady Free Stream", AIAA Paper 93-0555, January 1993.

Gursul, I., Srinivas, S. and Batta, G., "Active Control of Vortex Breakdown over Delta Wings", AIAA Journal, Volume 33, No 9, 1995, pp 1743-1745.

Karagounis, T., Maxworthy, T. and Spedding, G.R., "Generation and Control of Separated Vortices over a Delta Wing by Means of Leading Edge Flaps", AIAA Paper 89-0997, AIAA 2nd Shear Flow Conference, March 13-16, 1989, Tempe, AZ.

Lee, M. and Ho, C-M., "Lift Force of Delta Wings", *Applied Mechanics Reviews*, vol. 43, no. 9, 1990, pp. 209-221.

LeMay, S.P., Batill, S.M. and Nelson, R.C., "Vortex Dynamics on a Pitching Delta Wing", *Journal of Aircraft*, vol. 27, no. 2, February 1990, pp. 131-138.

Lowson, M. V., "Some experiments with vortex breakdown," *Journal of the Royal Aeronautical Society*, Vol. 68, 1964.

Payne, F. M., T. T. Ng and Nelson, R. C., "Visualization and wake surveys of vortical flow over a delta wing," *AIAA Journal*, Vol. 26, 1988.

Parmenter, K. and Rockwell, D., "Transient Response of Leading-Edge Vortices to Localized Suction", *AIAA Journal*, vol. 28, no. 6, June 1990, pp. 1131-1133.

Schaeffer, N.W., Rediniotis, O.K. and Telionis, D.P., "Control of the Transient Development of Leading Edge Vortices by Vortex Cavity Flaps", AIAA-94-1857, 25th AIAA Fluid Dynamics Conference, June 20-23, 1994, Colorado Springs, CO.

Spedding, G.R., Maxworthy, T. and Rignot, E., "Unsteady Vortex Flows over Delta Wings", *Proc. of 2nd AFOSR Workshop on Unsteady and Separated Flows*, Colorado Springs, July 1987, pp. 283-287.

Thompson, S. A., Batill, S. M. and Nelson, N. C., "Separated flowfield on a slender wing undergoing transient pitching motions", *Journal of Aircraft*, Vol. 28, No. 8, August, 1991.

Werle, H. "Sur l'eclatement des tourbillons d'apex d'une aile delta aux faibles vitesses", *La Recherche Aeronautique*, no. 74, January-February 1960, pp. 23-30.

Wolffelt, K. W., "Investigation on the movement of vortex burst position with dynamically changing angle of attack for a schematic delta wing in a water channel with correlation to similar studies in wind tunnel", In *Aerodynamic and Related Hydrodynamic Studies Using Water Facilities*, AGARD-CP-413, 1987.

Wood, N.J., Roberts, L. and Celik, Z., "Control of Asymmetric Vortical Flows over Delta Wings at High Angles of Attack", *Journal of Aircraft*, vol. 27, no. 5, pp. 429-435.

Woodgate, L., "Measurements of the oscillatory pitching-moment derivatives on a sharp-edge delta wing at angles of incidence for which vortex breakdowns occurs," *Aeronautical Research Council R & M*, No. 3628, Part 3, 1971.

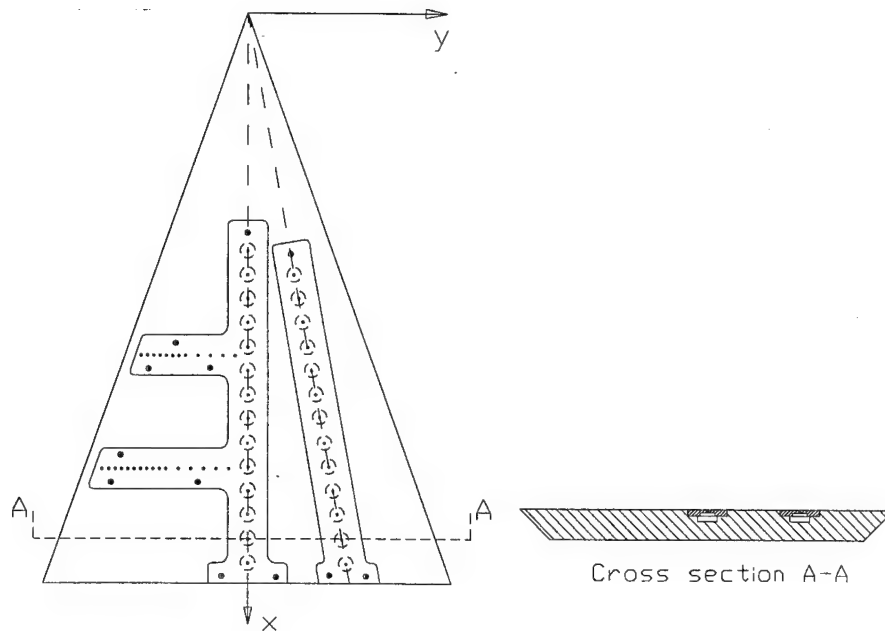


Figure 1. Top view (left) and cross section view (right) of delta wing model #1.

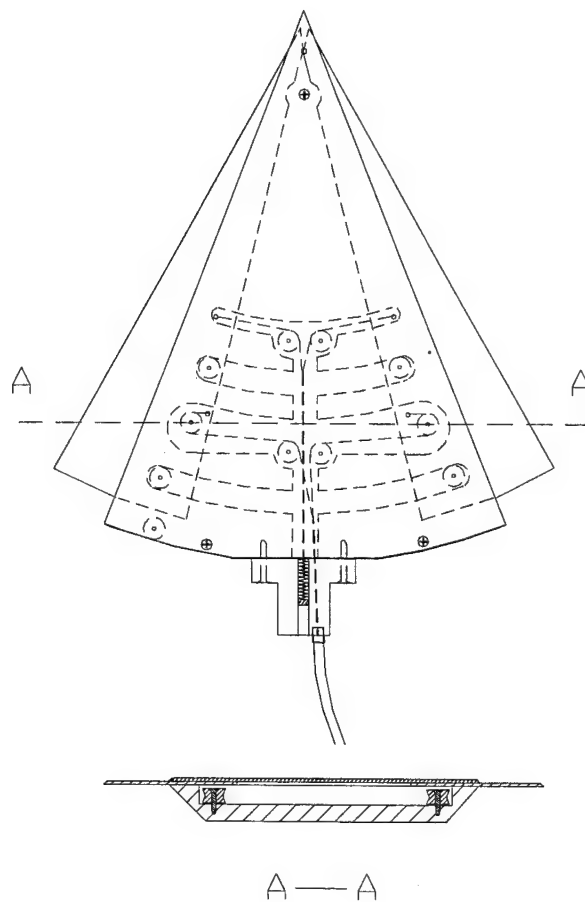


Figure 2. Schematic of delta wing model with variable sweep angle.

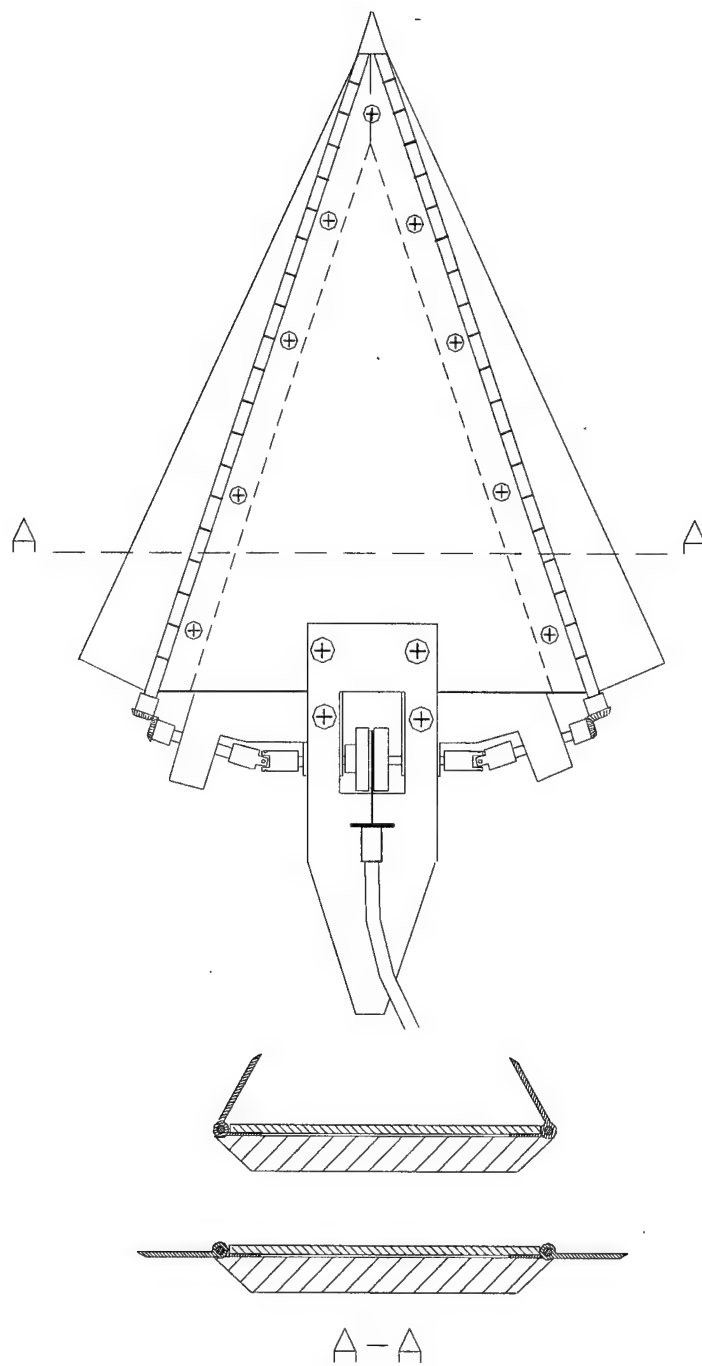


Figure 3. Schematic of delta wing model with leading-edge flaps.

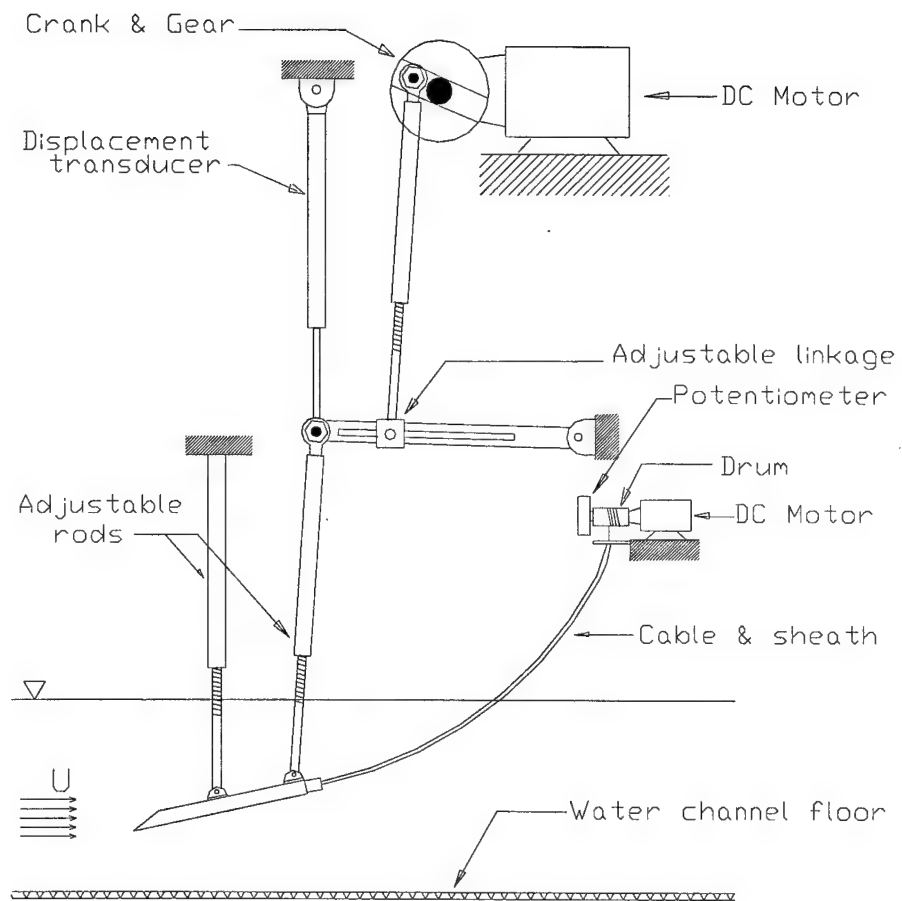


Figure 4. Experimental setup for water channel experiments.

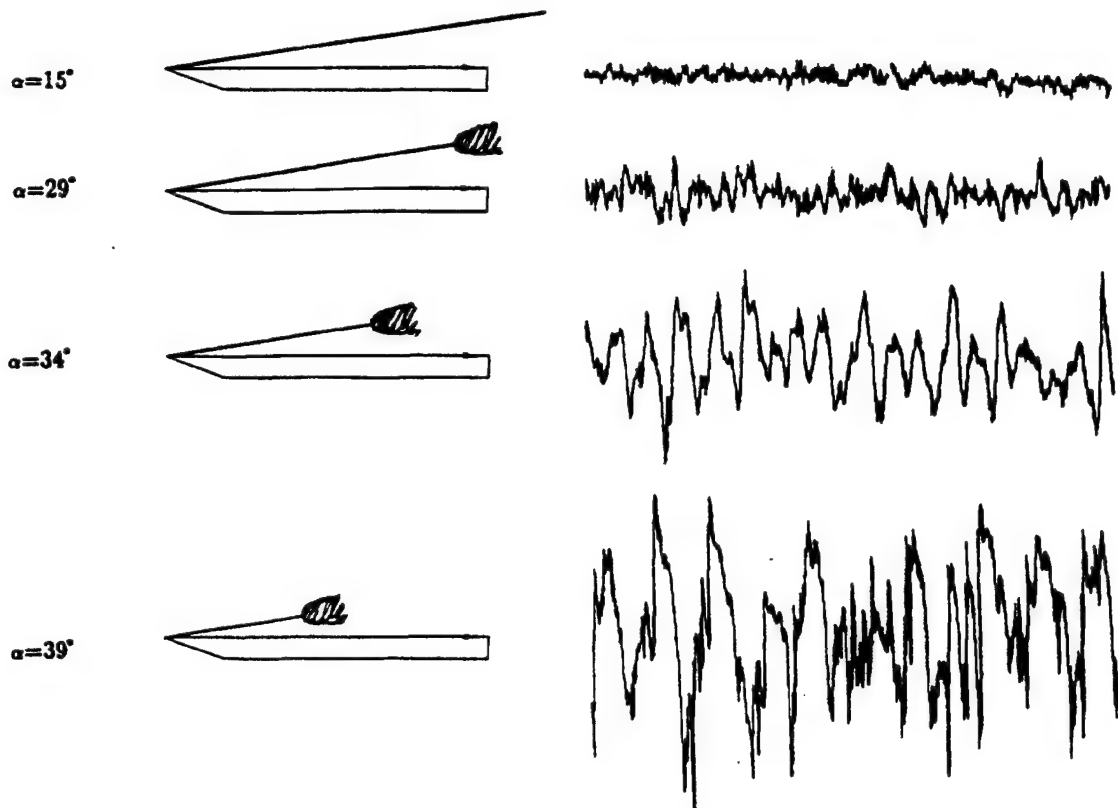


Figure 5. Location of vortex breakdown and pressure fluctuations near trailing-edge ($x/c=0.93$) for different angles of attack. Length of time record is approximately $10c/U_\infty$.

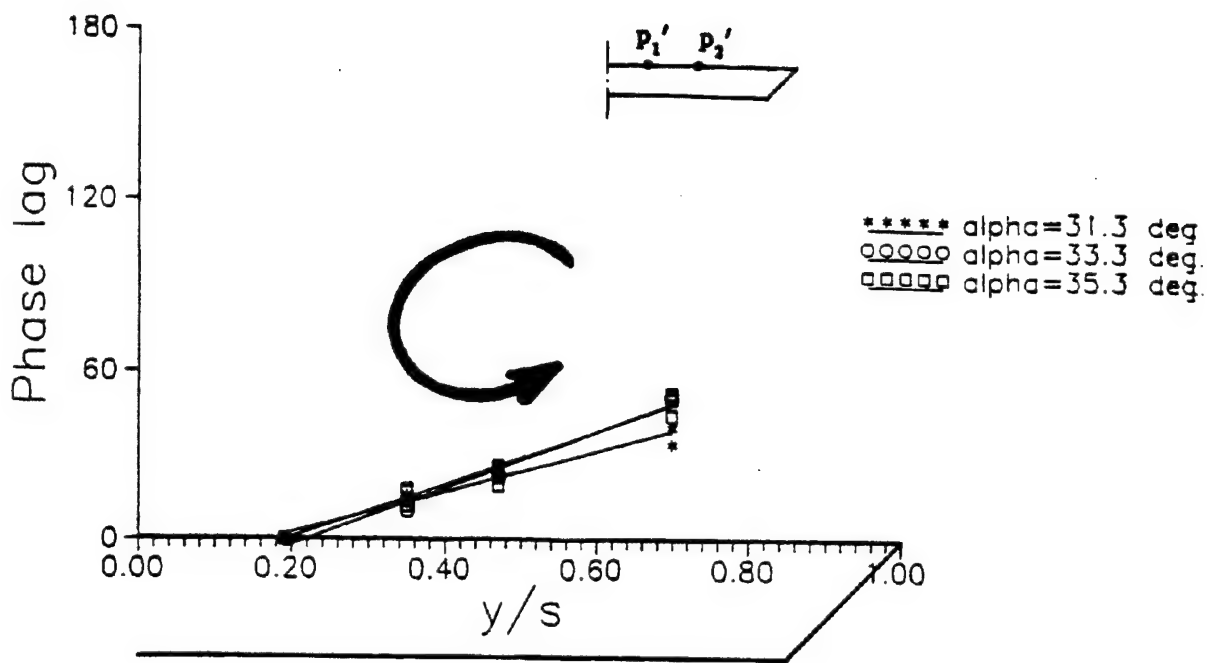


Figure 6. Variation of phase angle between pressure signals at two locations in the spanwise direction.

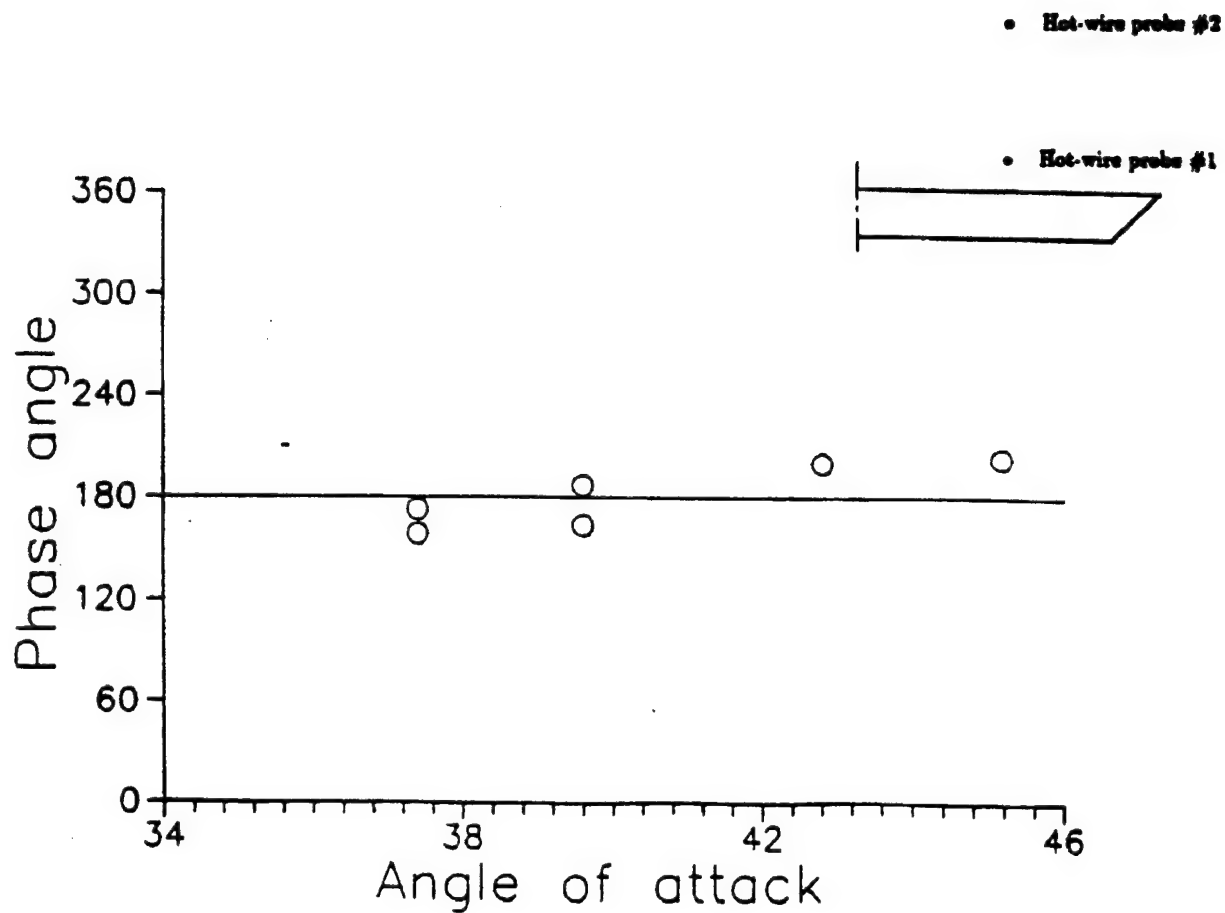


Figure 7. Variation of phase angle between hot-wire signals at two locations that are at either side of the vortex axis.

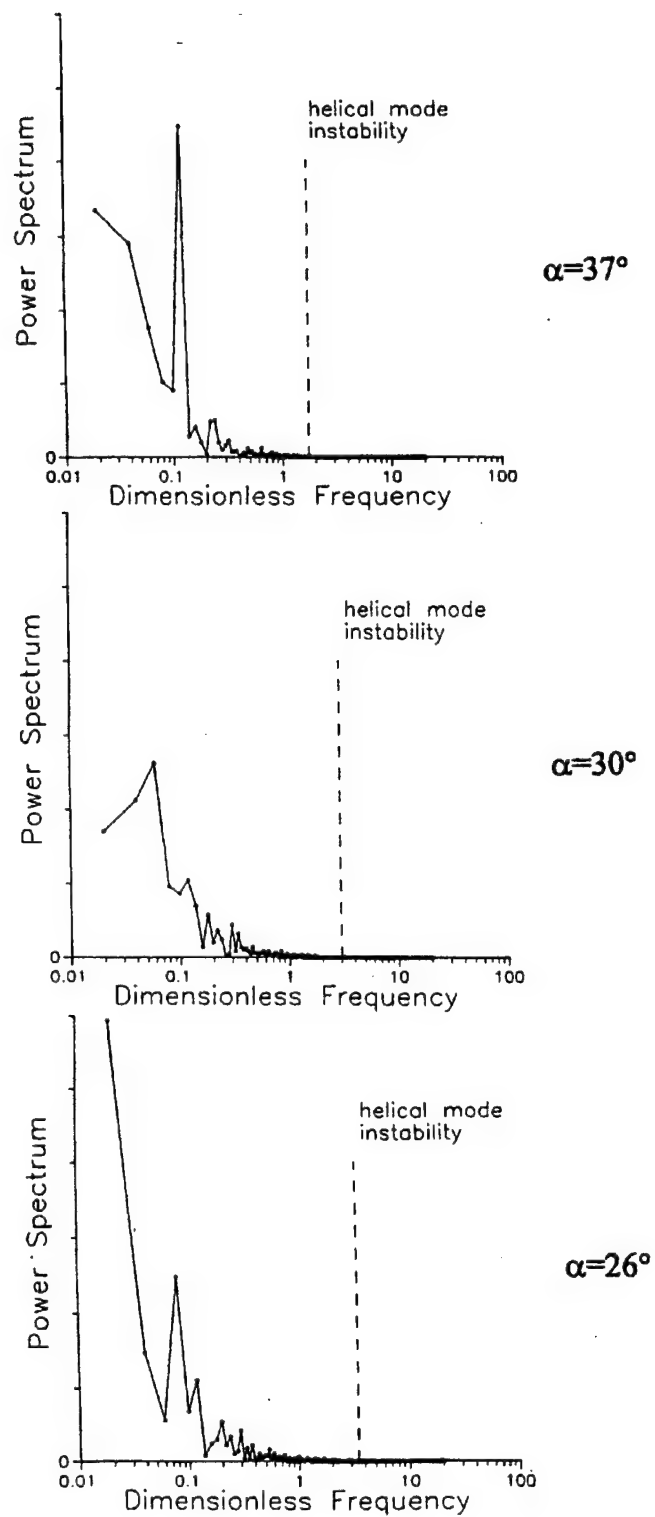


Figure 8. Spectra of fluctuations of breakdown location; vertical scale is linear and in arbitrary unit.

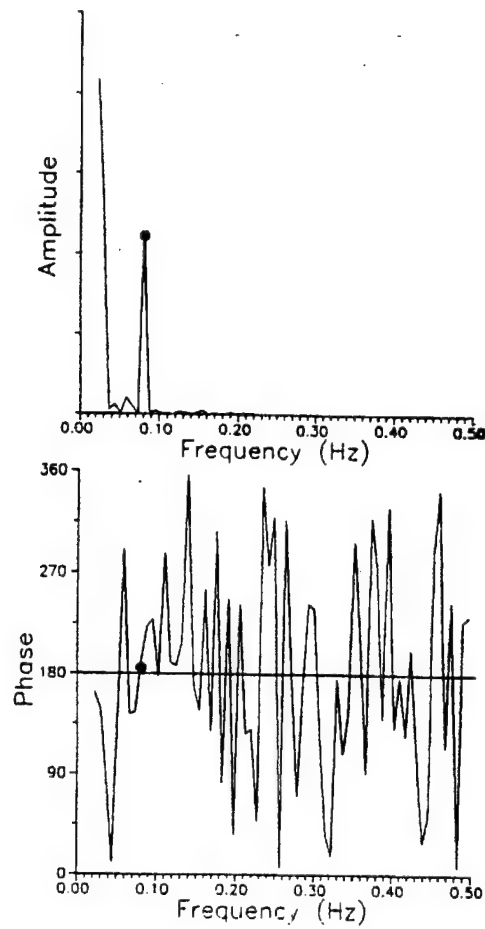


Figure 9. Cross-spectrum of fluctuation of left and right breakdowns, $\Lambda=70^\circ$ and $\alpha=37^\circ$.

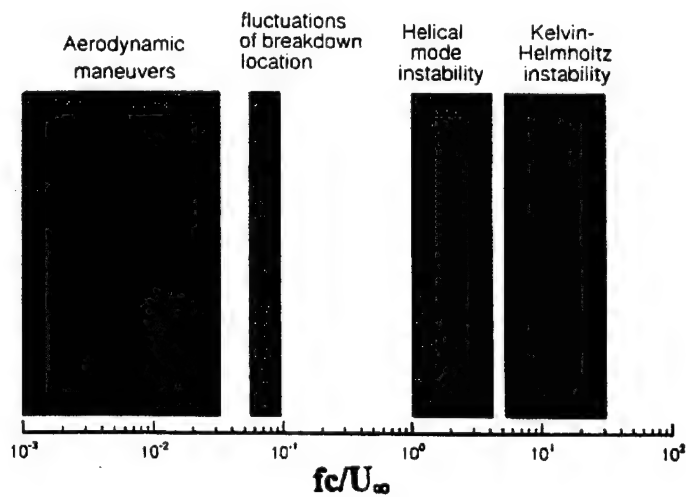


Figure 10. Spectrum of unsteady flow phenomena over delta wings.

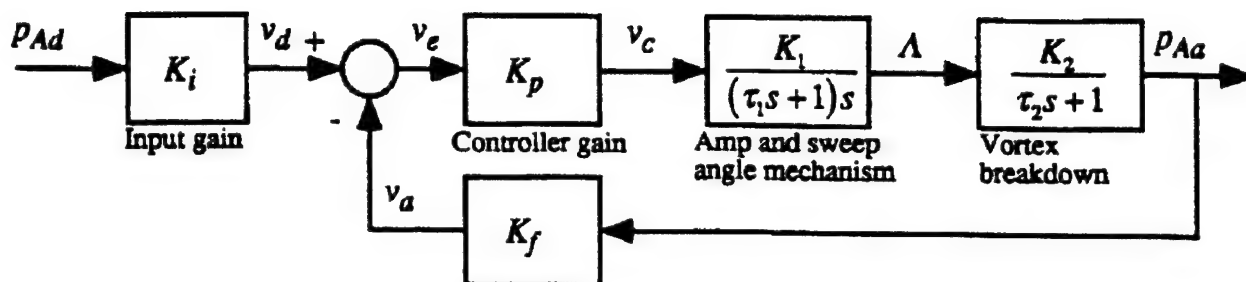


Figure 11. Block diagram of feedback control system.

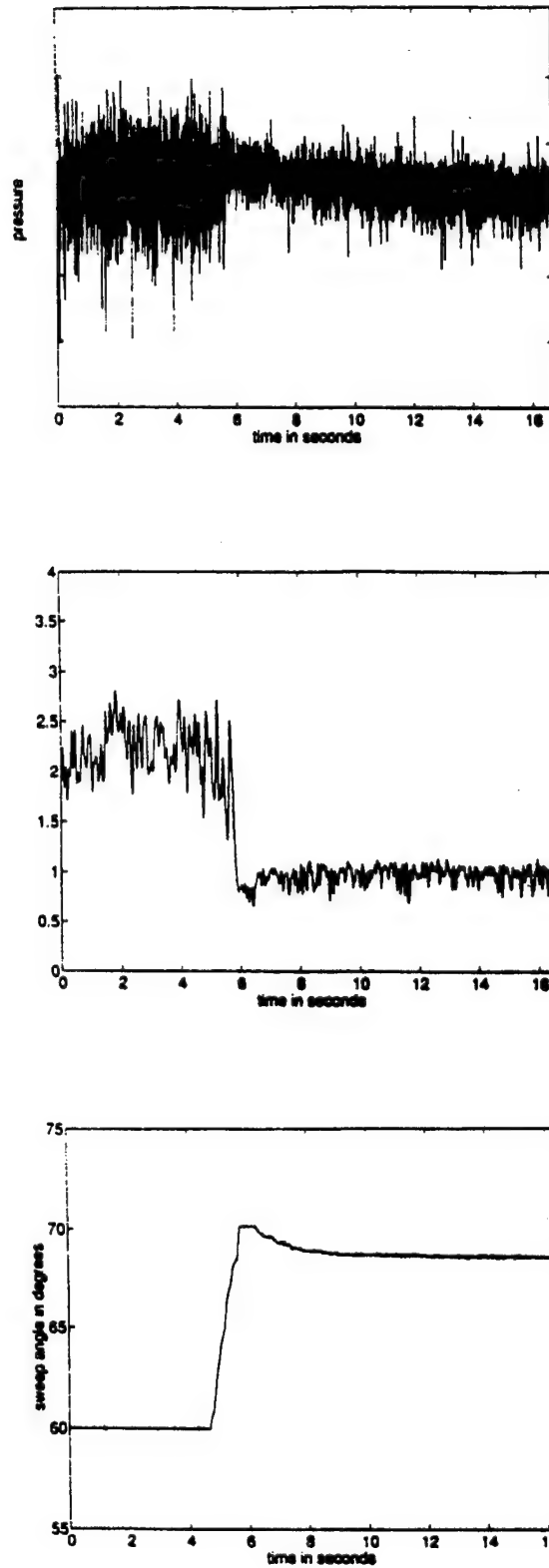


Figure 12: (From top to bottom) Variation of pressure fluctuation $p'(t)$, feedback voltage $v_a(t)$ and sweep angle $\Lambda(t)$ as a function of time. $\alpha=23^\circ$.

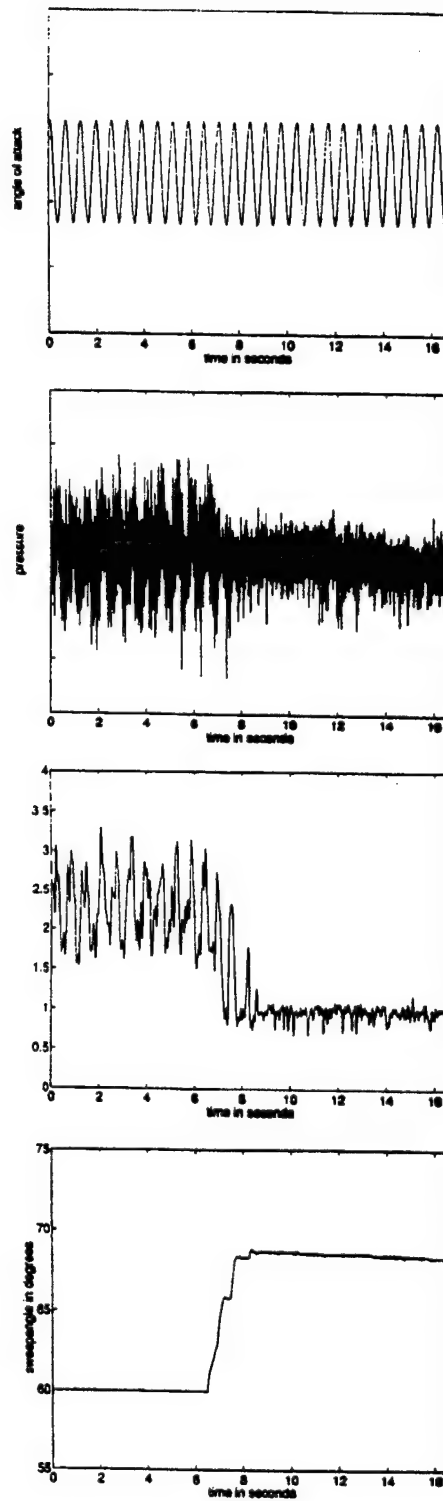


Figure 13: (From top to bottom) Variation of angle of attack $\alpha(t)$, pressure fluctuation $p'(t)$, feedback voltage $v_a(t)$ and sweep angle $\Lambda(t)$ as a function of time. $\alpha = 19^\circ + 4^\circ \cos(\omega t)$, $k = \omega c / 2U_\infty = 0.12$.

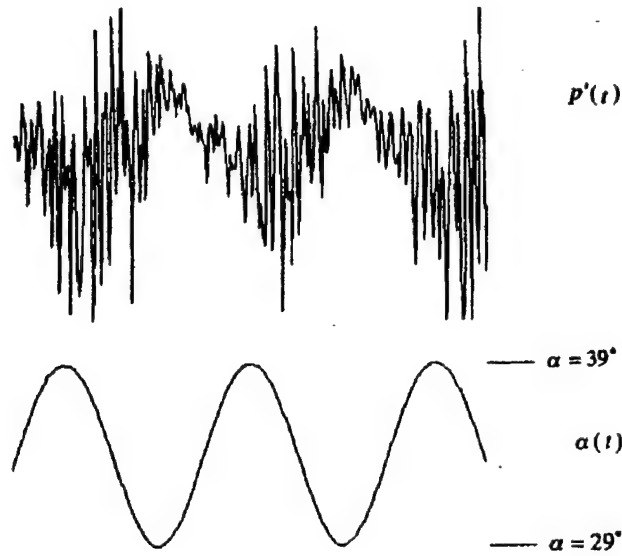


Figure 14. Pressure fluctuation and time history of angle of attack for a periodically pitching motion. Length of time record is 838ms; $x/c=0.55$, $y/s=0.5$, $k=0.35$.

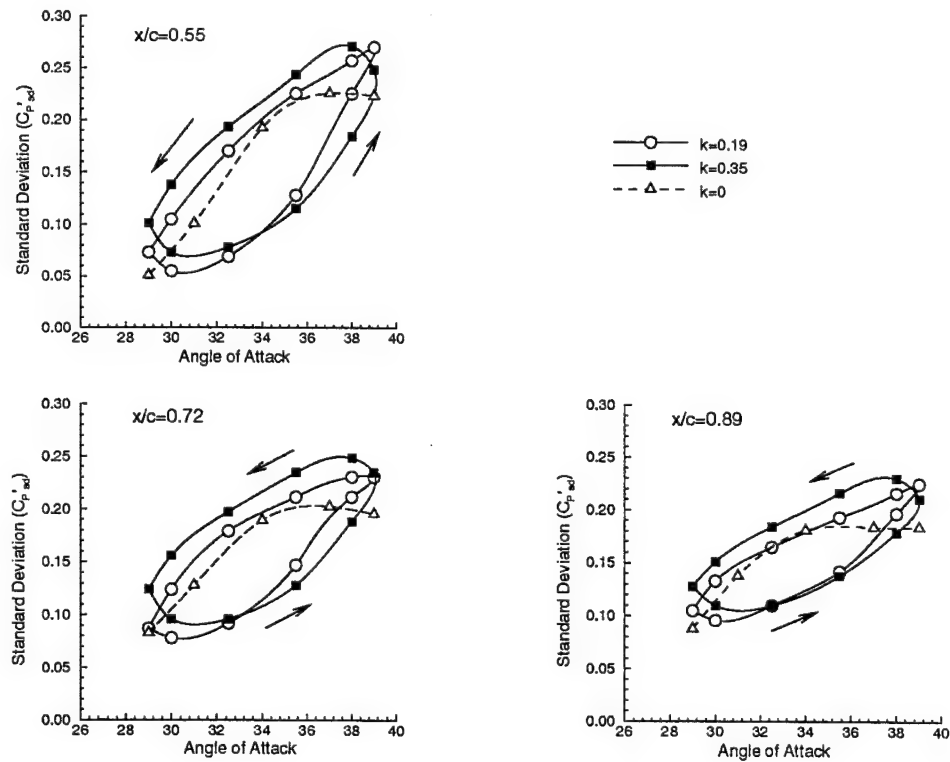


Figure 15. Variation of standard deviation as a function of angle of attack at different streamwise locations.

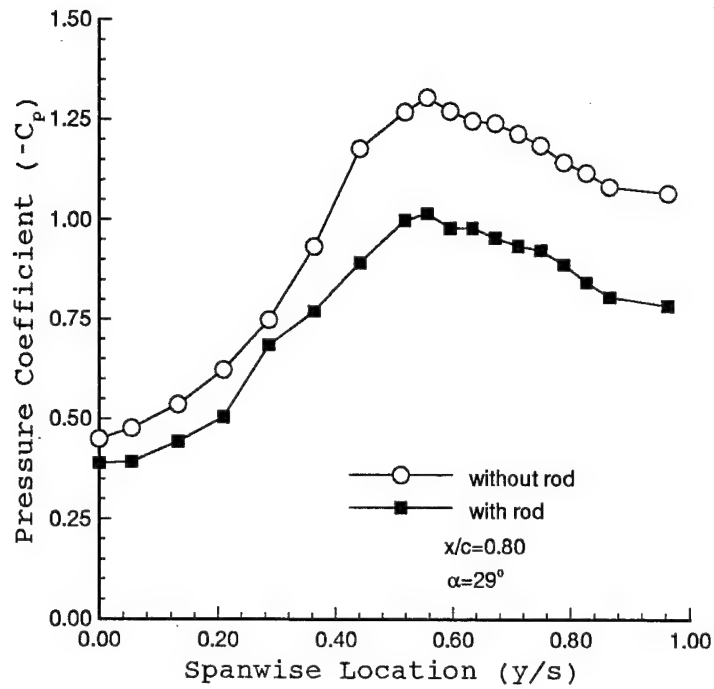


Figure 16. Mean pressure coefficient in spanwise direction.

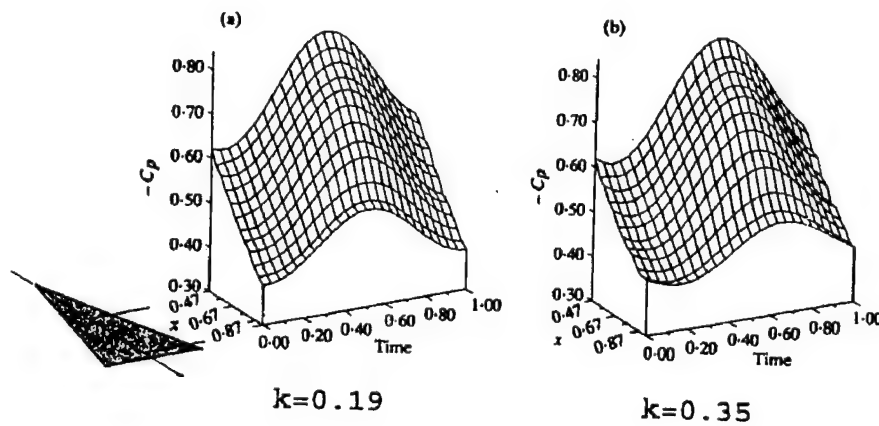


Figure 17. Variation of phase-averaged pressure along centerline.

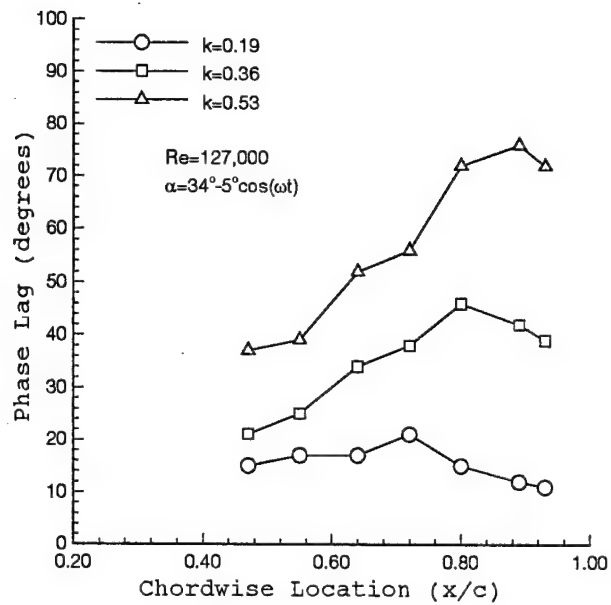


Figure 18. Phase lag as a function of chordwise location for $\alpha = 34^\circ - 5^\circ \cos \omega t$.

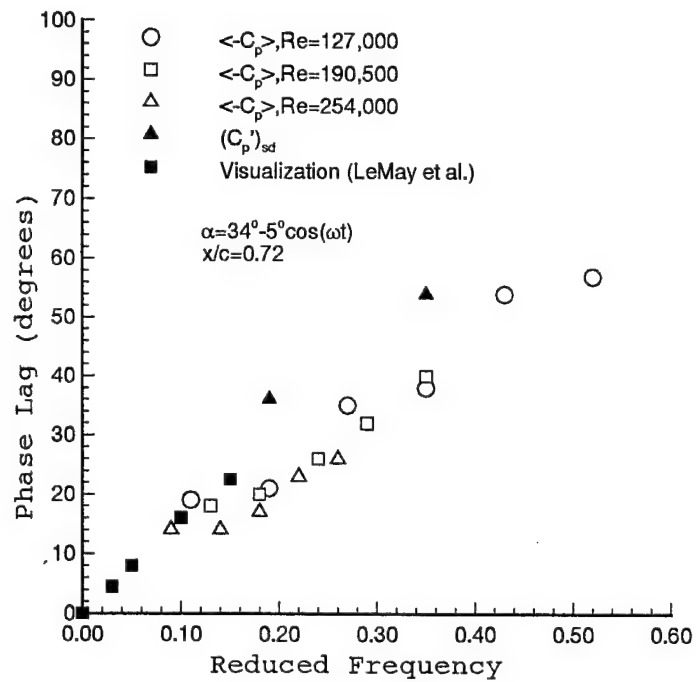


Figure 19. Phase lag as a function of reduced frequency, $x/c=0.72$.

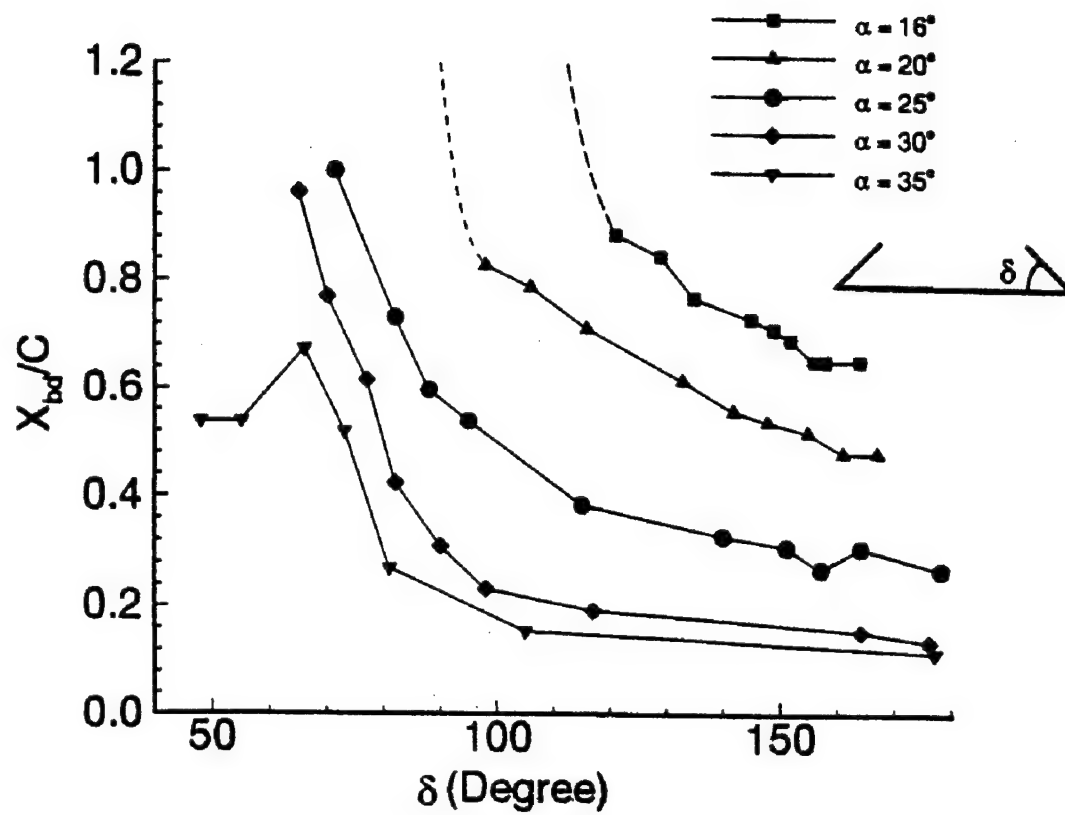


Figure 20. Variation of breakdown location as a function of flap angle for several values of angle of attack.

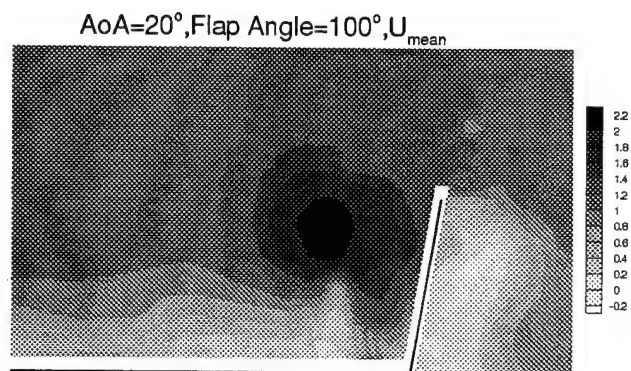
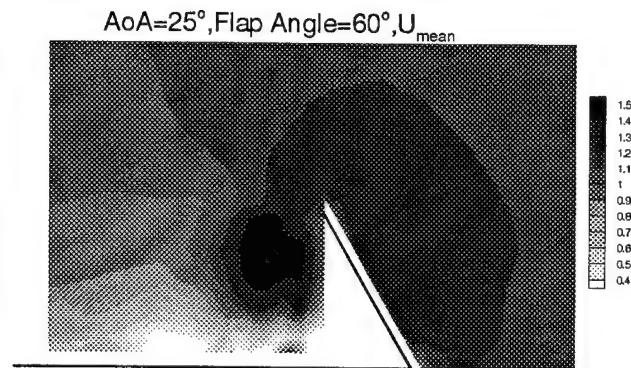
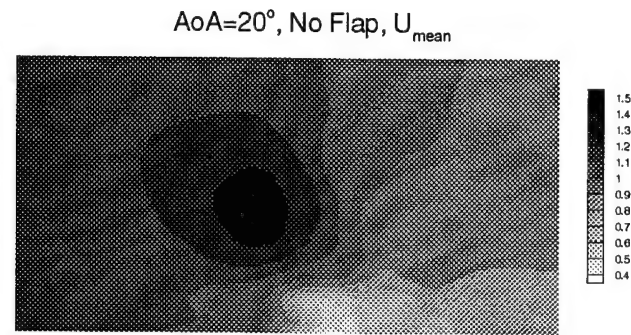


Figure 21. Constant contours of normalized axial velocity for $\delta=0^\circ$ (top, $\alpha=20^\circ$), $\delta=60^\circ$ (middle, $\alpha=25^\circ$), $\delta=100^\circ$ (bottom, $\alpha=20^\circ$).

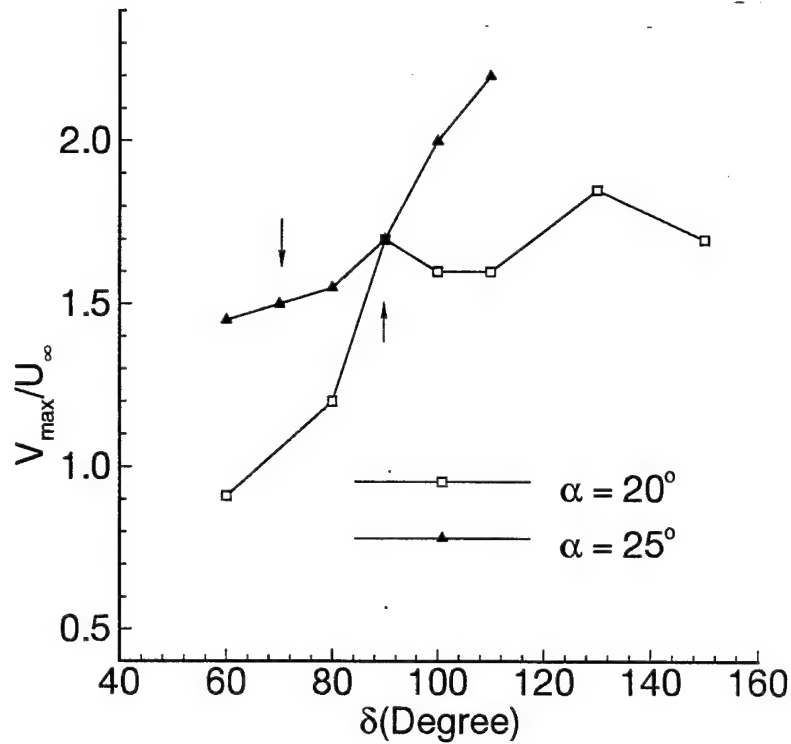


Figure 22: Variation of maximum swirl velocity as a function of flap angle for $\alpha=20^\circ$ and $\alpha=25^\circ$. The arrows indicate the flap angle at which breakdown is at the trailing-edge of the wing.

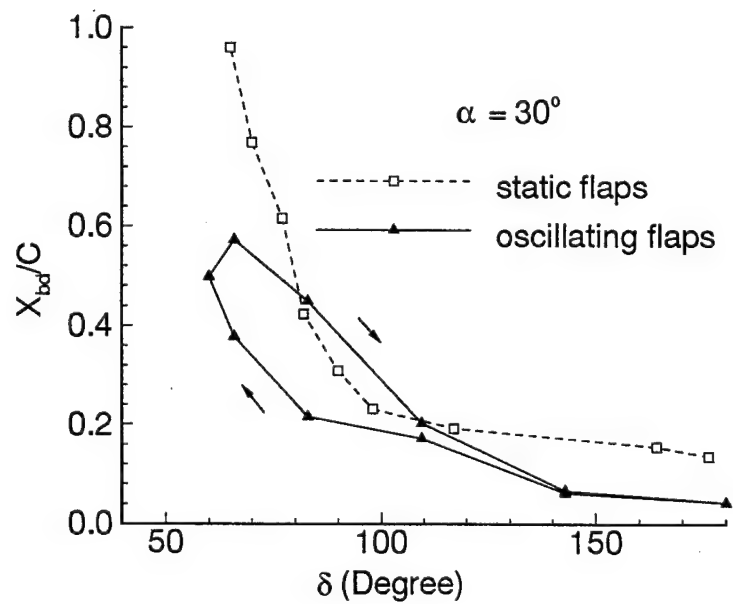


Figure 23: Variation of vortex breakdown location for harmonic variations of flap angle ($k=0.4$), and for static flaps ($\alpha=30^\circ$).

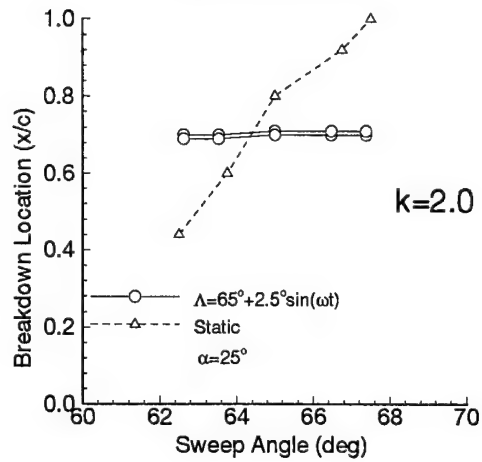
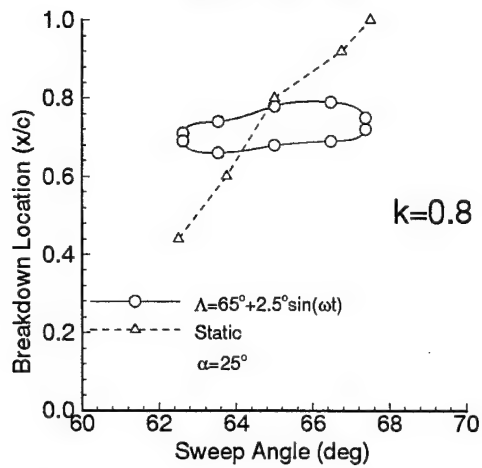
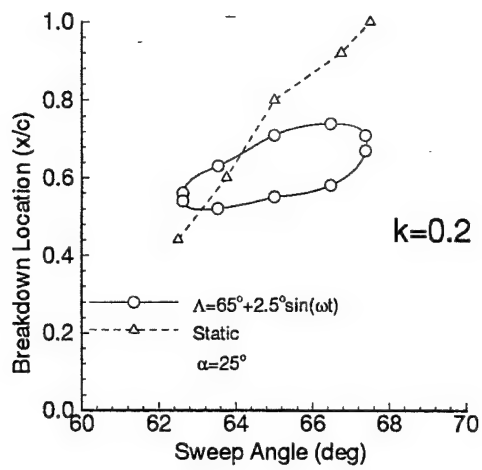


Figure 24: Variation of breakdown location for harmonic variations of sweep angle and for static case.

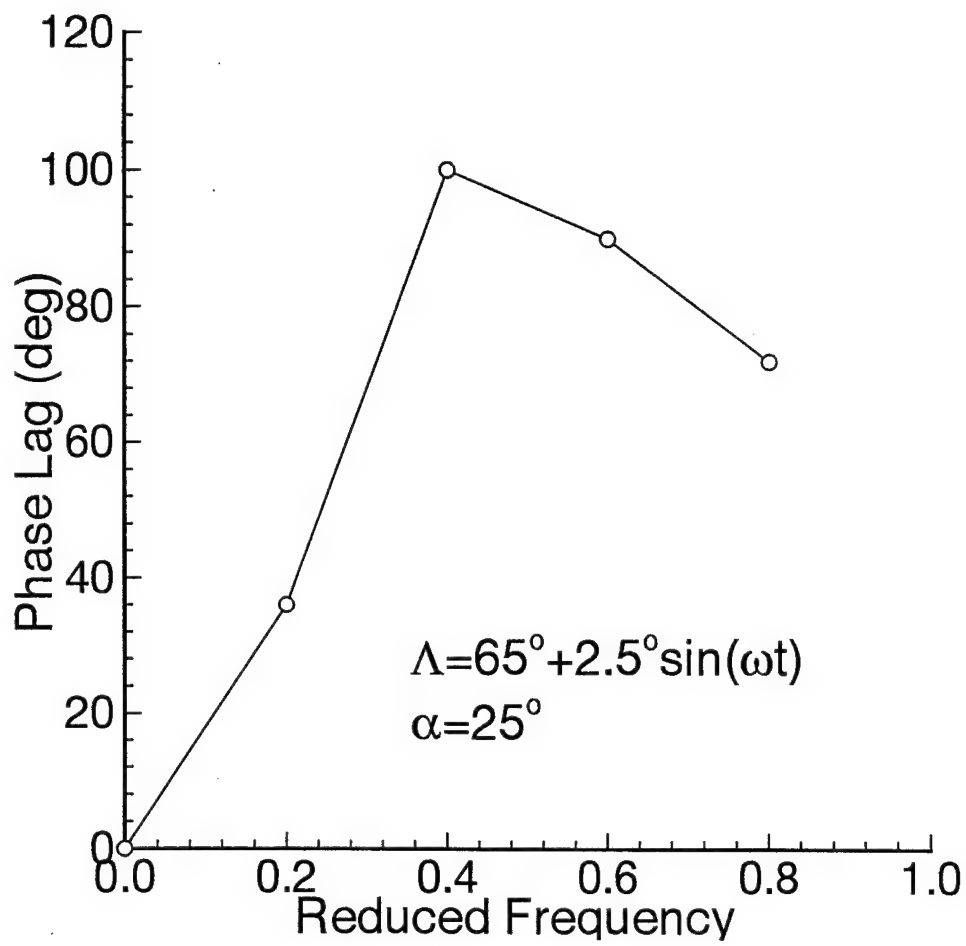
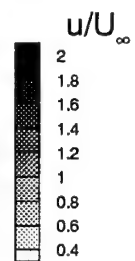
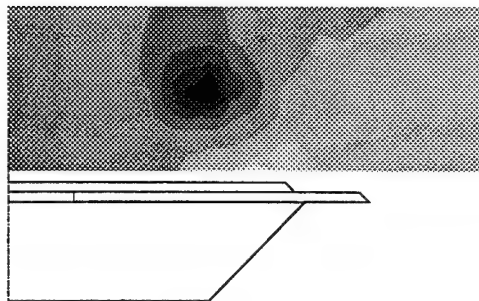
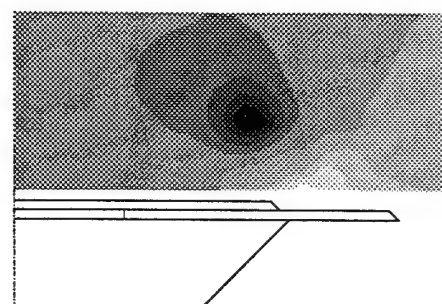
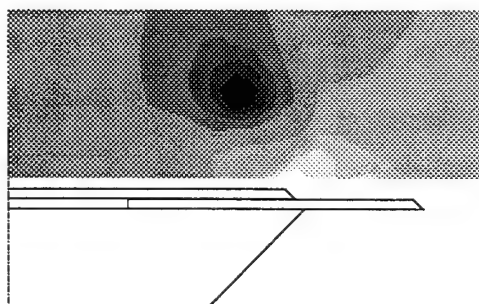


Figure 25: Variation of phase lag as a function of reduced frequency.

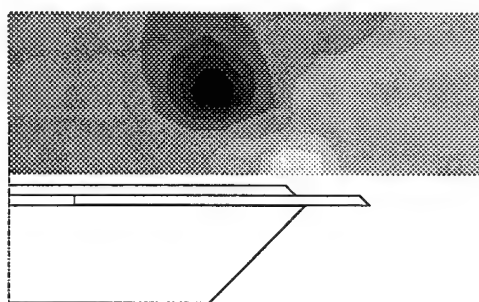
$\Lambda=66^\circ$



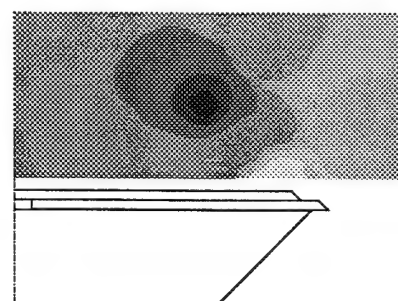
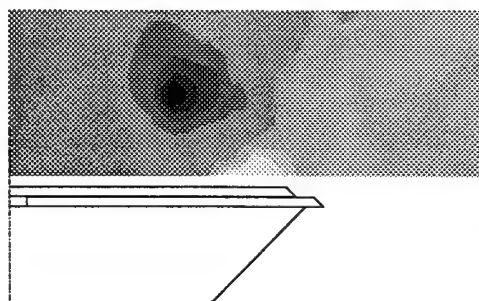
$\Lambda=63^\circ$



$\Lambda=66^\circ$



$\Lambda=69^\circ$



Dynamic

Static

Figure 26: Contours of axial velocity at different sweep angles.

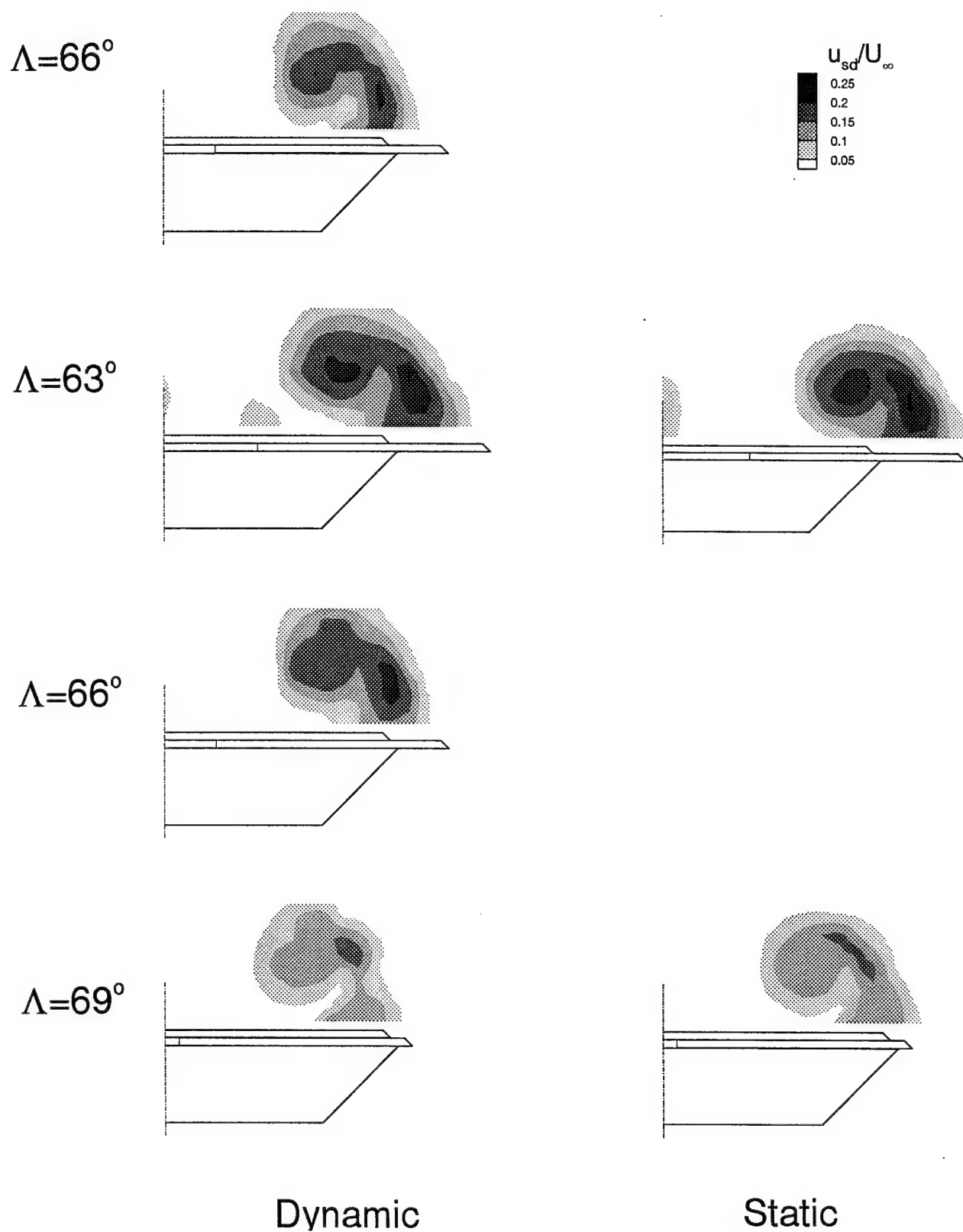


Figure 27: Contours of standard deviation and rms velocity (in the static case).

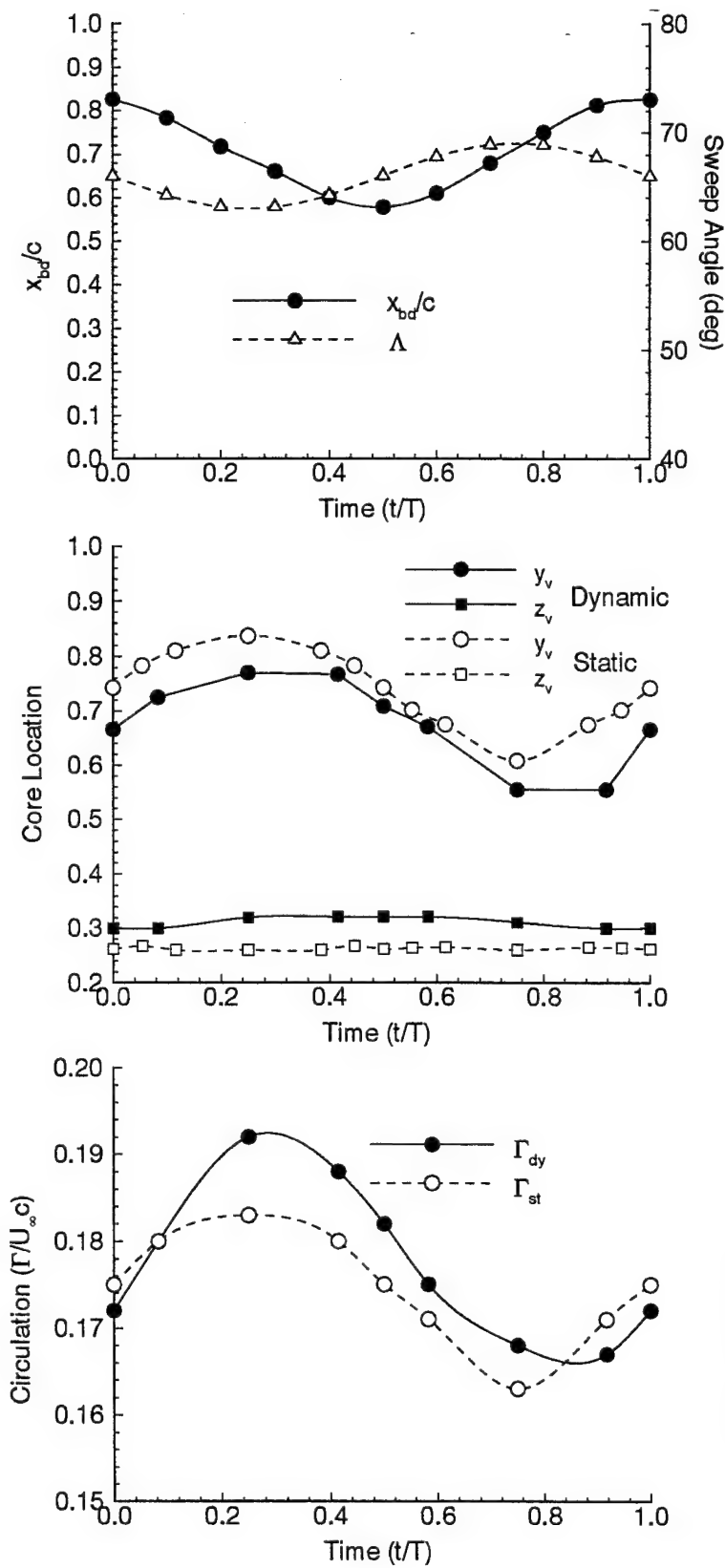


Figure 28. Variation of phase-averaged breakdown location, core location and circulation over a cycle.

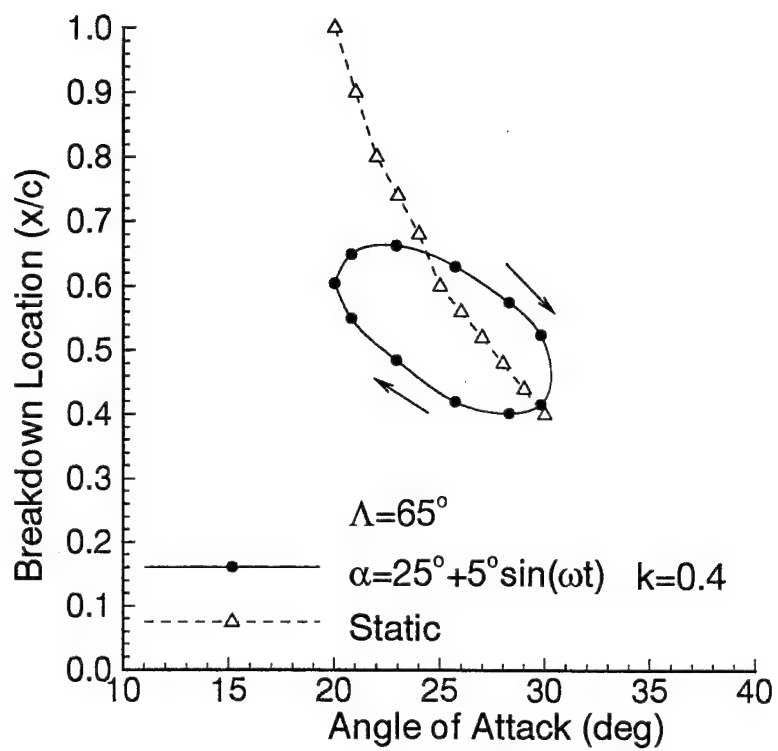


Figure 29: Variation of breakdown location for combined motion of pitching and variable sweep for different values of phase angle.

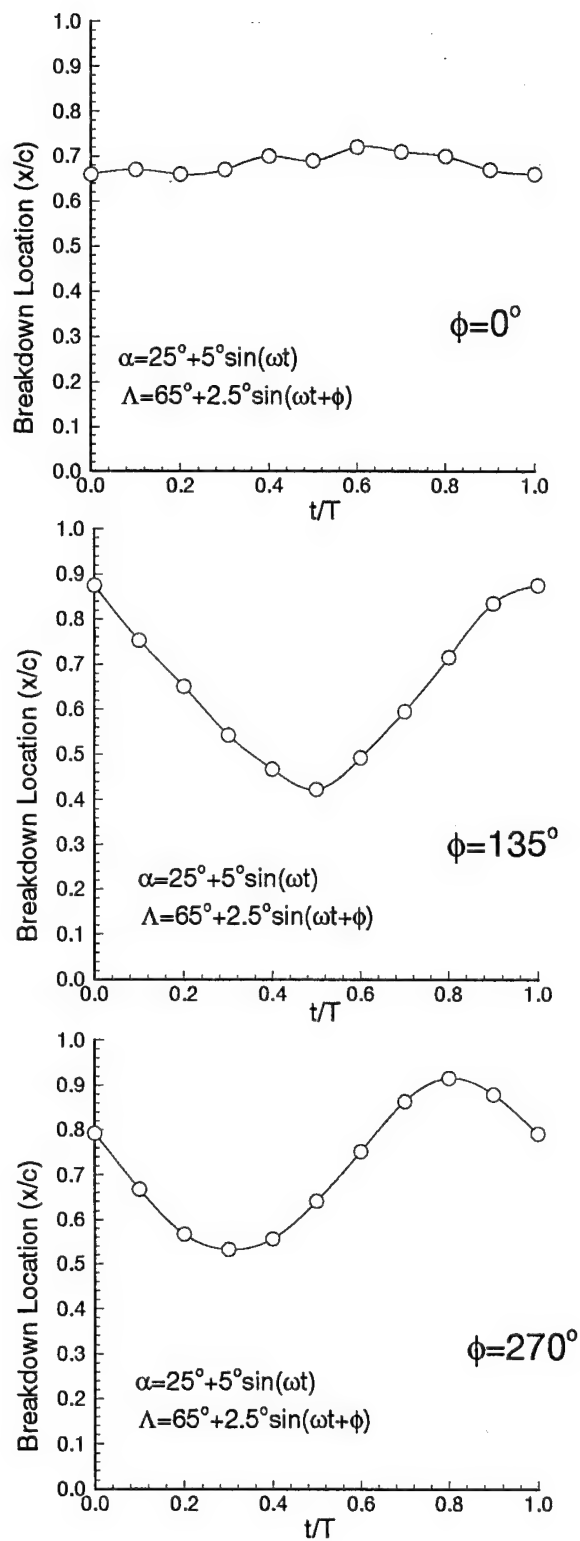


Figure 30. Variation of breakdown location for combined motion of pitching and variable sweep for different values of phase angle.

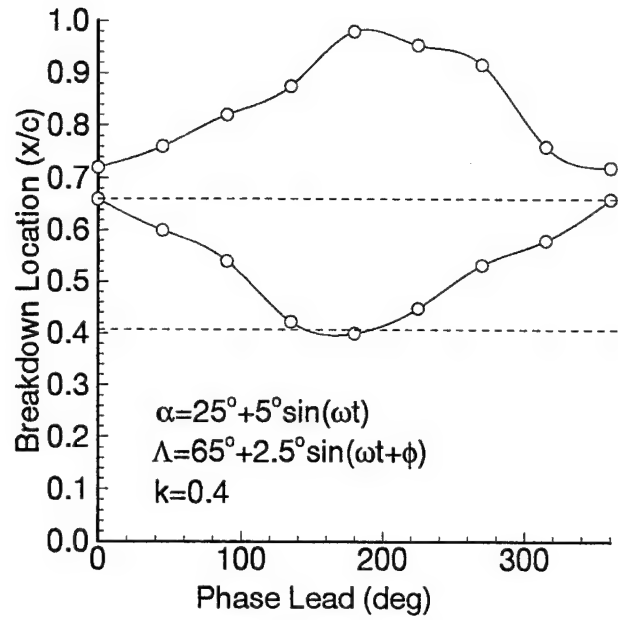


Figure 31: Maximum and minimum locations of breakdown as a function of phase angle. The dashed line is for pitching motion only for the average sweep angle.

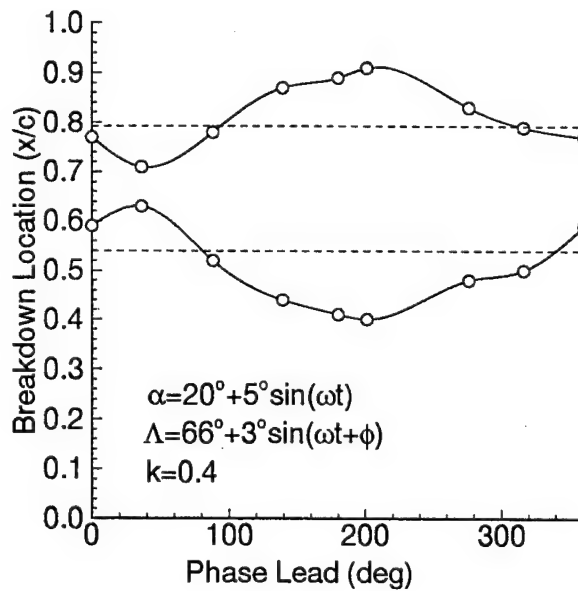


Figure 32: Maximum and minimum locations of breakdown as a function of phase angle. The dashed line is for pitching motion only for the average sweep angle.

Appendix A

Unsteady Flow Phenomena over Delta Wings at High Angle of Attack

Ismet Gursul*

University of Cincinnati, Cincinnati, Ohio 45221

Experiments show that coherent pressure fluctuations observed on delta wings are due to the helical mode instability of the vortex breakdown flowfield. No dominant frequency in the spectra of pressure fluctuations on the wing surface was observed after the breakdown reached the apex of the wing, although the vortex shedding could be detected in the wake. Measurements of pressure fluctuations at different streamwise locations on the wing suggest that the dimensionless frequency fx/U_∞ is nearly constant for a given geometry, which implies increasing wavelength in the streamwise direction. For different wings, this nondimensional frequency is shown to be a function of nondimensional circulation $\Gamma/U_\infty x$ only. Both the wavelength of the disturbances and the core radius increase with the nondimensional circulation at a fixed streamwise location. The wavelength normalized by the core radius is around 3–4, which is much smaller than the predictions for the Q vortex.

Nomenclature

c	= root chord
f	= frequency
k	= axial wave number
n	= azimuthal wave number
p	= pressure
q	= parameter for Q vortex
Re	= Reynolds number
r	= radial distance from vortex axis
r_0	= characteristic core size
s	= local semispan
U_∞	= freestream velocity
U_c	= phase speed
U_x	= axial velocity excess or deficit
V	= azimuthal velocity
W	= axial velocity
x	= chordwise distance from wing apex
y	= spanwise distance from wing root
z	= distance above wing surface
α	= angle of attack
Γ	= leading-edge vortex circulation
θ	= phase angle
Λ	= sweep angle
λ	= wavelength
ρ	= density
Φ	= phase angle
ϕ	= azimuthal angle
ω	= radial frequency

Introduction

ALTHOUGH interest in high angle-of-attack aerodynamics has increased, little is known about unsteady flow in vortex breakdown/postbreakdown flowfields. Sharply increased fluctuations in the normal-force coefficient for delta wings were observed when vortex breakdown moved over the wing.¹ Measurements of surface pressure fluctuations in the wake of breakdown showed coherent oscillations.^{2,3} Periodic oscillations were also observed in other swirling flows after breakdown occurred.^{4–7} Garg and Leibovich carried out LDV measurements in the wakes of breakdown in tubes and observed coherent oscillations. They suggested that the

measured frequencies correspond to the theoretical predictions found in Ref. 8 for the first helical mode ($n = -1$) of the time-averaged mean flow profiles, assuming that the oscillations are the disturbances with the maximum growth rate. [The disturbances are represented as $\exp[i(kx + n\phi - \omega t)]$, where ω is the frequency, k the wave number in the axial direction, and n the wave number (an integer) in the angular direction]. Thus, one possible source of the observed oscillations over delta wings is the hydrodynamic instability of breakdown wake.

On the other hand, based on the velocity measurements in the wake of a delta wing, vortex shedding was shown to occur.⁹ It was suggested that the alternate shedding at large angle of attack should induce asymmetry on the pressure distribution on the wing. The smallest angle of attack for which the periodic motion was detected was around 35 deg for the particular delta wing used. Although the authors do not report the location of vortex breakdown, it is estimated to be over the wing and close to the trailing edge.^{10,11} This suggests that vortex shedding may start when the breakdown moves over the wing. Although the time-averaged velocity measurements (for example, see Hummel¹²) reveal that the swirling flow persists in the wake of breakdown, little is known about the instantaneous flow structure. Since the axial convection of vorticity along the core is reduced after the breakdown, vortex shedding might start from the wing.

The purpose of this study is to investigate the characteristics of unsteady flow over delta wings of different sweep angle. The nature of coherent oscillations, their origin (helical mode instability vs vortex shedding), and their influence on unsteady loading will be discussed with the aid of measurements of pressure and velocity as well as flow visualization.

Experimental Setup

The experiments were carried out in an open-circuit wind tunnel having a cross section of 305 mm \times 305 mm. The flow entered through a 9.5:1 contraction section with honeycomb and screens, passed through the test section, and was exhausted by an axial fan. The turbulence intensity in the test section was about 0.25%. The freestream velocity spectrum was free from any sharp peaks. The angle of attack of the wings could be varied continuously from outside the tunnel.

Pressure and velocity measurements were made for four delta wings with sweep angles $\Lambda = 60, 65, 70$, and 75 deg. The chord lengths ranged from 120 mm to 150 mm, and the models were constructed of 9.5-mm-thick PVC. The lee surfaces were flat whereas the leading edges were beveled at 45 deg on the windward side. The models were sting mounted. The measurements were done at Reynolds numbers based on the chord length equal to 25,000–

Received Dec. 16, 1992; revision received June 1, 1993; accepted for publication June 2, 1993. Copyright © 1993 by Ismet Gursul. Published by the American Institute of Aeronautics and Astronautics, Inc., with permission.

*Assistant Professor, Department of Mechanical, Industrial, and Nuclear Engineering.

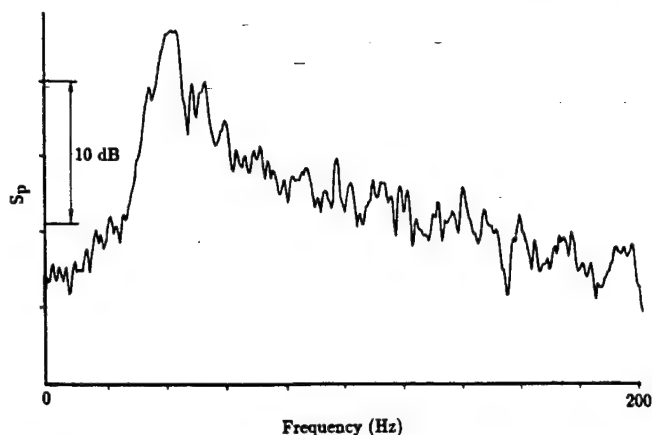


Fig. 1 Spectrum of pressure fluctuations at $x/c = 0.89$, $y/s = 0.42$, $\alpha = 35.3$ deg, $\Lambda = 70$ deg; vertical scale is logarithmic.

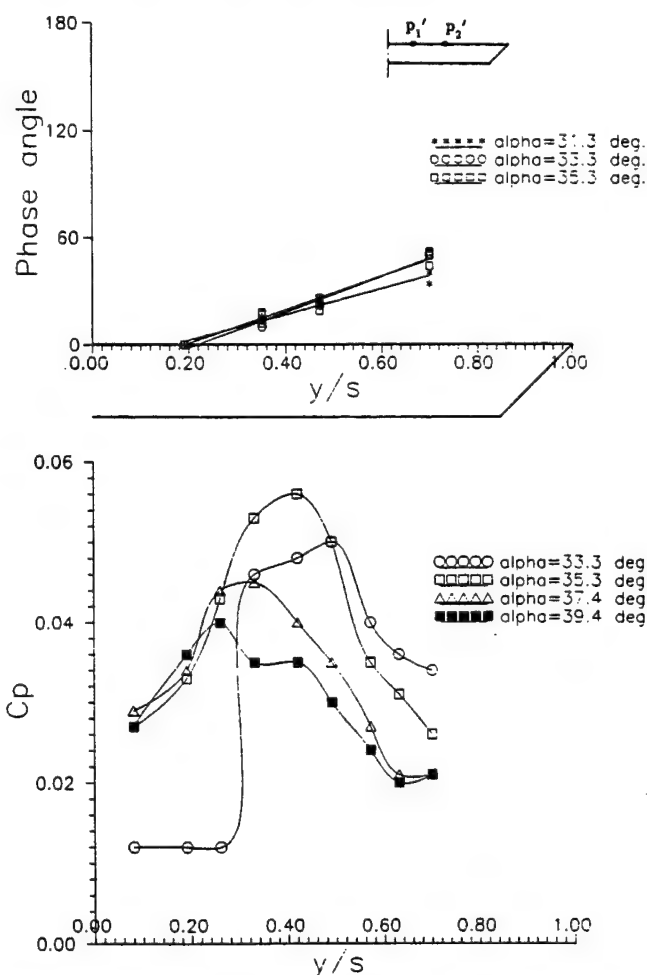


Fig. 2 Phase delay between the pressure fluctuations measured at points 1 and 2; point 1 is fixed, while the location of point 2 is varied (top). Variation of the amplitude of pressure fluctuations (bottom), $\Lambda = 70$ deg.

100,000, although most of the results reported here correspond to $Re = 100,000$. At the largest angle of attack, the blockage ratio was 0.094. A piezoelectric pressure transducer (PCB, model 103A) was used to measure the fluctuating pressure on the wing surface. The transducer has been flush mounted at the surface. The transducer and its leads were housed in the grooves running either along a ray from the apex to the trailing edge (at 40–60% of the local semispan, depending on the sweep angle) or along the spanwise direction. The pressure sensing part of the transducers had a diameter of 2.54 mm. Two pressure transducers were used for

simultaneous measurements in the spanwise and streamwise directions. A hot-wire probe was used to obtain the spectra of the velocity fluctuations over the wing and in the wake. Pressure and velocity signals were processed by a two-channel signal analyzer (HP 35660A). Smoke-wire visualization by a 0.1-mm-diam stainless steel wire, and the smoke injected near the apex provided information on the flow structure and vortex breakdown location. A light source consisting of two 600-W lamps was used to illuminate the flowfield. In addition to the still pictures taken, flow visualization was videotaped at low speeds. The measurement uncertainty for dimensionless pressure coefficient ranged from 10% to 0.6%, whereas the uncertainty for frequency and breakdown location were estimated as 1.4% and 3%, respectively.

Results

When the vortex breakdown moved over the wing, the pressure fluctuations exhibited coherent oscillations. An example of pressure fluctuation spectrum for sweep angle $\Lambda = 70$ deg, at an angle of attack $\alpha = 35.3$ deg is shown in Fig. 1. The measurement was taken at $x/c = 0.89$, $y/s = 0.42$ (where s is the local semispan) and the vortex breakdown location was $x_b/c \approx 0.3$. A sharp peak in the spectra was always observed in the wake of breakdown location, regardless of angle of attack and sweep angle for all of the delta wings tested. In the Reynolds number range investigated, the dimensionless dominant frequency fc/U_∞ seemed to be independent

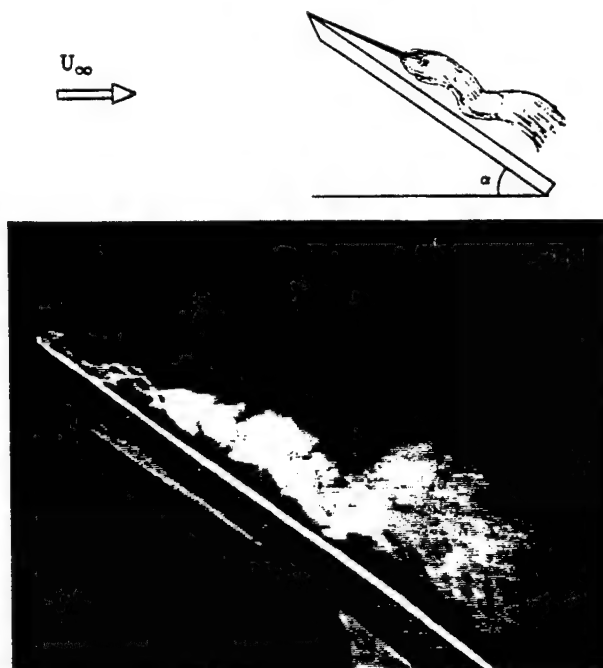


Fig. 3 Smoke visualization showing helical instability in the breakdown region ($\alpha = 35$ deg, $\Lambda = 70$ deg), $Re = 15,000$.

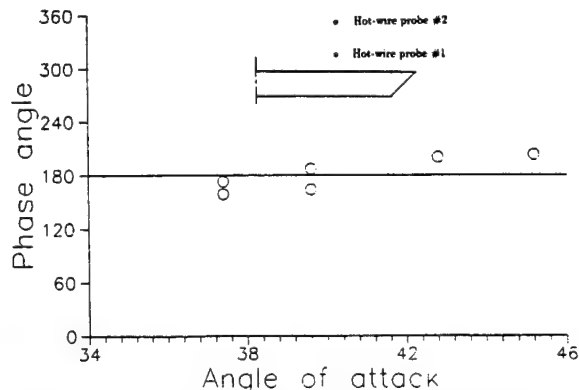


Fig. 4 Phase angle between the two hot-wire signals, $\Lambda = 75$ deg, $x/c = 0.89$.

of the Reynolds number. To understand the nature of these oscillations, measurements were taken with two pressure transducers located in the spanwise direction. Cross-spectral analysis provided the phase angle between the pressure fluctuations measured with the two transducers. If the pressure fluctuations are represented as $\cos(\omega t)$ and $\cos(\omega t - \theta)$ at points 1 and 2, respectively, the phase angle θ is shown in Fig. 2 together with the amplitude ($C_p = p'_{rms} / \frac{1}{2} \rho U_\infty^2$) distribution in the spanwise direction. In measuring the phase angle, the location of point 1 was fixed while the location of point 2 was varied. Increase in phase delay toward the leading edge is consistent with the direction of rotation in the vortex. The vortex shedding from the leading edge cannot cause this variation of the phase delay. Instead, the trend would likely be opposite (i.e., decreasing phase lag toward the leading edge). Thus, the evidence suggests that the oscillations may be due to the helical mode instability. Indeed, the flow visualization obtained by releasing smoke near the apex shows this type of instability (Fig. 3). In addition, the azimuthal wave number was estimated from the phase angle between the signals from two hot-wire probes located at $y/s = 0.5$ and $z/s = 0.25$ and $y/s = 0.5$ and $z/s = 0.75$. With respect to the vortex axis, these locations are approximately 180 deg apart. The probes were oriented so as to be most sensitive to tangential and axial velocities. The phase angle is shown in Fig. 4 for several values of angle of attack, which suggests that the azimuthal wave number is $n = 1$.

These results are consistent with the predictions of the linear stability theory.⁸ Lessen et al. carried out their calculations for a jet-like axial velocity profile and showed that the flow is most sensitive to the disturbances with negative azimuthal wave numbers ($n < 0$). Translation and inversion of the axial velocity profile does not affect the growth rate within the temporal analysis. However, the azimuthal wave number changes its sign.¹³ Therefore, for a wake-like profile such as found in breakdown region, the most unstable modes are the ones with positive azimuthal wave numbers ($n > 0$), which represent disturbances rotating in the same direction as the vortex. This is in agreement with the findings in Fig. 2. The theory cannot predict which azimuthal wave number will be amplified. However, experiments in a tube⁴ and tip vortex⁷ showed that $n = 1$. This is also in agreement with the present results (see Fig. 4). The $|n| = 1$ mode is necessary for a streakline released on the axis to take a helical shape,⁴ since the radial velocity component must be zero on the axis for all modes except $|n| = 1$. In the breakdown region shown in Fig. 3, the large-scale helical shape of smoke, which is originated from the axis, is an evidence of the helical mode instability. Since the disturbances with $n = 1$ will have a phase function $(kx + \phi - \omega t)$, one expects velocity/vorticity to be periodical in the x direction and be antisymmetric with

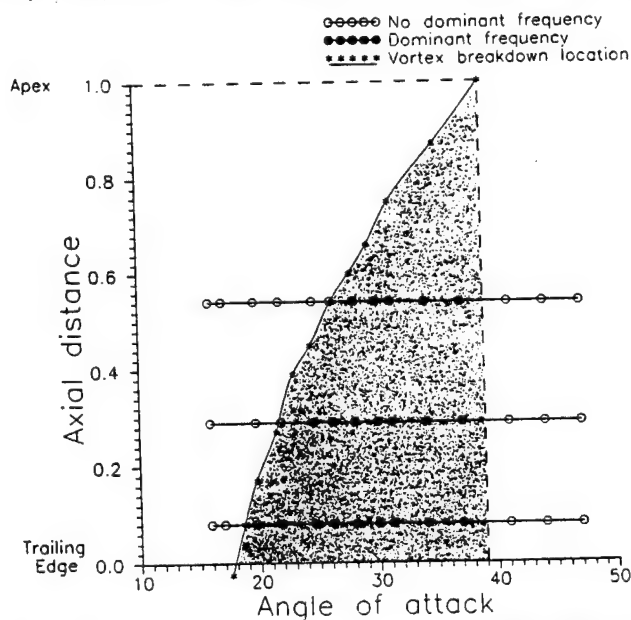


Fig. 5 Domain over which dominant frequency was observed for $\Lambda = 65$ deg.

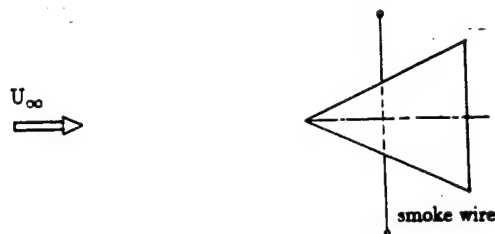


Fig. 6 Vortex shedding at large angle of attack ($\alpha = 60$ deg), $\Lambda = 60$ deg and $\Lambda = 75$ deg, $Re = 15,000$.

respect to the vortex axis. Indeed, the instantaneous azimuthal vorticity in a plane through the vortex axis¹⁴ shows that vorticity concentrations form the two rows of periodic structures located on either side of the axis with an antisymmetric configuration, resembling the well-known Karman vortex street.

With increasing angle of attack, the pressure spectra became free from any sharp peaks. The domain over which a sharp peak was observed in the spectrum for the wing with sweep angle $\Lambda = 65$ deg is shown in Fig. 5. A dominant frequency was observed at the measurement stations downstream of breakdown location, until the breakdown reached the apex of the wing. When the angle of attack is larger than the one that corresponds to the breakdown location at apex, no oscillations were observed in pressure fluctuations. The measurements for other wings gave results similar to Fig. 5. Thus, it is concluded that, until the breakdown reaches the apex of the wing, swirling flow persists over the wing and hydrodynamic instability of this flow is the only source of the unsteady loading on the wing. For larger angles of attack, the shear layer separated from the leading edge will not be able to form a swirling flow with axial motion. Thus, at large angle of attack, the vortex shedding from the wing starts as shown in Fig. 6. Whereas the shedding seems symmetric for the large aspect ratio wing, alternate shedding becomes dominant for the low aspect ratio wing. A

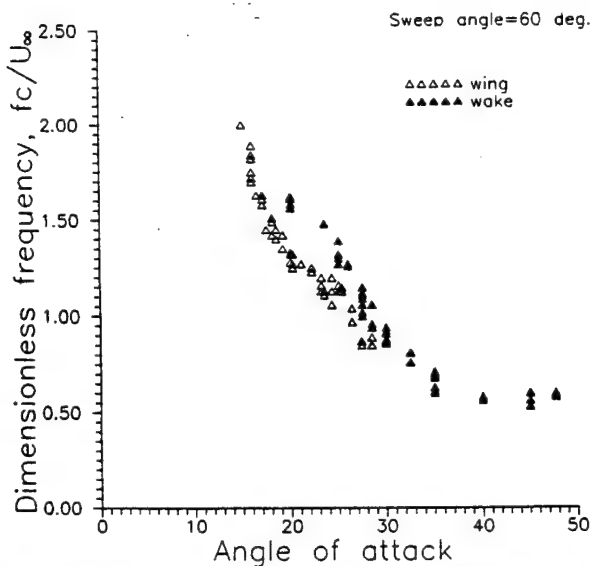


Fig. 7 Variation of dimensionless dominant frequency on the wing ($x/c = 0.89$) and at one chord length downstream of trailing edge as a function of angle of attack, $\Lambda = 60$ deg.

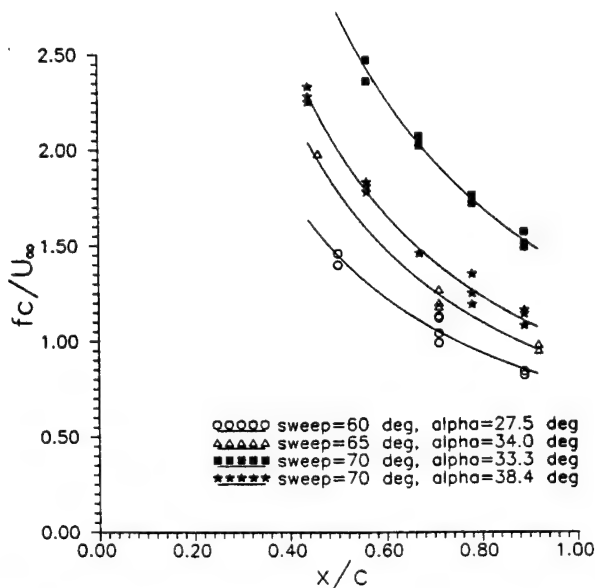


Fig. 8 Variation of dimensionless frequency fc/U_∞ as a function of streamwise distance.

signal from a hot-wire probe located at one chord length from the trailing edge was used to monitor unsteady flow in the wake. Dominant frequency detected in the wake was compared with the dominant frequency detected by the pressure transducer located near the trailing edge ($x/c = 0.89$) in Fig. 7. Until the breakdown location reaches the apex ($\alpha = 30$ deg for the wing with sweep angle $\Lambda = 60$ deg), both signals have the dominant frequency of the helical mode instability, although the frequencies differ slightly. This may be due to the streamwise gradients of the mean flow in the wake. Since no coherent pressure oscillations on the wing due to vortex shedding was detected (see also Fig. 5), this suggests that unsteady loading on the wing due to vortex shedding is negligible. After the helical mode instability disappears, vortex shedding frequency is detected in the wake. Although the relationship between the dominant frequency in the wake and angle of attack seems a continuous curve, it covers two different flow regimes. Indeed, in the vortex shedding regime, the frequency is pretty much constant. Similar trend was observed for a wing with $\Lambda = 76$ deg in other experiments.⁹

Measurements of pressure at different streamwise locations on the wing upper surface showed that the dominant frequency is not constant, but depends on the distance from the apex. Examples of variation of dimensionless frequency fc/U_∞ as a function of the streamwise distance for different wings is shown in Fig. 8. The scatter in the data is believed to be due to fluctuations in the breakdown location. It is well known that vortex breakdown location exhibits irregular variations. The dominant frequency decreases with increasing distance. This was also noticed by Roos and Kegelmann³ (for a wing with $\Lambda = 70$ deg and $\alpha = 33$ deg); moreover, it was shown that if the frequency is normalized with the distance x , the dimensionless frequency fx/U_∞ is nearly constant. This was attributed to disturbances rotating in the vortex core whose radius grows linearly with x . The variation of fx/U_∞ corresponding to the data in Fig. 8 is shown in Fig. 9. It seems that fx/U_∞ is nearly constant for a given Λ and α for all delta wings tested. Since the disturbances are shown to be helical waves, this implies that the wavelength increases with x . Indeed, the instantaneous azimuthal vorticity in a plane through the vortex axis, which was recently obtained by a particle image velocimetry technique,¹⁴ clearly shows vorticity concentrations with increasing wavelength between them. The instantaneous azimuthal vorticity concentrations seem to be located

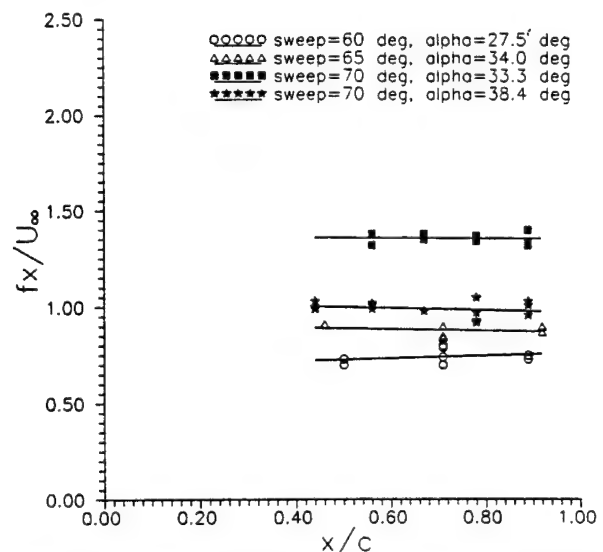


Fig. 9 Variation of dimensionless frequency fx/U_∞ as a function of streamwise distance.

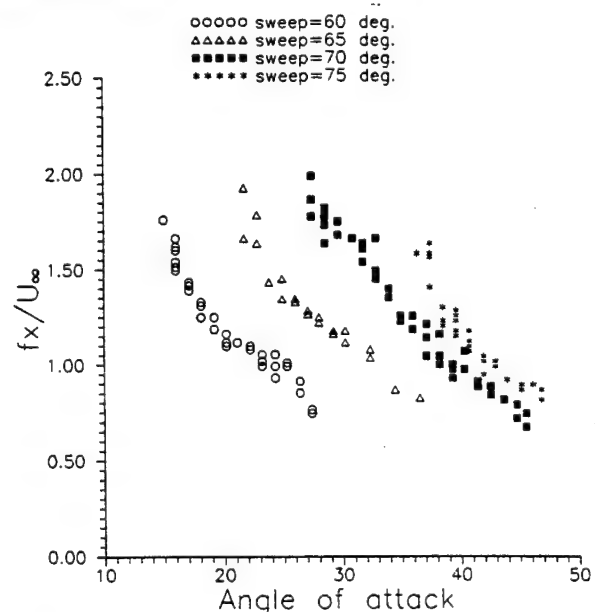


Fig. 10 Variation of dimensionless frequency fx/U_∞ as a function of angle of attack for different values of sweep angle.

on a cone. Moreover, the time-averaged velocity profile in the breakdown region was shown to be a function of r/x , indicating that the mean flow is conical.³ Thus, the wavelength of the disturbance is expected to increase linearly with x in a conical mean flowfield.

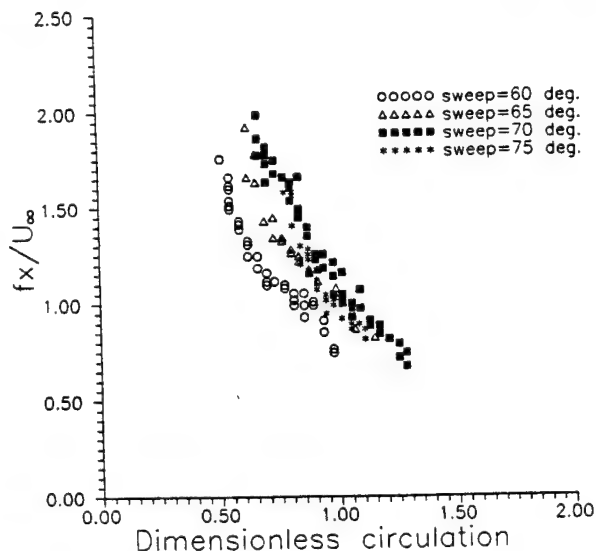


Fig. 11 Variation of dimensionless frequency f_x/U_∞ as a function of dimensionless circulation $\Gamma/U_\infty x$.

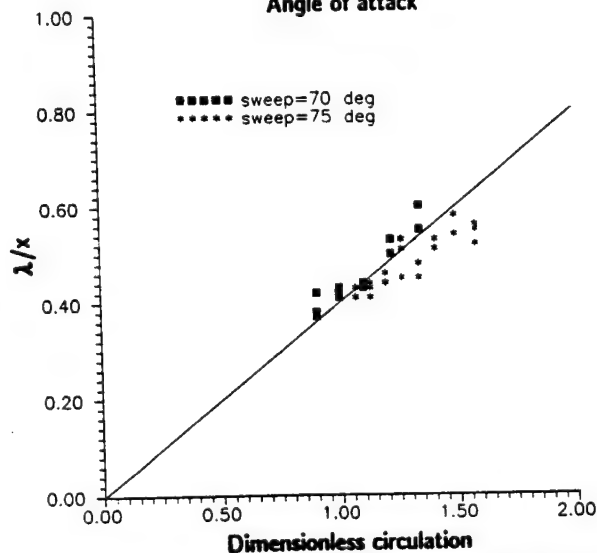
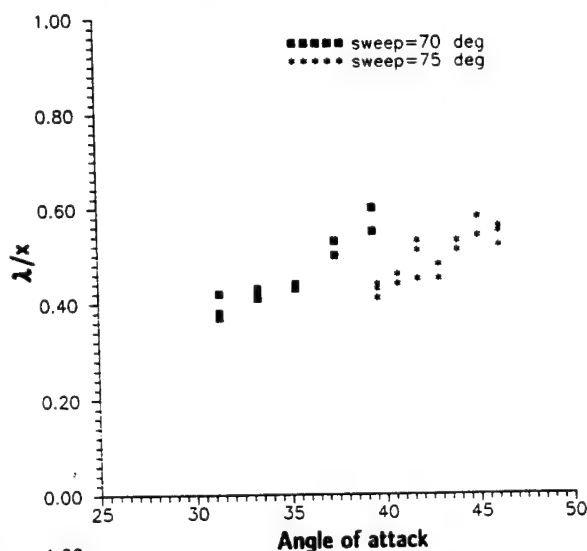


Fig. 12 Variation of normalized wavelength λ/x as a function of angle of attack (top) and dimensionless circulation (bottom), $x/c = 0.85$.

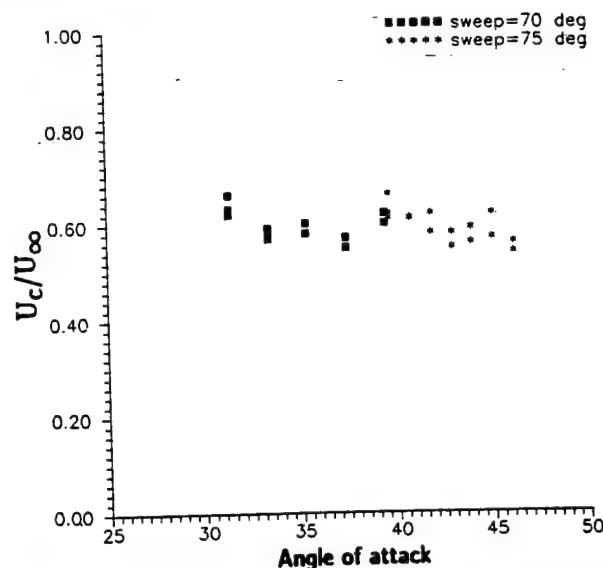


Fig. 13 Variation of phase speed as a function of angle of attack.

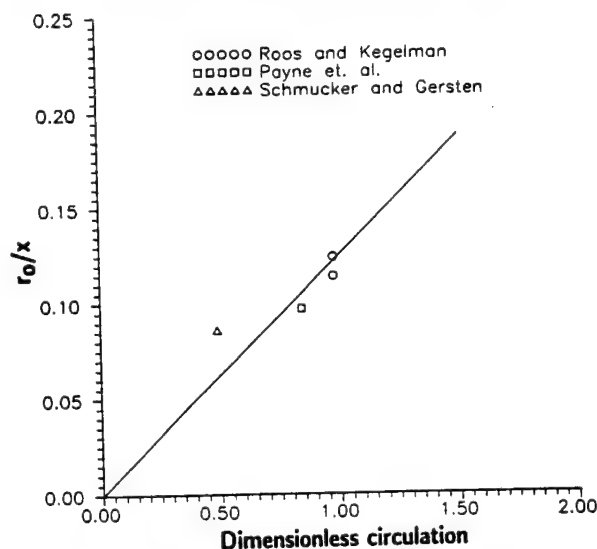


Fig. 14 Variation of normalized core radius r_0/x as a function of dimensionless circulation.

Having verified that f_x/U_∞ is nearly constant for a given geometry (angle of attack and sweep angle), the variation of the dimensionless frequency is shown in Fig. 10 as a function of angle of attack for the four wings tested. The range of the data is nearly the same for different wings. This suggests that a single relationship can be obtained if a unique parameter is found. The circulation of the leading-edge vortex is considered, which depends on both angle of attack α and sweep angle Λ . Experiments on vortex breakdown over delta wings in steady³ and unsteady freestream,¹⁵ as well as on trailing vortices,¹⁶ showed that the overall circulation is affected only very slightly after burst, although the vorticity concentration changes dramatically. Thus, it is reasonable to assume that the circulation continues to grow linearly, even after breakdown, because of continuous feeding of vorticity from leading edge. The dimensional analysis for the four variables Γ , U_∞ , f , and x shows that two nondimensional numbers can be found and a single relationship exists,

$$\frac{f_x}{U_\infty} = F\left(\frac{\Gamma}{U_\infty x}\right) \quad (1)$$

Since the circulation grows linearly with x , the dimensionless number $\Gamma/U_\infty x$ does not depend on x . The circulation for a given

angle of attack and sweep angle was estimated by using a slender wing theory.¹⁷ Figure 11 shows that all of the curves collapse except for $\Lambda = 60$ deg. Since the method used to calculate circulation is a good approximation for low aspect ratio wings, the discrepancy for $\Lambda = 60$ deg is believed to be due to the incapability of the method to estimate the circulation.

The wavelength of the disturbance was measured by two pressure transducers located in the streamwise direction. From the phase measurements obtained by the cross-spectral analysis, the wavelength was calculated as $\lambda = 2\pi/(\partial\Phi/\partial x)$, where Φ is measured in radians. Typical distance between the transducers was $\Delta x/c = 0.066$, corresponding to $\Delta x/\lambda = 0.13$. The midpoint between the transducers was located near the trailing edge ($x/c = 0.85$). Based on the previous results, the wavelength is expected to be linearly changing with x in the conical mean flowfield. The variation of λ/x as a function of angle of attack and dimensionless circulation is shown in Fig. 12. In addition, the variation of the phase speed $U_c = f\lambda$ is shown in Fig. 13. The quantity λ/x seems to be a linear function of the dimensionless circulation. A linear curve fit provided the following relation:

$$\frac{\lambda}{x} = 0.4 \frac{\Gamma}{U_\infty x} \quad (2)$$

Since the normalized convection speed U_c/U_∞ seems to be independent of the dimensionless circulation, it can be shown that

$$\frac{\lambda}{x} = \frac{U_c}{fx} \sim \frac{U_\infty}{fx} = \frac{1}{(fx/U_\infty)}$$

and using Eq. (2)

$$\frac{\lambda}{x} \sim \frac{1}{(fx/U_\infty)} \sim \frac{\Gamma}{U_\infty x}$$

Hence,

$$\frac{fx}{U_\infty} \sim \left(\frac{\Gamma}{U_\infty x} \right)^{-1} \quad (3)$$

Indeed, a curve fit to the data shown in Fig. 11 gives the following relationship:

$$\frac{fx}{U_\infty} = 1.038 \left(\frac{\Gamma}{U_\infty x} \right)^{-0.98}$$

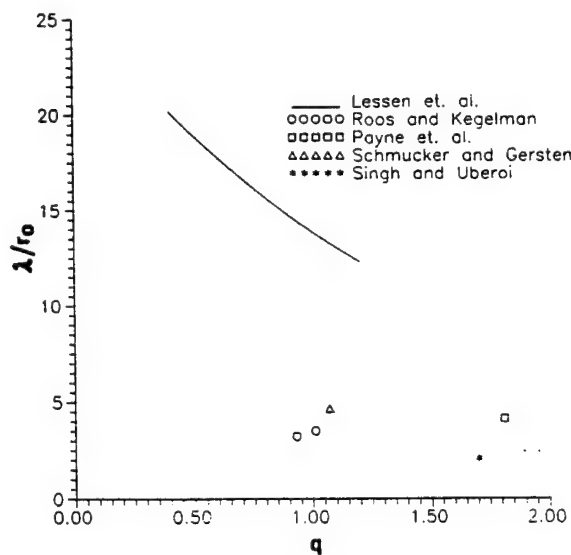


Fig. 15 Variation of λ/r_0 as a function of parameter q .

Lessen et al.⁸ calculated the most unstable wavelength for the first helical mode of the following time-averaged mean flow:

$$\begin{aligned} V/U_s &= \frac{q}{r/r_0} [1 - \exp(-r^2/r_0^2)] \\ W/U_s &= \exp(-r^2/r_0^2) \end{aligned} \quad (4)$$

where the circulation is $\Gamma = 2\pi q r_0 U_s$. This is known as Q vortex and the parameter q is directly proportional to the circulation and inversely proportional to the axial velocity excess or deficit U_s . The maximum swirl speed occurs at $r = 1.122 r_0$. Therefore, the parameter r_0 can be taken as the characteristic core size. The most unstable wavelength λ/r_0 for the first helical mode was calculated by Lessen et al.⁸ for several values of the parameter q . The core radius r_0 is expected to be a linear function of x in the conical flow over delta wings. From a limited number of mean velocity measurements,^{3,18,19} r_0/x was estimated and is shown in Fig. 14. The data suggests that the core radius increases with the increasing swirl level, which was predicted for a trailing vortex²⁰ and swirling flows in tubes.²¹ Although the data is very limited, there is a trend of a linear relationship between r_0/x and $\Gamma/U_\infty x$. This together with Eq. (2) suggests that the normalized wavelength λ/r_0 is roughly constant as is expected in a conical flowfield. The variation of λ/r_0 with the estimated parameter q is shown in Fig. 15, which indicates that the disturbances have a much smaller wavelength than the predictions for the Q vortex. This may be due to slowly varying mean flow in the streamwise direction. Garg and Leibovich⁴ showed that the measured frequencies in vortex-tube experiments agree very well with the temporal stability predictions for the Q vortex, assuming that the disturbances have the wavelength and phase speed corresponding to the maximum growth rate. On the other hand, the experimental result for a trailing vortex⁷ (for which the streamwise gradient is also negligible) is closer to the results for leading-edge vortex over delta wings. The discrepancy between the predictions for Q vortex and the present experimental results remains to be explained.

Conclusions

Experiments showed that coherent pressure fluctuations are observed on delta wings as long as vortex breakdown is over the wing. Cross-spectral analysis of two-point pressure and velocity measurements as well as flow visualization confirm that these oscillations are in the form of helical waves with azimuthal wave number $n = 1$, which is the result of the instability of swirling breakdown wake flow. The source of unsteady loading on the wing is due to this helical mode instability as opposed to vortex shedding which starts after the breakdown reaches the apex of the wing. Vortex shedding takes the form of symmetric or alternate depending on the aspect ratio of the wing. The influence of vortex shedding on unsteady pressure fluctuations is negligible and could not be detected in the experiments, although the velocity fluctuations in the wake show coherent oscillations.

Measurements of unsteady pressure at different streamwise locations on the wing surface showed that the dimensionless frequency fx/U_∞ is nearly constant for a fixed angle of attack and sweep angle. Based on the results from this work and other experiments, it is suggested that the wavelength of the disturbances increases linearly with x in the conical mean flowfield, resulting in constant fx/U_∞ . The nondimensional frequency is found to be a function of nondimensional circulation $\Gamma/U_\infty x$ only, where the circulation was calculated by assuming conical flow and using a slender-wing theory.

Measurements of the wavelength and phase speed indicates that λ/x increases with increasing $\Gamma/U_\infty x$, whereas the phase speed is roughly constant $U_c/U_\infty \approx 0.6$. The core radius r_0 which is approximately equal to the radius at which the swirl speed becomes maximum, also increases with increasing $\Gamma/U_\infty x$. The normalized wavelength λ/r_0 seems to be around 3–4, which is much smaller than the predictions for the Q vortex.

Finally, it should be noted that the existence of helical mode instability does not have any implications with regard to the breakdown mechanism. The flows upstream of breakdown location are known to be stable to disturbances. However, whether the instabilities in downstream region promote breakdown is not known.⁴

Acknowledgments

Part of this work was supported by the Air Force Office of Scientific Research. The author would like to thank F. Roos for making some of his data available.

References

- ¹Earnshaw, P. B., and Lawford, J. A., "Low Speed Wind Tunnel Experiments on a Series of Sharp-edged Delta Wings," Aeronautical Research Council, R & M 3424, Aug. 1964.
- ²Mabey, D. B., "Beyond the Buffet Boundary," *Aeronautical Journal*, April 1973, pp. 201-215.
- ³Roos, F. W., and Kegelman, J. T., "Recent Explorations of Leading-edge Vortex Flowfields," NASA High-Angle-of-Attack Technology Conference, NASA Langley Research Center, Hampton, VA, Oct. 30-Nov. 1, 1990.
- ⁴Garg, A. K., and Leibovich, S., "Spectral Characteristics of Vortex Breakdown Flowfields," *Physics of Fluids*, Vol. 22, No. 11, 1979, pp. 2053-2064.
- ⁵Chanaud, R. C., "Observations of Oscillatory Motion in Certain Swirling Flows," *Journal of Fluid Mechanics*, Vol. 21, 1965, pp. 111-127.
- ⁶Cassidy, J. J., and Falvey, H. T., "Observations of Unsteady Flow Arising after Vortex Breakdown," *Journal of Fluid Mechanics*, Vol. 41, 1970, pp. 727-736.
- ⁷Singh, P. I., and Uberoi, M. S., "Experiments on Vortex Stability," *Physics of Fluids*, Vol. 19, No. 12, 1976, pp. 1858-1863.
- ⁸Lessen, M., Singh, P. J., and Paillet, F., "The Stability of a Trailing Line Vortex, Part 1, Inviscid Theory," *Journal of Fluid Mechanics*, Vol. 63, 1974, pp. 753-763.
- ⁹Rediniotis, O. K., Stapountzis, H., and Telionis, D. P., "Vortex Shedding over Delta Wings," *AIAA Journal*, Vol. 28, No. 5, 1990, pp. 944-946.
- ¹⁰Wentz, W. H., and Kohlman, D. L., "Vortex Breakdown on Slender Sharp-Edged Wings," *Journal of Aircraft*, Vol. 8, No. 2, 1971, pp. 156-161.
- ¹¹Erickson, G. E., "Water-Tunnel Studies of Leading-Edge Vortices," *Journal of Aircraft*, Vol. 19, No. 3, 1982, pp. 442-448.
- ¹²Hummel, D., "Untersuchungen über das Aufplatzen der Wirbel an schlanken Deltaflügeln," *Zeitschrift fuer Flugwissenschaft*, Vol. 13, 1965, pp. 158-168.
- ¹³Khorrami, M., "On the Viscous Modes of Instability of a Trailing Line Vortex," *Journal of Fluid Mechanics*, Vol. 225, 1991, pp. 197-212.
- ¹⁴Rockwell, D., Magness, C., Robinson, O., Towfighi, J., Akin, O., Gu, W., and Corcoran, T., "Instantaneous Structure of Unsteady Separated Flows via Particle Image Velocimetry," Fluid Mechanics Labs., Lehigh Univ., Rept. PI-1, Bethlehem, PA, Feb. 1992.
- ¹⁵Gursul, I., and Ho, C. M., "Vortex Breakdown over Delta Wings in Unsteady Free Stream," AIAA Paper 93-0555, Jan. 1993.
- ¹⁶Solignac, J. L., and Leuchter, O., "Etudes experimentales d'écoulements tourbillonnaires soumis à des effets de gradient de pression adverse," *Aerodynamics of Vortical Type Flows in Three Dimensions*, AGARD CP-342, July 1983.
- ¹⁷Smith, J. H. B., "Improved Calculations of Leading-Edge Separation from Slender, Thin, Delta Wings," *Proceedings of the Royal Society, A*, Vol. 306, 1968, pp. 67-90.
- ¹⁸Payne, F. M., Ng, T. T., Nelson, R. C., and Schiff, L. B., "Visualization and Wake Surveys of Vortical Flow over a Delta Wing," *AIAA Journal*, Vol. 26, No. 2, 1988, pp. 137-143.
- ¹⁹Schmucker, A., and Gersten, K., "Vortex Breakdown and its Control on Delta Wings," *Fluid Dynamics Research*, Vol. 3, 1988, pp. 268-272.
- ²⁰Mager, A., "Dissipation and Breakdown of a Wing-Tip Vortex," *Journal of Fluid Mechanics*, Vol. 55, 1972, pp. 609-628.
- ²¹Keller, J. J., Egli, W., and Althaus, R., "Vortex Breakdown as a Fundamental Element of Vortex Dynamics," *Fluid Dynamics Research*, Vol. 3, 1988, pp. 31-42.

Appendix B

On fluctuations of vortex breakdown location

Ismet Gursul and Houbin Yang

Department of Mechanical, Industrial, and Nuclear Engineering, University of Cincinnati, Cincinnati, Ohio 45221-0072

(Received 19 July 1994; accepted 30 September 1994)

Flow visualization and velocity measurements are performed in order to investigate the unsteady nature of vortex breakdown location over a delta wing. The results indicate that the fluctuations of vortex breakdown location occur at much lower frequencies than the frequency of the hydrodynamic instability of the flow in the wake of the vortex breakdown. It is suggested that the helical mode instability does not influence the unsteady nature of breakdown location. © 1995 American Institute of Physics.

It has been observed in several experiments that vortex breakdown location is not steady and exhibits fluctuations in the streamwise direction.¹⁻⁴ Garg and Leibovich² reported fluctuations of the order of the test-section radius in their vortex-tube experiments. The magnitude of the fluctuations corresponds approximately to five times the core diameter (after breakdown) in their experiments. The experiments for delta wings showed fluctuations of breakdown location up to 10% of the chord length of the delta wing.¹ The purpose of this Brief Communication is to report the results of the experiments on the fluctuations of vortex breakdown location.

One possible source of the observed fluctuations is the hydrodynamic instability of the "breakdown wake" (i.e., the flow in the wake of the vortex breakdown) where wake-like axial velocity profiles are observed. Garg and Leibovich² carried out velocity measurements in the breakdown wakes and observed coherent oscillations. They suggested that these oscillations correspond to the first helical mode instability of the time-averaged velocity profiles. Periodic oscillations due to the helical mode instability were observed in a variety of swirling flows after breakdown occurred. For delta wings, the existence of the first helical mode instability was shown with the help of the two-point pressure measurements on the suction surface of the delta wings.⁵ Examples of pressure fluctuations⁶ at a fixed point underneath the vortex and near the trailing edge are shown in Fig. 1. At small angle of attack ($\alpha=15^\circ$), the vortex breakdown is not over the wing. With the increasing angle of attack, the vortex breakdown moves toward the apex of the wing. At angle of attack $\alpha=34^\circ$, the breakdown location is approximately 60% of the chord length from the wing apex. The length of the time record is approximately $10c/U_\infty$, where c is the chord length and U_∞ is the free stream velocity. As noted by Garg and Leibovich,² although the existence of the wake instability has been well documented, its role in vortex breakdown phenomena remains unclear. The quasiperiodic nature of the flow in the wake of breakdown may interact with the breakdown process through upstream influence. It has not been possible to determine, from the previous experiments, the role of the helical mode instability in the unsteady nature of breakdown location. The main objective of this study is to investigate the relationship between the helical mode instability and the unsteadiness of vortex breakdown location.

For this purpose, flow visualization and laser Doppler

velocimetry (LDV) measurements were carried out over a delta wing. The experiments were performed in a water channel with a cross-sectional area of 61 by 61 cm. The delta wing has a sweep angle of $\Lambda=70^\circ$ and chord length of $c=268$ mm. The lee surface was flat, whereas the leading edges were beveled at 45° on the windward side. The Reynolds number based on the chord length was around $Re=50\,000$ and the turbulence level was 0.6%. The velocity measurements were made with a single component LDV system and the free-stream velocity was $U_\infty=20$ cm/s.

Figure 2 shows an example of the streamwise velocity fluctuations spectrum taken just outside of the vortex core at an angle of attack $\alpha=37^\circ$. The velocity spectrum at different cross-stream locations was very similar. The axial location of the measurement point is approximately $0.08c$ downstream of the time-averaged breakdown location. The sharp peak in the spectrum is due to the helical mode instability. The dimensionless frequency of the instability fc/U_∞ is around 1.72. This number is in agreement with the results from the pressure measurements⁵ on delta wings, which showed that the dimensionless frequency is on the order of unity for a large range of angle of attack and sweep angle.

Flow visualization of vortex breakdown was performed by injecting fluid with food coloring dye near the apex of the model. The motion of vortex breakdown location was recorded with a 30 frames/s VCR, a CCD camera and zoom lens. The videotape recording of the motion was analyzed

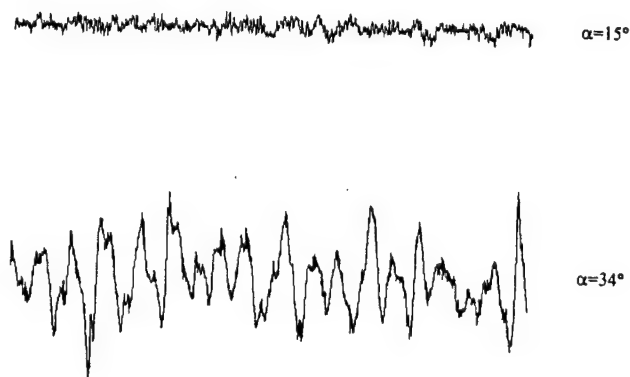


FIG. 1. Pressure fluctuations near trailing edge ($x/c=0.93$) for different angles of attack.⁶ Length of time record is approximately $10c/U_\infty$.

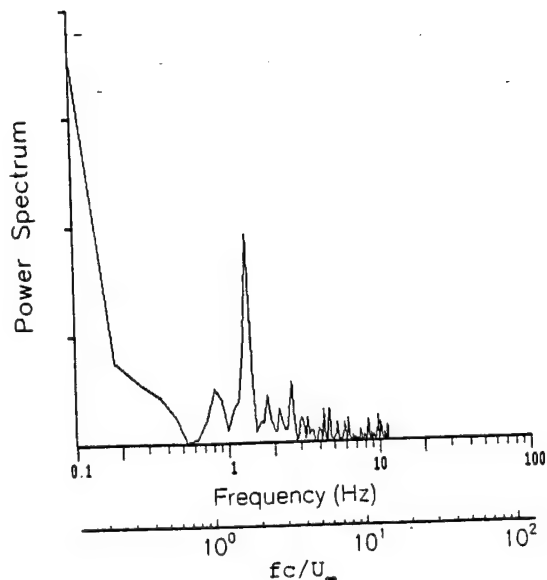


FIG. 2. Spectrum of streamwise velocity fluctuation in breakdown wake; vertical scale is linear and in arbitrary units.

frame by frame and the chordwise distance of breakdown location from the apex was measured. The breakdown was spiral type, as generally observed over delta wings. The location of breakdown was taken as the location where the streakline marking the core makes an abrupt kink to form a spiral. The measurement uncertainty for the breakdown location is $0.004c$. The time history of the vortex breakdown location was observed for a total length of time record of approximately $100c/U_\infty$ (see Fig. 3). For the experimental conditions, the time resolution is limited by the frame speed and corresponds to $0.025c/U_\infty$. Therefore, the frequencies up to $fc/U_\infty = 20$ can be resolved in the frequency domain. For $\alpha = 37^\circ$, from the time history of breakdown location, the time-averaged breakdown location and root-mean-square (RMS) value of it were calculated as $\bar{x}/c = 0.297$ and $x_{\text{RMS}}/c = 0.032$.

Figure 4 shows the spectrum of the fluctuations of vortex breakdown location for $\alpha = 37^\circ$ along with the spectra for $\alpha = 30^\circ$ and 26° . The frequency of the helical mode instability is also shown in each plot with dashed lines. It is seen that the fluctuations of breakdown location occur at a much lower frequency range compared to the helical mode instability. It is concluded that there is no correlation between the fluctuations of breakdown location and helical mode instability. Indeed, most of the energy of fluctuations of breakdown location is below $fc/U_\infty = 0.2$. For $\alpha = 37^\circ$, it is also seen that a sharp peak exists around $fc/U_\infty \approx 0.12$. The dominant frequency of the oscillations of breakdown location and the



FIG. 3. Time history of breakdown location. Length of time record is approximately $100c/U_\infty$.

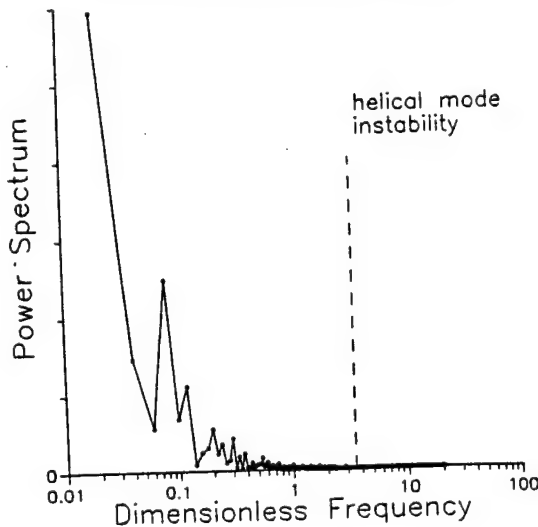
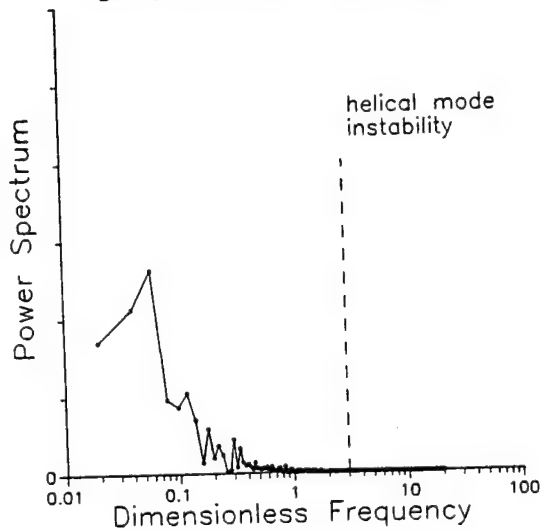
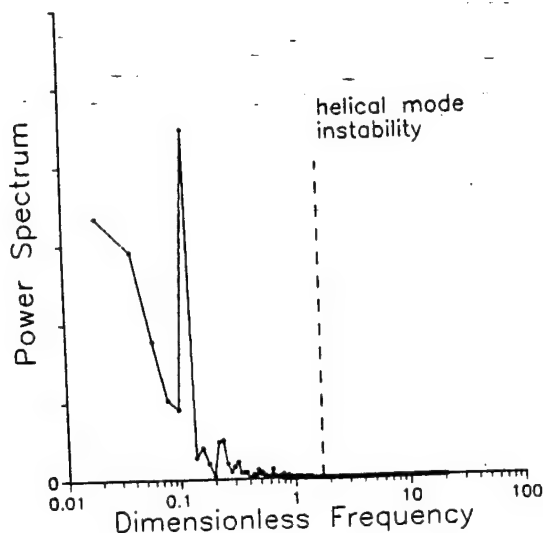


FIG. 4. Spectrum of fluctuations of breakdown location; vertical scale is linear and in arbitrary units.

frequency of the helical mode instability vary with angle of attack. The fact that dominant frequency of the oscillation of breakdown location varies with angle of attack suggests that the oscillations are not related to the facility dependent conditions such as the disturbances in the free-stream velocity.

The most coherent oscillations occur for the largest angle of attack $\alpha=37^\circ$, when the breakdown location is closest to the apex. For all three angles of attack, the main conclusion is the same: the oscillations of breakdown occur at a much lower frequency than that of the helical mode instability in breakdown wake.

It should also be noted that, the Kelvin-Helmholtz instability of the shear layer separated from the leading edge has a much higher frequency range,^{7,8} $fc/U_\infty=10-30$. Therefore, it is not related to the fluctuations of breakdown location either. When compared with the frequency of the helical mode instability, the frequency range of the spectrum of breakdown location for a stationary delta wing is much closer to the frequency range of typical aerodynamic maneuvers (up to $fc/U_\infty \approx 0.03$). The response of breakdown location and possible coupling between the wing motion and breakdown location in this frequency range is very important.

ACKNOWLEDGMENT

The authors appreciate the support of the Air Force Office of Scientific Research.

- ¹M. V. Lowson, "Some experiments with vortex breakdown," *J. R. Aeronaut. Soc.* **68**, 343 (1964).
- ²A. K. Garg and S. Leibovich, "Spectral characteristics of vortex breakdown flowfields," *Phys. Fluids* **22**, 2053 (1979).
- ³F. M. Payne, T. T. Ng, and R. C. Nelson, "Visualization and wake surveys of vortical flow over a delta wing," *AIAA J.* **26**, 137 (1988).
- ⁴S. A. Thompson, S. M. Batill, and R. C. Nelson, "Separated flowfield on a slender wing undergoing transient pitching motions," *J. Aircraft* **28**, 489 (1991).
- ⁵I. Gursul, "Unsteady flow phenomena over delta wings at high angle of attack," *AIAA J.* **32**, 225 (1994).
- ⁶I. Gursul and H. Yang, "Vortex breakdown over a pitching delta wing," *AIAA Paper No. 94-0536*, 1994.
- ⁷M. Gad-el-Hak and R. F. Blackwelder, "The discrete vortices from a delta wing," *AIAA J.* **23**, 961 (1985).
- ⁸R. Gordnier and M. R. Visbal, "Unsteady vortex structure over a delta wing," *J. Aircraft* **31**, 243 (1994).

Appendix C

Active Control of Vortex Breakdown over a Delta Wing

I. Gursul,* S. Srinivas,† and G. Batta*

University of Cincinnati, Cincinnati, Ohio 45221-0072

Introduction

THE objective of this study is to accomplish active control of vortex breakdown over delta wings. The first step in this effort is to identify a physical quantity that indicates the existence of vortex breakdown and can be used as a feedback signal for active control. Previous studies^{1,2} suggest that pressure fluctuations induced by the helical mode instability of vortex breakdown is a good candidate. Measurement of pressure fluctuations at a single location on the wing surface can be sufficient for control purposes. The variation of the amplitude of pressure fluctuations (or rms value of pressure) with the breakdown location seems monotonic.² Hence, in this study, the rms value of pressure was chosen as the control variable, and a feedback control strategy was considered.

The second element in active control of vortex breakdown is to identify a flow controller to influence the vortex breakdown location. Several methods were shown to delay vortex breakdown. Blowing and suction in the tangential direction along the leading edge,^{3,4} suction applied around the vortex axis,^{5,6} and use of leading-edge flaps⁷ are among them. For most of the techniques mentioned, however, the relationship between the control parameter and the vortex breakdown location is unknown or undesirable (i.e., not monotonic). A desirable controller should have a monotonic relationship between the control parameter and breakdown location. Sweep angle has such a relationship. Therefore, variable sweep angle control was employed in this study. The relationship between the sweep angle and vortex breakdown location is very well known from static experiments.

A delta wing with variable sweep was fabricated (see Fig. 1a). Measured rms value of pressure coefficient at a fixed point close to the trailing edge ($x/c = 0.94$, $y/c = 0.27$) is shown as a function of angle of attack and sweep angle in Fig. 1b. The flat region near $\Lambda = 70$ deg shows the pressure fluctuation level in the absence of the vortex breakdown over the wing ($C_p \approx 0.05$). With increasing angle of attack or decreasing sweep angle, the vortex breakdown moves over the wing as the rms pressure level increases and finally reaches a saturation. This approximate monotonic relation between the sweep angle Λ and rms C_p suggests that a feedback control may be feasible. The increase in pressure fluctuations with the decreasing sweep angle is due to the increasing length of the breakdown region over the wing, as well as increasing circulation of the leading-edge vortex.⁸

An important consideration for the feedback control is the system dynamic response. It is well known that the dynamic response of the vortex breakdown location in unsteady flows is characterized by time-lag effects. It was suggested that the response of the breakdown location is similar to that of a first-order system.⁸ Estimated values of the time constant for different types of motion are summarized in Ref. 8. Flow-visualization experiments⁷ for variable sweep angle in a water channel showed that the normalized time constant is $\tau U_\infty/c = 2-7$. The idealization as a first-order system suggested that either proportional or integral control (or a combination of both) could be suitable for this application.

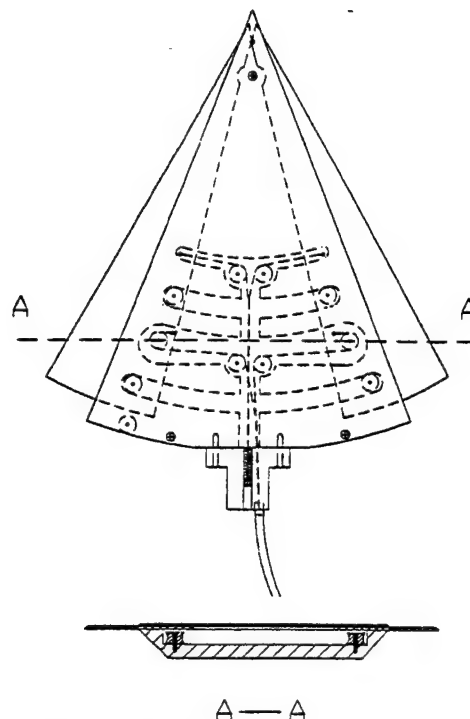


Fig. 1a Schematic of variable sweep delta wing.

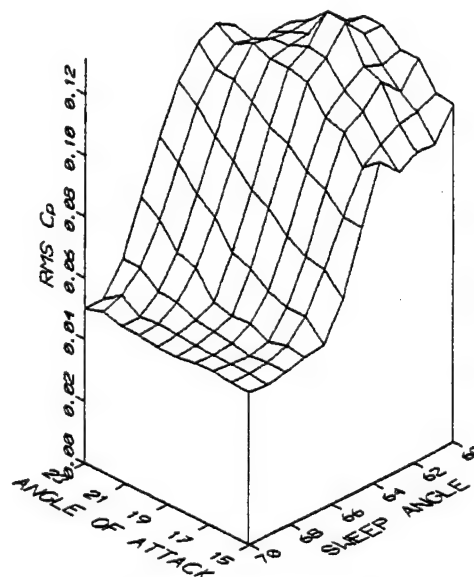


Fig. 1b RMS value of pressure coefficient as a function of angle of attack and sweep angle.

Experimental Setup

Experiments were carried out in a closed-circuit wind tunnel with a cross-sectional area of 61 by 61 cm. Details of the experimental setup and model can be found in Ref. 8. The chord length of the wing shown in Fig. 1a was $c = 268$ mm and the Reynolds number was $Re = 190,000$. The range of sweep angle was from $\Lambda = 60$ to $\Lambda = 70$ deg. Two thin plates were used to change the sweep angle. The motion of the plates was guided with a cable-pulley-pin system. A bicycle brake cable, whose sheath was fixed near the trailing edge and outside the wind tunnel, was attached to a drum, which was driven by a dc motor servo system. This flexible system allowed the use of variable sweep even for a pitching motion of the delta wing. The unsteady surface pressure was measured by a high-sensitivity

Received Dec. 12, 1994; revision received May 18, 1995; accepted for publication June 1, 1995. Copyright © 1995 by the authors. Published by the American Institute of Aeronautics and Astronautics, Inc., with permission.

*Assistant Professor, Department of Mechanical, Industrial and Nuclear Engineering.

†Graduate Student, Department of Mechanical, Industrial and Nuclear Engineering.

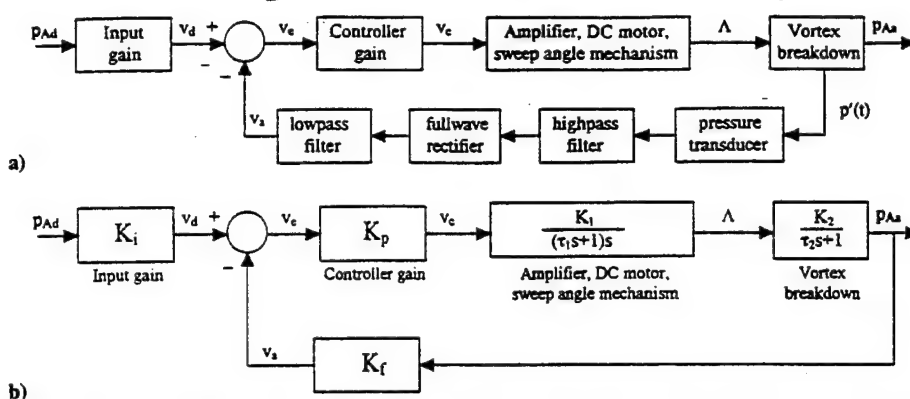


Fig. 2 Block diagram: a) feedback control system showing signal conditioning components and b) with transfer functions.

piezoelectric transducer (PCB model 103A). The measurement location was $x/c = 0.94$, $y/c = 0.27$, which was chosen based on previous measurements.¹ The active control experiments were conducted both for a stationary and a pitching delta wing. The pitching mechanism was similar to the one used by LeMay et al.⁹ The angle of attack was varied between 15 and 23 deg. A variable speed dc motor and a speed controller were used to drive the pitching mechanism.

Since the rms value of pressure was chosen as the control variable, an approximation for the rms pressure was necessary in a real-time control loop. The raw pressure fluctuation signal $p'(t)$ was rectified and low-pass filtered.⁸ The latter quantity is denoted by p_A , which represents the amplitude of the pressure fluctuations. The signal $p_A(t)$ was used as the control variable. The overall objective of the control system was translated into a control objective of maintaining a particular value of pressure amplitude $p_A(t)$. The implementation of the controller can be more easily understood by considering the block diagram representation of the system as shown in Fig. 2a. The plant in this control system consists of two parts: the mechanical position dynamics of the sweep angle mechanism and the vortex breakdown process. The pressure amplitude $p_A(t)$ was obtained by rectifying and low-pass filtering, after the signal from the pressure transducer was passed through a high-pass filter. The rectification was obtained using a full-wave bridge rectifier. The signal conditioning circuits and the feedback control system for the sweep angle were implemented using operational amplifiers. These circuits were constructed on a breadboard. The block diagram of the feedback control system with the transfer functions is shown in Fig. 2b. The power amplifier, dc motor, and sweep angle mechanism were modeled as a dc motor with a directly coupled inertia. Frequency response tests of the sweep angle mechanism indicate that this is a reasonable approximation. The transfer function for this model is shown in Fig. 2b. The time constant τ_1 was estimated from the step response tests as $\tau_1 \approx 0.25$ s, $(9.3c/U_\infty)$. As indicated earlier, the vortex breakdown process is modeled as a first-order dynamic system with time constant τ_2 . The time constant τ_2 was estimated from the water channel experiments⁷ as $\tau_2 = (2-7)c/U_\infty$.

Since the sweep angle positioning mechanism provides an integral relationship in the forward path, an integral controller for the overall control system was relatively easy to implement. In addition, integral control has the advantage of small steady-state error. The only parameter needed in the controller design was the gain K_p . Since specific values of the plant parameters were not easily obtained, the gain K_p was chosen by trial and error.

Results

First, the active control experiments were conducted for the stationary delta wing at angle of attack $\alpha = 19$ and 23 deg. The results for $\alpha = 23$ deg are shown in Fig. 3. Initially, the sweep angle was set to $\Lambda = 60$ deg and the desired voltage v_d (corresponding to a desired pressure amplitude p_{Ad}) was chosen as 1.0 V. For this value of sweep angle, the vortex breakdown location was over the wing and closer to the apex. In Fig. 3, plots of pressure fluctuation $p'(t)$, feedback voltage $v_a(t)$, and sweep angle $\Lambda(t)$ are shown. At around $t = 5$ s, the feedback control was turned on. Note that the

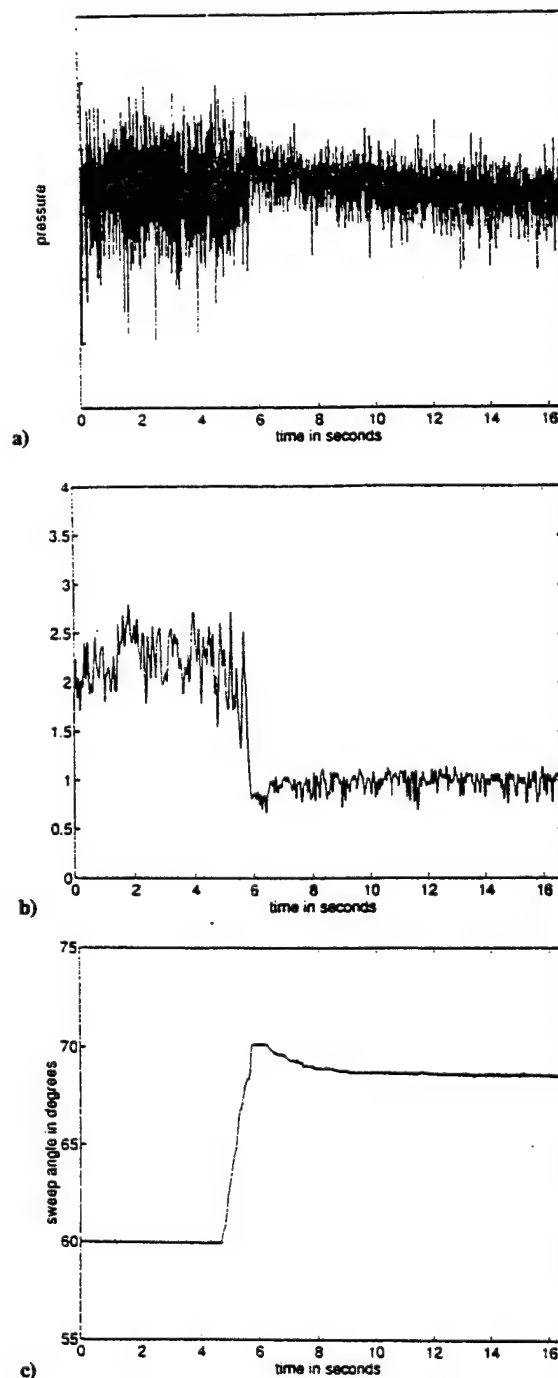


Fig. 3 Variation of a) pressure fluctuation $p'(t)$, b) feedback voltage $v_a(t)$, and c) sweep angle $\Lambda(t)$ as a function of time, $\alpha = 23$ deg.

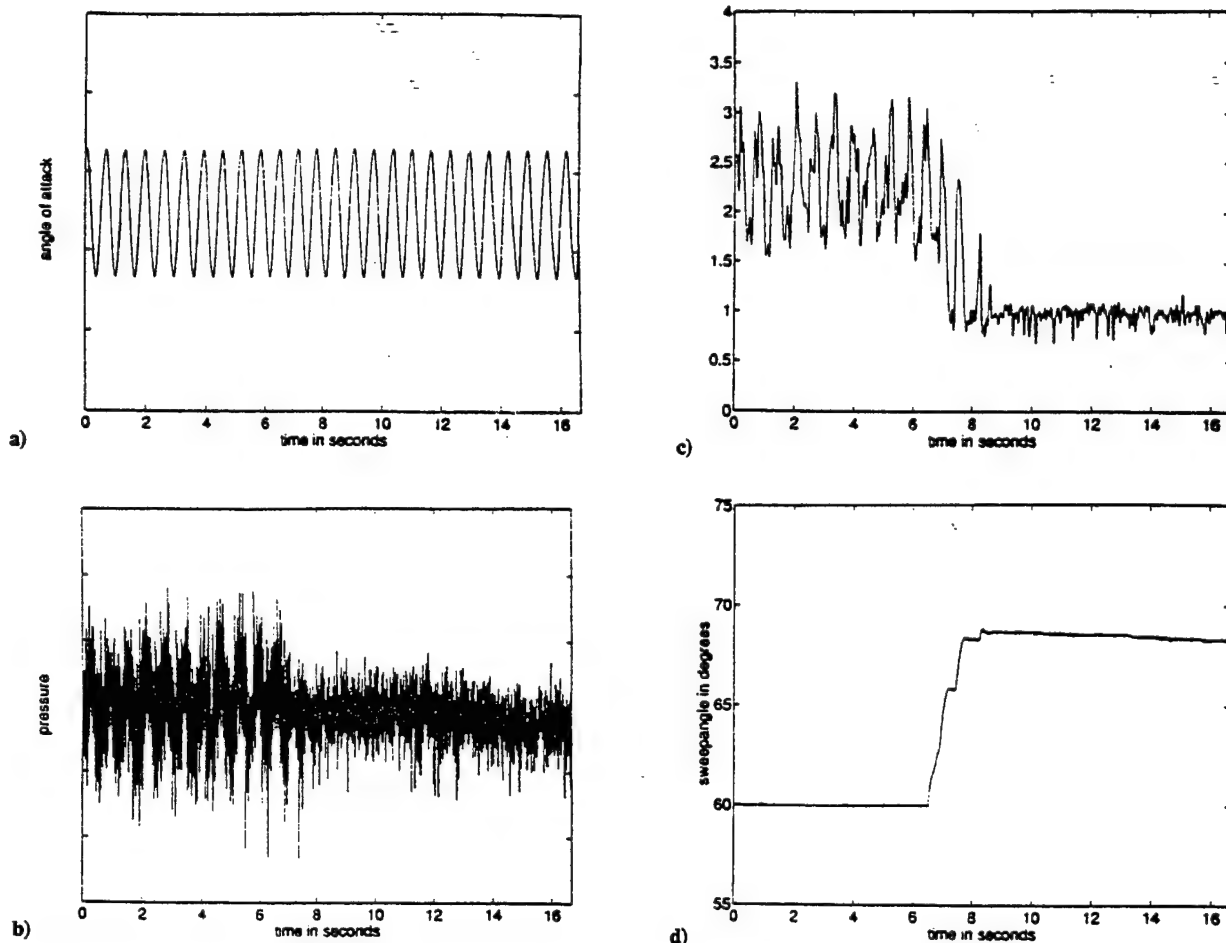


Fig. 4 Variation of a) angle of attack $\alpha(t)$, b) pressure fluctuation $p'(t)$, c) feedback voltage $v_d(t)$, and d) sweep angle $\Lambda(t)$ as a function of time, $\alpha(t) = 19 + 4 \cos(\omega t)$ (deg), $k = \omega c / 2U_\infty = 0.12$.

sweep angle $\Lambda(t)$ increases and becomes nearly constant around $\Lambda \cong 68.5$ deg after a small overshoot. This new sweep angle corresponds to a case where the breakdown location is downstream of the wing. The decrease in raw pressure fluctuations and feedback voltage accompany the variation of sweep angle. Similar results were obtained for $\alpha = 19$ deg. Experiments for different values of the desired voltage v_d , which represents the desired pressure amplitude, were carried out. When this parameter was increased to $v_d = 1.5$ V, the overshoot of the sweep angle was not observed.

The active control experiments for the pitching delta wing were conducted in a similar way. As the delta wing was pitched periodically between 15 and 23 deg, i.e., $\alpha(t) = 19 + 4 \cos(\omega t)$ (deg), the initial sweep angle was set to 60 deg. For this range of angle of attack, the vortex breakdown was over the wing during the whole cycle. The plots of angle of attack $\alpha(t)$, pressure fluctuation $p'(t)$, feedback voltage $v_d(t)$, and sweep angle $\Lambda(t)$ are shown in Fig. 4 for a desired voltage $v_d = 1.0$ V and a reduced frequency $k = \omega c / 2U_\infty = 0.12$, where ω is the radial frequency of the pitching motion. Again, the feedback control was turned on suddenly. It is seen that the sweep angle $\Lambda(t)$ increases and becomes nearly constant around a new value for which the breakdown location is downstream of the wing. It is also seen that the magnitude of pressure fluctuations decreases substantially as a result of feedback control.

Conclusions

It is shown that pressure fluctuations induced by the helical mode instability of vortex breakdown can be used to control the vortex breakdown location. Measurement of pressure fluctuations at a single location on the delta wing is sufficient for this purpose. The monotonic variation of the amplitude of the pressure fluctuations with vortex breakdown location makes the feedback control

possible. Based on previous experiments on the dynamic response of vortex breakdown location, the system was idealized as a first-order system, and integral control was used. The active control of vortex breakdown was achieved for stationary as well as pitching delta wings.

Acknowledgment

This research was supported by the Air Force Office of Scientific Research Grant F49620-92-J-0532.

References

- ¹Gursul, I., "Unsteady Flow Phenomena over Delta Wings at High Angle of Attack," *AIAA Journal*, Vol. 32, No. 2, 1994, pp. 225-231.
- ²Gursul, I., and Yang, H., "Vortex Breakdown over a Pitching Delta Wing," *AIAA Paper 94-0536*, Jan. 1994.
- ³Wood, N. J., Roberts, L., and Celik, Z., "Control of Asymmetric Vortical Flows over Delta Wings at High Angles of Attack," *Journal of Aircraft*, Vol. 27, No. 5, pp. 429-435.
- ⁴Gu, W., Robinson, O., and Rockwell, D., "Control of Vortices on a Delta Wing by Leading-Edge Injection," *AIAA Journal*, Vol. 31, No. 7, 1993, pp. 1177-1186.
- ⁵Werle, H., "Sur l'éclatement des tourbillons d'apex d'une aile delta aux faibles vitesses," *La Recherche Aeronautique*, No. 74, Jan.-Feb. 1960, pp. 23-30.
- ⁶Parmenter, K., and Rockwell, D., "Transient Response of Leading-Edge Vortices to Localized Suction," *AIAA Journal*, Vol. 28, No. 6, 1990, pp. 1131-1133.
- ⁷Gursul, I., Yang, H., and Deng, Q., "Control of Vortex Breakdown with Leading-Edge Devices," *AIAA Paper 95-0676*, Jan. 1995.
- ⁸Srinivas, S., Gursul, I., and Batta, G., "Active Control of Vortex Breakdown over Delta Wing," *AIAA Paper 94-2215*, June 1994.
- ⁹LeMay, S. P., Batill, S. M., and Nelson, R. C., "Vortex Dynamics on a Pitching Delta Wing," *Journal of Aircraft*, Vol. 27, No. 2, 1990, pp. 131-138.

Appendix D

VORTEX BREAKDOWN OVER A PITCHING DELTA WING

I. GURSUL AND H. YANG

*Department of Mechanical, Industrial and Nuclear Engineering, University of Cincinnati
Cincinnati, OH 45221, U.S.A.*

(Received 5 August 1994 and in revised form 21 February 1995)

Unsteady pressure measurements were carried out on a pitching delta wing in order to study the effects of pressure gradient on the phase lag between the wing motion and the movement of breakdown location. The results indicate that the observed time lag of breakdown location is strongly linked to the external pressure gradient generated by the wing. © 1995 Academic Press Limited

1. INTRODUCTION

SEVERAL EXPERIMENTAL STUDIES of vortex breakdown over pitching delta wings (see Figure 1) have shown that there is a phase shift between the motion of the wing and the movement of the breakdown location (Woodgate 1971; Wolffelt 1987; LeMay *et al.* 1990; Atta & Rockwell 1990). The phase delay mainly depends on the reduced frequency (LeMay *et al.* 1990) and can be as large as 180° , which means that the breakdown location moves toward the apex as the angle of attack decreases (Atta & Rockwell 1990). As an example, the results of flow visualization studies for sweep angle $\Lambda = 70^\circ$ are summarized in Figure 2. Although the data are for periodic pitching motion (see Figure 1) with different ranges of angle of attack (mean value and amplitude), there is a consistent trend of increasing phase delay with increasing reduced frequency. The physics of this phase lag is not well understood.

It is well known that there are two important parameters which determine the breakdown location: swirl angle and external pressure gradient outside the vortex core. Hall (1972) suggested that vortex breakdown occurs as a result of adverse pressure gradient along the vortex axis which leads to a stagnation point. He showed theoretically that the pressure gradient along the vortex axis is the sum of external pressure gradient and swirl velocity contribution. This is consistent with the observations that an increase in swirl angle or in the magnitude of adverse external pressure gradient causes an earlier breakdown (i.e., the breakdown location moves upstream). Hall's theory also explains the observations that less swirl is needed for breakdown if the magnitude of adverse external pressure gradient is increased (Sarpkaya 1974).

For a leading-edge vortex, the external pressure gradient is generated by the wing itself, and it is adverse due to the presence of a trailing-edge (Polhamus 1971). The circulation (or swirl angle) and adverse external pressure gradient depend on geometrical parameters such as angle of attack and sweep angle (Gursul 1992a). Thus, for a pitching wing, both the swirl angle and streamwise pressure gradient vary during a maneuver.

It has been suggested that delta-wing vortex breakdown in unsteady flow is driven by

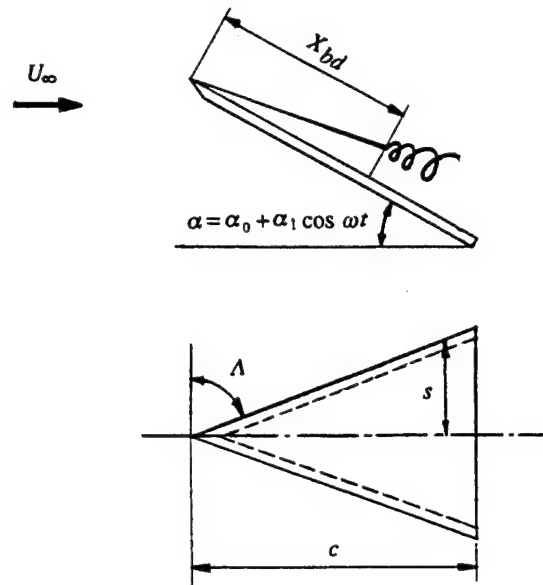


Figure 1. Definition diagram for the pitching delta wing.

the external pressure gradient (Gursul & Ho 1994). Likewise, the observed phase delay of the breakdown location for pitching delta wings may be related to the variations of the adverse pressure gradient on the wing surface. In order to test this hypothesis, unsteady pressure on a pitching delta wing was measured and correlated with the movement of the breakdown location.

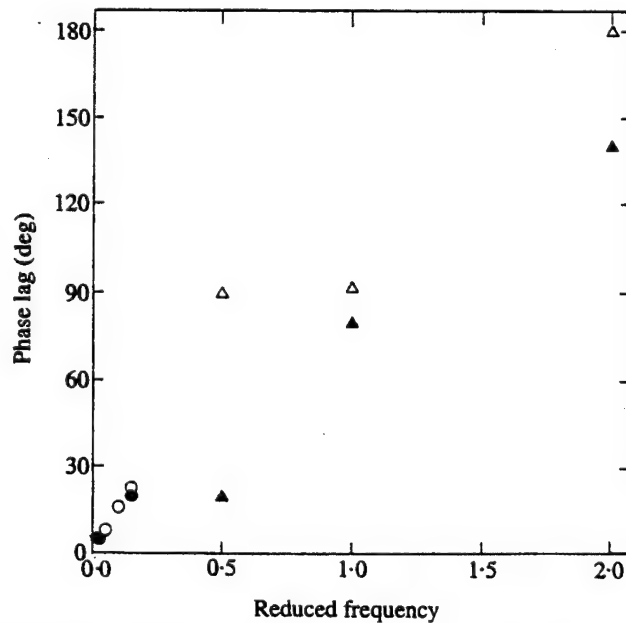


Figure 2. Phase lag as a function of reduced frequency, $\Lambda = 70^\circ$: \circ , LeMay *et al.* ($\alpha_0 = 34^\circ$, $\alpha_1 = 5^\circ$); \bullet , LeMay *et al.* ($\alpha_0 = 22.5^\circ$, $\alpha_1 = 22.5^\circ$); \triangle , Woodgate ($\alpha_0 = 30^\circ$, $\alpha_1 = 1^\circ$); \blacktriangle , Woodgate ($\alpha_0 = 35^\circ$, $\alpha_1 = 1^\circ$).

2. EXPERIMENTAL FACILITY

Experiments were carried out in a closed-circuit wind tunnel with a cross-sectional area of 610 mm by 610 mm. The model delta wing (sweep angle of 70°) was made of 19 mm thick plexiglas and had a chord length of $c = 356$ mm (see Figure 3). The lee surface was flat, whereas the leading-edges were beveled at 45° on the windward side. The Reynolds number was varied from 127,000 to 254,000, although most of the results are for $Re = 254,000$. At the largest angle of attack, the blockage ratio was 0.08.

Unsteady pressure measurements were made along the centerline ($y/s = 0$) and along the ray $y/s = 0.5$. The unsteady surface pressure was measured by a high sensitivity piezoelectric transducer (PCB model 103A). The measurement uncertainty for the dimensionless pressure coefficient, C_p , was estimated as 0.005. The pressure transducer has a built-in accelerometer to cancel vibration sensitivity. It is 5.6 mm high, 9.4 mm in diameter and has a pressure orifice measuring 2.54 mm in diameter. The sensing area of the transducer was reduced by using a 1 mm diameter pinhole of 2 mm depth. The amplitude distortion and phase shift of the pressure signal due to the very short pinhole are negligible, since the natural frequency of the system was found to be much higher than the frequency range of interest. The transducer and its leads were housed in the grooves shown in Figure 3. The pressure taps were also used for mean pressure measurements. Additional pressure taps were located in the spanwise direction at $x/c = 0.6$ and $x/c = 0.8$. The mean pressure was measured with a Setra transducer (model 239). The pressure taps were connected to the transducer with the

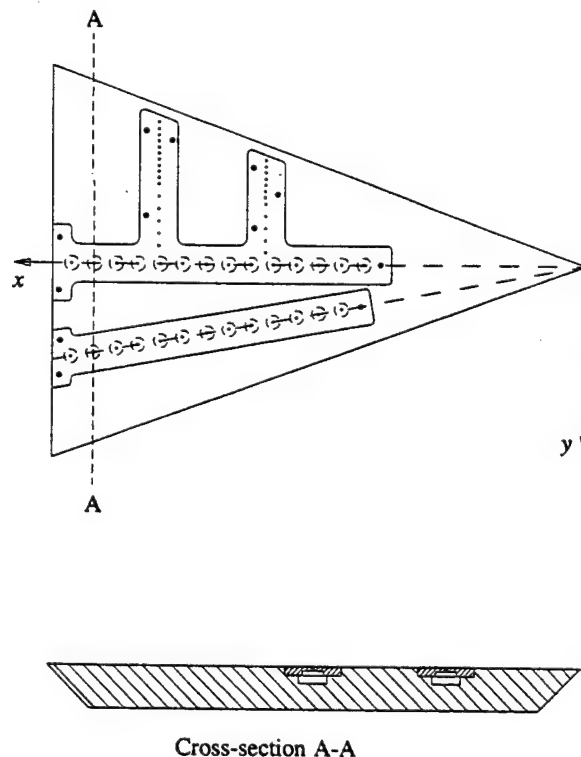


Figure 3. Top view of the delta wing model (top), cross-section of the delta wing model (bottom).

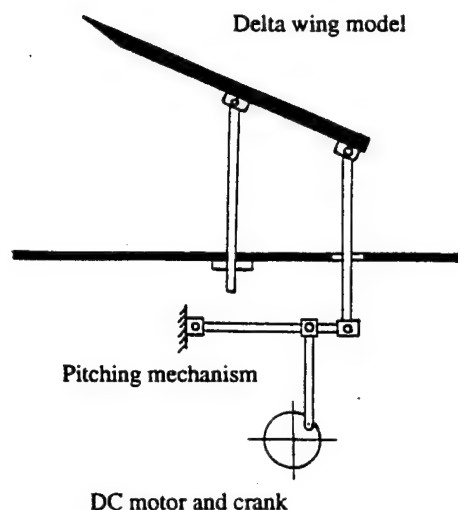


Figure 4. Schematic of experimental set-up.

enclosed chamber (see Figure 3) and plastic tubing. All unused taps were sealed by tape.

A schematic of the experimental set-up is shown in Figure 4. The model was pitched sinusoidally about a point located at the one-half root-chord position and 28.5 mm below the model suction surface. The pitching mechanism was similar to the one used by LeMay *et al.* (1990). A variable speed DC motor and speed controller were used to drive the pitching mechanism. The model was pitched periodically at different reduced frequencies up to $\omega c/2U_\infty = 0.53$. A displacement transducer was used to monitor the variation of the angle of attack. In order to make a comparison with the results of flow visualization by LeMay *et al.* (1990), the angle of attack range was chosen as $29\text{--}39^\circ$. In addition, experiments for the range of $10\text{--}15^\circ$ (for which breakdown is absent over the wing) were performed for comparison.

Pressure signals were digitized and processed by a laboratory computer. The dynamic variation of breakdown location was monitored with the help of signal analysis of the pressure fluctuations as described in the next section.

3. RESULTS

It was shown in an earlier investigation that vortex breakdown flowfields over delta wings show helical-mode instability which produces coherent pressure fluctuations on the suction surface (Gursul 1992b). The pressure fluctuations measured on the steady model (at $x/c = 0.93$, $y/s = 0.5$) are shown for different angles of attack in Figure 5. For the smallest angle of attack $\alpha = 15^\circ$, the breakdown location is not over the wing. For the range of $\alpha = 29^\circ$ to $\alpha = 39^\circ$, the breakdown location moves from $x/c \approx 0.90$ to $x/c \approx 0.45$ (LeMay *et al.* 1990). With increasing angle of attack, the amplitude of the pressure fluctuations due to the signature of breakdown increases. This can be understood qualitatively by modeling the vortex breakdown as a spiral vortex filament (Jumper *et al.* 1993). Because the circulation of the leading-edge vortex, as well as the length of the breakdown region over the wing, increase as the angle of attack is increased, the pressure fluctuations also increase with angle of attack. Figure 5 shows that the frequency content also varies with the angle of attack. However, the pressure

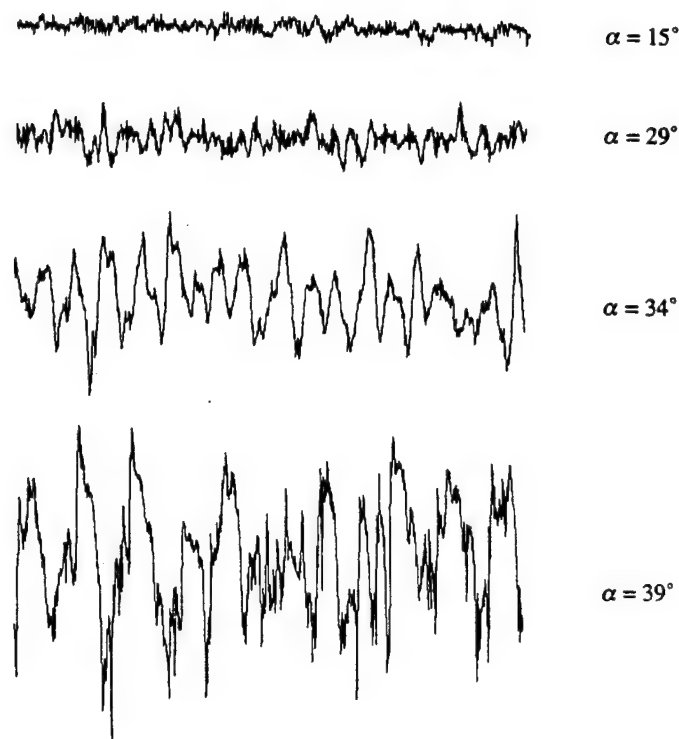


Figure 5. Pressure fluctuations on steady model for different angles of attack. Length of time record is 250 ms, $x/c = 0.93$, $y/s = 0.5$.

signature of breakdown has a much higher frequency range compared with the frequency of a typical aerodynamic maneuver (Gursul 1994).

When the delta wing is pitched sinusoidally (between 29 and 39°), the instantaneous pressure signature of the breakdown varies as the breakdown location moves back and forth in the streamwise direction (Figure 6). It is evident that the maximum fluctuation level due to the breakdown occurs not at the maximum angle of attack, but later, at a smaller angle of attack as the wing pitches down. This is an indication of phase delay between the motion of the wing and the location of vortex breakdown. In order to quantify the phase delay, the phase-averaging technique was applied to the pressure signal, i.e.

$$C_p = \langle C_p \rangle + C'_p,$$

where $\langle C_p \rangle$ is the phase-averaged pressure coefficient. The standard deviation from the phase-averaged value,

$$C'_{p, sd} = \sqrt{\langle (C'_p)^2 \rangle},$$

was calculated as a function of the angle of attack. The variation of the standard deviation shown in Figure 7 reveals hysteresis loops. The loops become wider with increasing reduced frequency, which is an indication of increasing phase delays. The maximum amplitudes reached during the maneuver decrease in the streamwise direction as the trailing-edge is approached. The phase angles for two streamwise locations are shown in Figures 14 and 15. These phase angles were found by plotting the variation of the standard deviation as a function of time (not shown here). Comparison of these figures shows that the phase lag at different streamwise locations

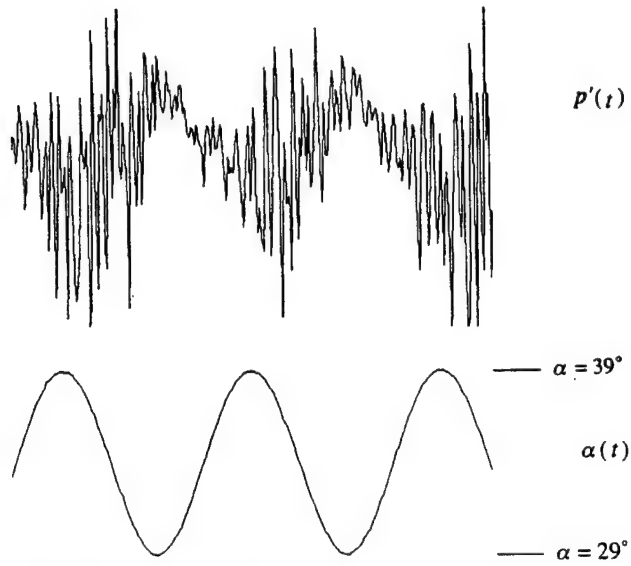


Figure 6. Pressure fluctuations and time history of angle of attack for a periodically pitching motion. Length of time record is 838 ms; $x/c = 0.55$, $y/s = 0.5$, reduced frequency $k = 0.35$.

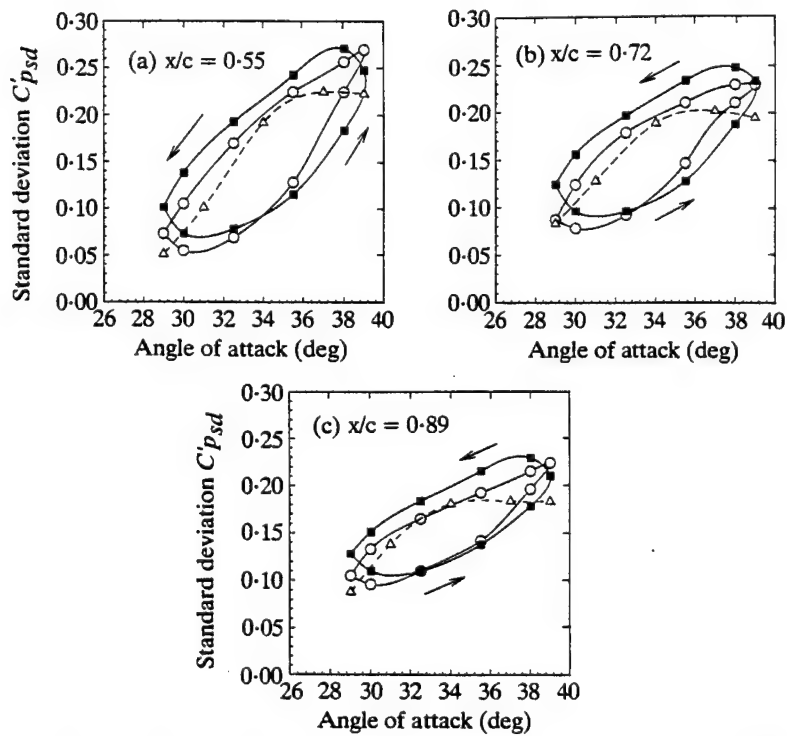


Figure 7. Variation of standard deviation $C'_{p_{sd}}$ as a function of angle of attack at different streamwise locations and $y/s = 0.5$: \circ —, $k = 0.19$, \blacksquare —, $k = 0.35$, \triangle —, $k = 0$.

is approximately the same, and is in agreement with the trend of the flow visualization experiments (Le May *et al.* 1990).

In order to investigate the possible relationship between the pressure field and the dynamic character of the breakdown location, pressure measurements were carried out along the centerline ($y/s = 0$) and $y/s = 0.5$. For the leading-edge vortex, the pressure gradient on the suction surface of the wing acts as the external pressure gradient. However, interpretation of the pressure along $y/s = 0.5$ is not straightforward, since the measurement locations are approximately underneath the vortex. Whether the unsteady variation of pressure is the end result of vortex breakdown remains uncertain. For example, Thompson *et al.* (1990) measured the pressure underneath the vortex and observed a time lag with respect to the wing motion. However, one cannot conclude whether the time lag is because of the movement of vortex breakdown. On the other hand, along the centerline $y/s = 0$, the effects of vortex on pressure are negligible. This is verified by the following experiment. A control cylinder with diameter $d/c = 0.047$ was placed at $x/c = 0.92$, $z/s = 0.37$ (for $\alpha = 29^\circ$) which caused a premature breakdown (Figure 8). The control cylinder spanned across the entire cross-section of the wind tunnel. Although the exact location of vortex breakdown with respect to the cylinder is not known, its streamwise location is estimated to be around $x/c = 0.90$ (LeMay *et al.* 1990) in the absence of the cylinder. The breakdown location moved upstream after the control cylinder was placed. This was monitored by the pressure signal taken at the same location as in Figure 5. The pressure signals with and without the cylinder and the comparison with those in Figure 5 confirm that the breakdown location moved upstream. The vertical location of the cylinder was chosen so that the largest amplitude of the pressure fluctuations was obtained. The mean pressure

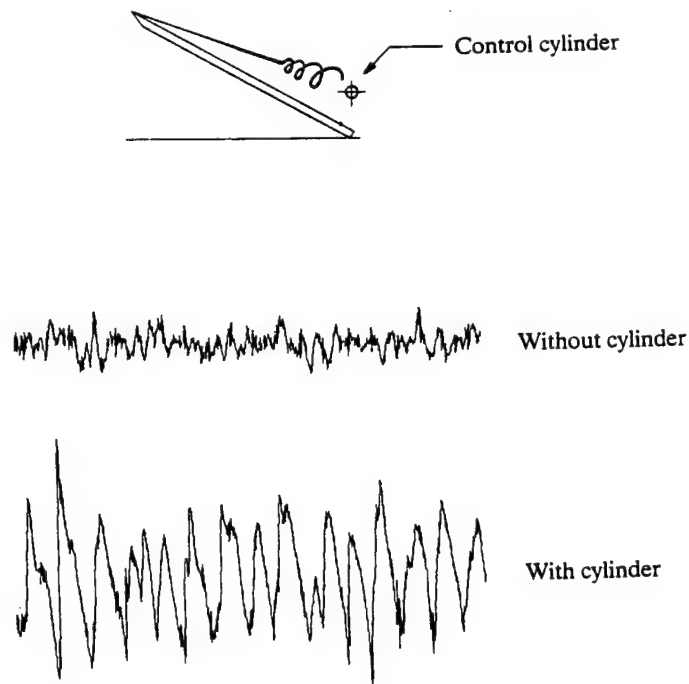


Figure 8. Pressure fluctuations at $x/c = 0.93$, $y/s = 0.5$ for $\alpha = 29^\circ$ with and without control cylinder. Dimensionless diameter of the cylinder $d/c = 0.047$; location of the cylinder $x/c = 0.92$, $z/s = 0.37$. Dot on the wing surface indicates the location of pressure transducer.

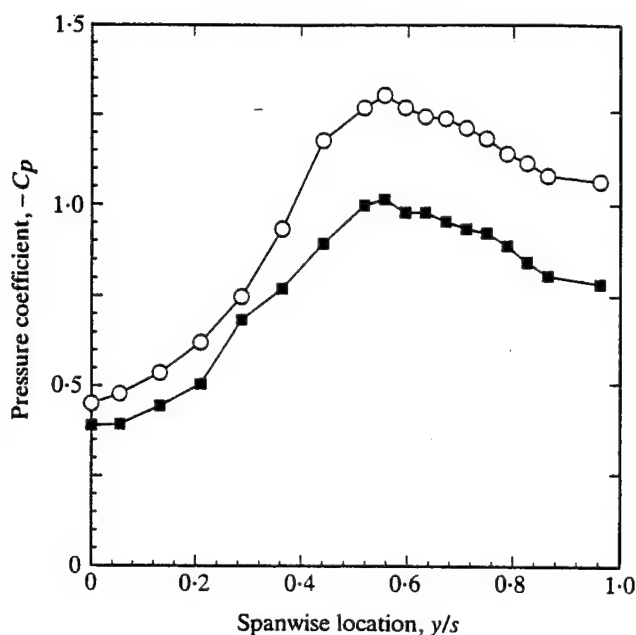


Figure 9. Mean pressure coefficient in spanwise direction at $x/c = 0.80$, $\alpha = 29^\circ$; —○—, without rod; —■—, with rod.

coefficient along the spanwise direction at $x/c = 0.80$ for the cases with and without the cylinder shows that there is a large reduction in the induced pressure underneath the vortex due to the breakdown, whereas the effects are minimum at the centerline (Figure 9). The measurements along the centerline (Figure 10) confirm that the pressure is unaffected by the breakdown, hence by the vortex itself.

The variation of phase-averaged pressure along the centerline as a function of time is shown in Figure 11 for two different values of the reduced frequency. The angle of attack varies as

$$\alpha = 34^\circ - 5^\circ \cos \omega t.$$

The pressure along the centerline varies in magnitude as a function of time. For the smaller reduced frequency ($k = 0.19$), the maximum pressure (suction) occurs when the angle of attack is closer to the maximum angle of attack; however, there exists a time delay. For $k = 0.35$, this phase delay is larger. The pressure field for a pitching wing seems to be delayed in time compared to the quasi-steady case. Accordingly, the pressure gradient has a delay compared to the quasi-steady case. This phase delay is close to that of the breakdown location obtained from the pressure fluctuations (i.e., from the variation of the standard deviation $C'_{p,u}$ shown in Figure 7). Thus, there exists a definite relationship between the pressure field on the wing and the location of vortex breakdown. Hall (1972) showed that small external pressure gradients can be amplified along the core of the vortices, leading to a stagnation point. Thus, the large sensitivity of the vortex breakdown location to a streamwise pressure gradient along the exterior of the vortex is very much expected. Recent computational studies (Visbal 1993) confirm that the time lag of vortex breakdown over a pitching delta wing is linked to the pressure gradient along the vortex axis. This pressure gradient, which depends on the angle of attack and pitching motion (Visbal 1993), is strongly affected by the external pressure gradient generated by the wing.

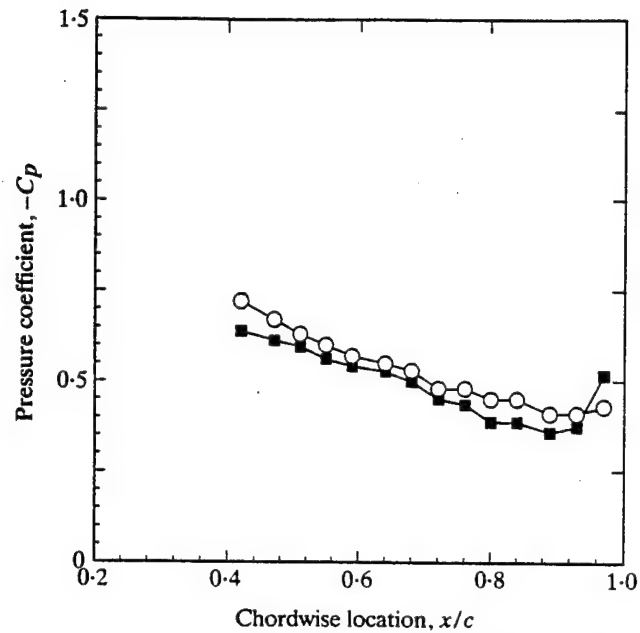


Figure 10. Mean pressure coefficient in streamwise direction for $y/s = 0$, $\alpha = 29^\circ$: —○—, without rod; —■—, with rod.

The Fourier analysis of the phase averaged signal showed that most of the energy was concentrated at the fundamental frequency. The phase angle between the angle of attack α and $\langle -C_p \rangle$ was calculated at each measurement station and plotted in Figure 12. The phase delay increases with increasing reduced frequency. At large reduced frequencies, there is also considerable variation of the phase angle in the streamwise direction. However, it should be kept in mind that the amplitude of the pressure variations becomes smaller toward the trailing-edge where the largest phase angles are observed.

Pressure measurements were also made for a smaller angle-of-attack range, for

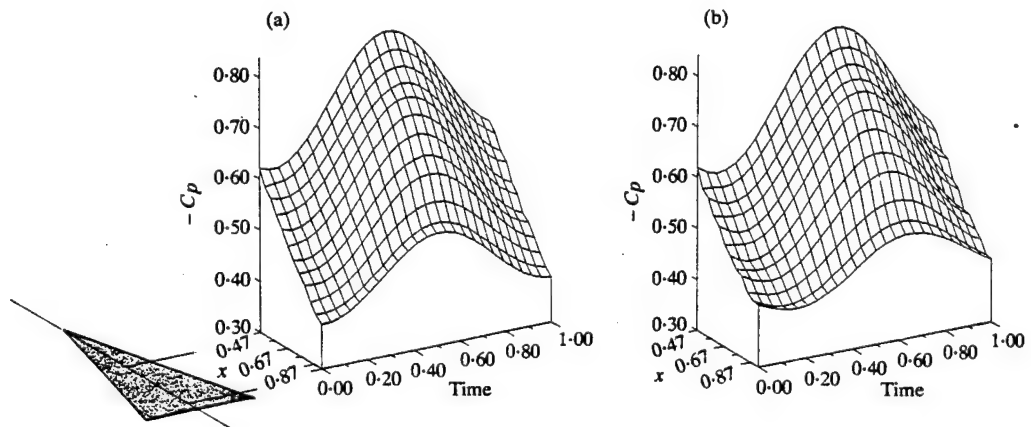


Figure 11. Variation of phase-averaged pressure along the centerline ($y/s = 0$) as a function of time for $\alpha = 34^\circ - 5^\circ \cos \omega t$: (a) $k = 0.19$; (b) $k = 0.35$.

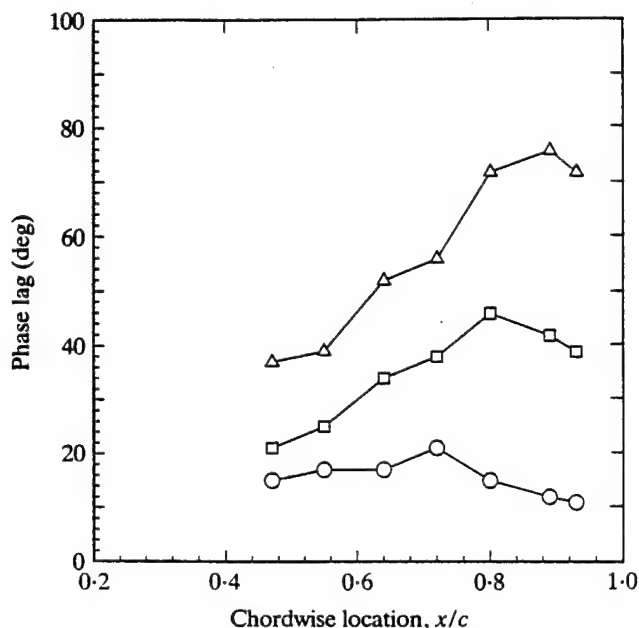


Figure 12. Phase lag of phase-averaged pressure as a function of chordwise location for $\alpha = 34^\circ - 5^\circ \cos \omega t$, $y/s = 0$, $Re = 127,000$: —○—, $k = 0.19$, —□—, $k = 0.36$, —△—, $k = 0.53$.

which the breakdown is absent (this was checked by monitoring the pressure fluctuations):

$$\alpha = 12.5^\circ - 2.5^\circ \cos \omega t.$$

Similar variations of phase lag shown in Figure 13 indicate that the source of the phase delay is not the breakdown process itself. Similar phase lags for the normal force coefficient were predicted with a panel method in the absence of vortex breakdown over a delta wing (Ashley *et al.* 1991). Thus, there is enough evidence that the external pressure gradient is responsible for the observed phase lag of breakdown location.

For the case with breakdown, i.e. $\alpha = 34^\circ - 5^\circ \cos \omega t$, the variation of phase lag between the wing motion and $\langle -C_p \rangle$ at two streamwise locations is shown as a function of reduced frequency in Figures 14 and 15 for different values of Reynolds number. The results show that the measured phase lags are not sensitive to the Reynolds number. Also shown are the phase lags obtained from the pressure fluctuations (i.e., the variation of the standard deviation $C'_{p_{std}}$ shown in Figure 7) and determined by flow visualization for a similar model (LeMay *et al.* 1990).

4. CONCLUSIONS

In order to study the effect of pressure gradient on vortex breakdown, unsteady pressure measurements on a pitching delta wing were carried out. It was shown that the pressure fluctuations induced by the helical mode instability of vortex breakdown can be used to quantify the phase lag between the wing motion and breakdown location. Variation of the standard deviation of pressure fluctuations from the phase-averaged value is shown to be a useful tool to detect the vortex breakdown.

With the help of time-averaged pressure measurements with and without forced breakdown, it was shown that the pressure along the centerline ($y/s = 0$) (where the

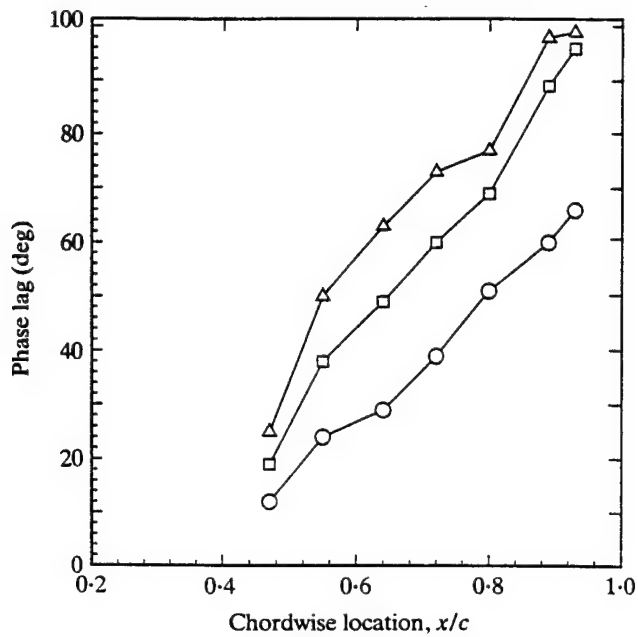


Figure 13. Phase lag of phase-averaged pressure as a function of chordwise location for $\alpha = 12.5^\circ - 2.5^\circ \cos \omega t$, $y/s = 0$, $Re = 127,000$: \circ —, $k = 0.19$, \square —, $k = 0.35$, \triangle —, $k = 0.52$.

effect of the vortex is negligible) is representative of the external pressure field for the leading-edge vortices. Variation of the phase-averaged pressure along the wing centerline as a function of time shows that there is a phase delay between the wing motion and the pressure field. This phase delay is close to the phase delay of the

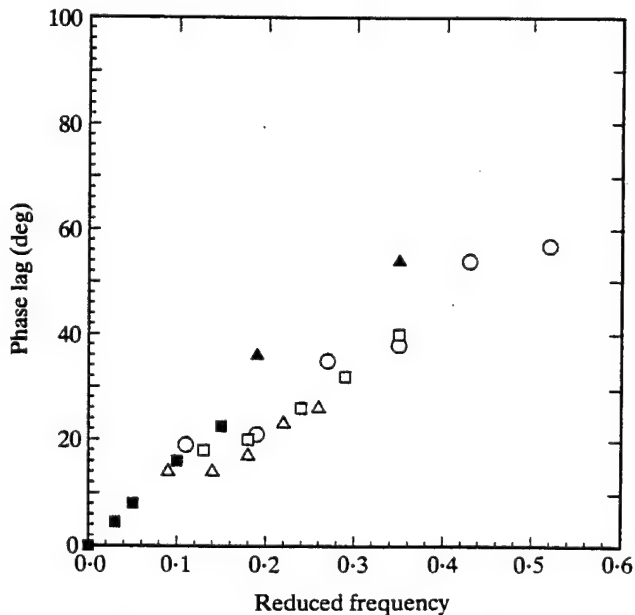


Figure 14. Phase lag as a function of reduced frequency for $x/c = 0.72$, $\alpha = 34^\circ - 5^\circ \cos \omega t$: \circ , $\langle -C_p \rangle$, $Re = 127,000$; \square , $\langle -C_p \rangle$, $Re = 190,500$; \triangle , $\langle -C_p \rangle$, $Re = 254,000$; \blacktriangle , $C_{p_{ad}}$; \blacksquare , visualization (LeMay *et al.* 1990).

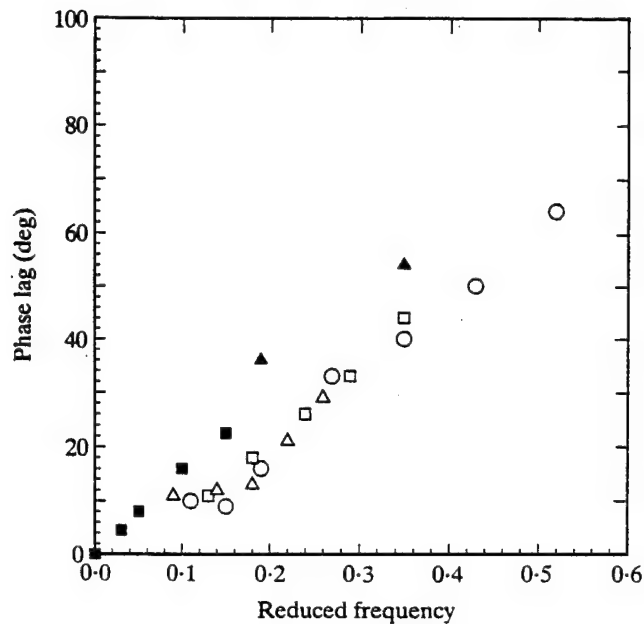


Figure 15. Phase lag as a function of reduced frequency for $x/c = 0.89$, $\alpha = 34^\circ - 5^\circ \cos \omega t$: \circ , $\langle -C_p \rangle$, $Re = 127,000$; \square , $\langle -C_p \rangle$, $Re = 190,500$; \triangle , $\langle -C_p \rangle$, $Re = 254,000$; \blacktriangle , $C'_{p,ld}$; \blacksquare , visualization (LeMay *et al.* 1990).

movement of breakdown location. The phase delay of pressure increases with increasing reduced frequency and is not sensitive to Reynolds number variation. Similar phase lags for pressure were found for a smaller angle-of-attack range for which the breakdown is absent. This confirms that the observed time delays in breakdown location is related to the variation of the external pressure gradient generated by the wing.

The phase lag of the external flow field is due to the shedding of vorticity from the wing (Ashley *et al.* 1991). It should also be noted that the swirl level, which is the other important parameter for vortex breakdown, was not measured in this study. However, the pressure measurements suggest that the external pressure gradient plays a major role.

ACKNOWLEDGMENT

This research was supported by the Air Force Office of Scientific Research Grant No. F49620-92-J-0532. The authors would like to express their appreciation to Doug Hurd for the design and construction of the model wing and pitching mechanism.

REFERENCES

- ASHLEY, H., KATZ, J., JARRAH, M. A. & VANECK, T. 1991 Survey of research on unsteady aerodynamic loading of delta wings. *Journal of Fluids and Structures* **5**, 363–390.
- ATTA, R. & ROCKWELL, D. 1990 Leading-edge vortices due to low Reynolds number flow past a pitching delta wing. *AIAA Journal* **28**, 995–1004.
- GURSUL, I. 1992a Vortex breakdown over unsteady wings. In *Proceedings Workshop on Supermaneuverability: Physics of Unsteady Separated Flows at High Angle of Attack* (eds D. Fant & D. Rockwell), Lehigh University, Bethlehem, PA, U.S.A., 9–10 April 1992.
- GURSUL, I. 1992b Unsteady flow over delta wings at high angle-of-attack. *Bulletin of the American Physical Society* **37**, 1711.

- GURSUL, I. 1994 Unsteady flow phenomena over delta wings at high angle-of-attack. *AIAA Journal* **32**, 225-231.
- GURSUL, I. & HO, C.-M. 1994 Vortex breakdown over delta wings in unsteady free stream. *AIAA Journal* **32**, 433-436.
- HALL, M. G. 1972 Vortex breakdown. *Annual Review of Fluid Mechanics* **4**, 195-218.
- JUMPER, E. J., NELSON, R. C. & CHEUNG, K. 1993 A simple criterion for vortex breakdown. Paper AIAA-93-0866, 31st Aerospace Sciences Meeting and Exhibit, 11-14 January 1993, Reno, NV, U.S.A.
- LEMAY, S. P., BATILL, S. M. & NELSON, R. C. 1990 Vortex dynamics on a pitching delta wing. *Journal of Aircraft* **27**, 131-138.
- POLHAMUS, E. C., 1971, Prediction of vortex-lift characteristics by leading-edge suction analogy. *Journal of Aircraft* **8**, 193-199.
- SARPKAYA, T., 1974, Effect of the adverse pressure gradient on vortex breakdown. *AIAA Journal* **12**, 602-607.
- THOMPSON, S., BATILL, S. & NELSON, R. 1990 Unsteady surface pressure distributions on a delta wing undergoing large amplitude pitching motions. AIAA Paper 90-0311.
- VISBAL, M. R. 1993 Structure of vortex breakdown on a pitching delta wing. Paper AIAA-93-0434, 31st Aerospace Sciences Meeting and Exhibit, 11-14 January 1993, Reno, NV, U.S.A.
- WOLFFELT, K. W. 1987 Investigation on the movement of vortex burst position with dynamically changing angle of attack for a schematic delta wing in a water channel with correlation to similar studies in wind tunnel. In *Aerodynamic and Related Hydrodynamic Studies Using Water Facilities*, AGARD-CP-413.
- WOODGATE, L. 1971 Measurements of the oscillatory pitching-moment derivatives on a sharp-edge delta wing at angles of incidence for which vortex breakdown occurs. *Aeronautical Research Council R & M No. 3628*, Part. 3.

APPENDIX: NOMENCLATURE

c	chord length
C_p	pressure coefficient
$\langle C_p \rangle$	phase-averaged pressure coefficient
C'_p	fluctuating pressure coefficient
$C'_{p,rd}$	standard deviation of pressure coefficient
d	diameter of control cylinder
k	reduced frequency, $\omega c/2U_\infty$
p'	pressure fluctuations
Re	Reynolds number, $U_\infty c/\nu$
s	local semispan
U_∞	freestream velocity
x	chordwise distance from wing apex
y	spanwise distance from wing root
z	distance above wing surface
α	angle of attack
α_0	mean angle of attack
α_1	amplitude of pitching motion
Λ	sweep angle
ω	radial frequency
$\langle \rangle$	phase-averaged quantity

Appendix E



AIAA 95-0676

**Control of Vortex Breakdown with
Leading-Edge Devices**

**I. Gursul, H. Yang and Q. Deng
University of Cincinnati
Cincinnati, OH**

**33rd Aerospace Sciences
Meeting and Exhibit
January 9-12, 1995 / Reno, NV**

CONTROL OF VORTEX BREAKDOWN WITH LEADING-EDGE DEVICES

I. Gursul*, H. Yang** and Q. Deng**

University of Cincinnati
Department of Mechanical, Industrial and Nuclear Engineering
Cincinnati, OH 45221-0072

Abstract

Effect of leading-edge devices on vortex breakdown was investigated. Stationary as well as oscillating leading-edge flaps were shown to alter the structure of the leading-edge vortices, and consequently the location of vortex breakdown. Also, periodic variations of the sweep angle were used to control the breakdown location for a pitching delta wing.

Introduction

Control of vortex breakdown continues to be of vital importance because the breakdown may have a considerable effect on aircraft performance, such as the effect on the time-averaged lift force¹. Breakdown is also important because of the unsteady nature of flow downstream of vortex breakdown². The unsteadiness may affect the stability of the aircraft and also cause buffeting. These concerns have stimulated research on potential (active and passive) control methods to delay vortex breakdown.

This control problem is particularly important for unsteady delta wings as well as for unsteady free stream³⁻⁵. The vortex breakdown may appear on the wing even if no breakdown is observed in the steady case⁶. The time-dependent nature of breakdown location may affect unsteady loading on the wing. One of the objectives of this work is to study the possibility of controlling the breakdown in unsteady flows.

It is well known that there are two important parameters which determine the breakdown location: *swirl angle* and *external pressure gradient* outside the vortex core. The principle of any control method is to alter either or both of these parameters. Blowing and suction in the tangential direction along a rounded leading-edge^{7,8}, and suction applied around the vortex

axis^{9,10} were shown to delay breakdown. The former is believed to be due to a change in the strength and location of the leading-edge vortices. This is achieved by affecting the location of separation on the rounded leading-edge. Direct control of the separation point modifies the vortex properties such that a reduction in the swirl angle is achieved. The purpose of applying suction around the vortex axis is to reduce the local adverse pressure gradient, which is achieved by accelerating the axial flow along the core.

Since all of the vorticity of the leading-edge vortices originates from the separation point along the leading-edge, leading-edge devices are particularly attractive tools that can be used to influence the strength and structure of these vortices. For example, leading-edge flaps are known to be capable of controlling the circulation and location of the leading-edge vortices¹¹⁻¹³. These studies concentrated primarily on the effect of leading-edge flaps at low angle of attack where vortex breakdown was not observed over the wing. Recently, the effect of vortex cavity flaps at high angles of attack has been reported¹⁴. The purpose of this paper is to explore the effect of leading-edge flaps on the vortex breakdown phenomena. Stationary as well as oscillating flaps may provide further insight into the possibility of control of vortex breakdown. Also studied was vortex breakdown over a delta wing with variable sweep angle, since this method allows a direct control of the strength and structure of the leading-edge vortices. Again, periodic variations of sweep angle were studied with the control of vortex breakdown in mind. Application of this technique in unsteady flows was demonstrated for a pitching delta wing.

Experimental Facility

Experiments were carried out in a water channel with a cross-sectional area of 61 cm by 61 cm. The model delta wing with leading-edge flaps and the variable sweep delta wing are shown in Figures 1 and 2, respectively. For both models, the base model has a sweep angle of $\Lambda=70^\circ$. The chord lengths are $c=254$ mm and 268 mm for the model with flaps and the variable sweep delta wing, respectively. The Reynolds

* Assistant Professor

** Graduate Student

breakdown appears on the wing when the swirl level reaches a certain value. For $\alpha=20^\circ$, the swirl level does not change much with the flap angle δ when the breakdown is over the wing. On the other hand, for $\alpha=25^\circ$, the swirl level increases rapidly with the flap angle (when the breakdown is over the wing), explaining the sensitivity of breakdown location with respect to the variations in the flap angle.

In addition to the changes in the swirl level (or strength of the vortex), the location of the vortex core (in the cross plane) exhibits variations with the flap angle. The location of the vortex core was obtained from the velocity measurements (not shown here), which suggested that the existence of the flap may affect the pressure gradient outside of the vortex core. For example, for $\alpha=20^\circ$, there is a gradual variation of breakdown location with the flap angle, although the swirl level does not change much in the same range. This implies that the external pressure gradient for the vortex core is affected by the changes in the geometry of the wing.

Experiments with oscillating flaps were also conducted. The variation of vortex breakdown location for harmonic variations of flap angle between 60° and 180° is shown in Figure 7 together with that of the steady flap angles. The reduced frequency is $k=\omega c/2U_\infty=0.4$, where ω is the radial frequency and U_∞ is the free stream velocity. The variation of breakdown location reveals a hysteresis loop. This is an indication of a time lag response, which is similar to the response of a pitching delta wing. Clearly, development of the detailed flow structure is needed in order to understand the response of vortex breakdown. For this purpose, experiments to obtain the phase-averaged flow field for harmonic variations of flap angle are currently underway.

Vortex Breakdown over a Delta Wing with Variable Sweep Angle

In static experiments, the location of vortex breakdown moves toward the apex with decreasing sweep angle (or aspect ratio), as known from a number of experiments with different aspect ratio wings. Therefore, in the steady case, the location of breakdown shows a monotonic variation with the sweep angle, as opposed to the variation with the flap angle. This feature may be advantageous for active control purposes¹⁵.

The variation of breakdown location was studied for harmonic variations of sweep angle, i.e.

$$\Lambda = \Lambda_0 + \Lambda_1 \sin \omega t$$

The variations of the ensemble-averaged breakdown location are shown in Figure 8 for $\Lambda_0=65^\circ$ and

$\Lambda_1=2.5^\circ$ for different values of the reduced frequency, which show hysteresis loops. The loops become narrower with increasing reduced frequency. Actually, at very large reduced frequency ($k=2.0$ and $k=4.0$ (not shown here)), the ensemble-averaged breakdown location is almost constant. The phase lag of vortex breakdown location with respect to that of the quasi-steady case was found by plotting the time history of breakdown location. This is shown in Figure 9. It seems that the phase lag reaches a maximum at $k=0.4$ and then decreases. This time-lag behavior seems to be an inherent response of breakdown location in unsteady flows, regardless of the type of motion^{4,15}.

In order to understand the phase lag of vortex breakdown, phase-averaged velocity measurements were carried out in a cross plane (at $x/c=0.5$) upstream of breakdown location for a reduced frequency of $k=0.4$. It should be noted that the flow field of the leading-edge vortex develops very gradually before vortex breakdown. Indeed, the velocity changes drastically only in a small neighborhood of the breakdown location. It is also known that the swirl level of the leading edge vortex does not vary much in the streamwise direction⁵. Therefore, these measurements give a good indication of the upstream conditions before breakdown. Contours of constant phase-averaged axial velocity are shown at different sweep angles for $\Lambda_0=66^\circ$ and $\Lambda_1=3^\circ$ in Figure 10. Also shown are the mean velocity contours in the steady case for the minimum sweep angle $\Lambda=63^\circ$ and the maximum sweep angle $\Lambda=69^\circ$. As the sweep angle varies dynamically, the location of the vortex core (defined as the location at which the phase-averaged axial velocity is maximum) varies mostly in the spanwise direction. Note that the axial velocity contours are very similar for the dynamic and static cases. Also the two flow fields for the mean sweep angle $\Lambda_0=66^\circ$ (for increasing and decreasing sweep angle) are not very different from each other. All these suggest that the structure of leading edge vortex is not affected much by the unsteadiness and is approximately quasi-steady. Nevertheless, there is a small phase lag in the development of the vortical flow. This is evident from the contours of constant standard deviation from the phase-averaged velocity shown in Figure 11. It should be noted that the shape of the contours of the standard deviation (or rms velocity fluctuations in the steady case) is related to the main vortex as well as the shear layer and secondary separation region.

The variations of the main parameters are summarized in Figure 12. The variation of sweep

Conclusions

Control of vortex breakdown with leading-edge devices was considered. The main idea is to control the strength and location of leading-edge vortices, which in turn determine the swirl level (and possibly the external pressure gradient) for the swirling flow.

The effect of leading-edge flaps on vortex breakdown was investigated. It was shown that the effect of flaps and sensitivity of breakdown location strongly depends on angle of attack. Velocity measurements showed that, with the varying flap angle, large changes take place in the vortex core diameter and location, in axial and swirl velocity profiles, and in the secondary vortex structure. In general, with the increasing flap angle, larger swirl velocities are observed. The variation of maximum swirl velocity seems to be correlated with the variations of breakdown location as the flap angle is varied.

Experiments with oscillating flaps showed that there exists a hysteresis loop in the variation of breakdown location. This is an indication of a time-lag response, which is similar to the response of a pitching delta wing.

Harmonic variations of sweep angle were studied for a delta wing with variable sweep. The variation of vortex breakdown location showed hysteresis loops and phase lag which depend on the reduced frequency. However, measurements of the phase-averaged axial velocity in a cross flow plane upstream of breakdown location showed no major unsteady effects in the development of the flow field. The larger time lag of vortex breakdown location cannot be explained with the variations in the upstream conditions since the location and strength of the vortex exhibit smaller phase lags. This suggests that the *external pressure gradient* plays a major role in the dynamic response of breakdown location.

Use of variable sweep for breakdown control was demonstrated for a pitching delta wing. Oscillations of sweep angle with the same frequency as pitching, but with a phase angle were considered. It was shown that, at an optimum phase angle, the perturbations of sweep angle decrease the amplitude of the variations of breakdown location. In some cases, it was also observed that the average breakdown location moved downstream.

Acknowledgment

This research was supported by the Air Force Office of Scientific Research Grant No. F49620-92-J-0532. The authors would like to express their

appreciation to Doug Hurd for the design and construction of the model wings.

List of References

1. Lee, M. and Ho, C-M., "Lift Force of Delta Wings", *Applied Mechanics Reviews*, vol. 43, no. 9, 1990, pp. 209-221.
2. Gursul, I. "Unsteady Flow Phenomena over Delta Wings at High Angle of Attack", *ALAA Journal*, vol. 32, no. 2, February 1994, pp. 225-231.
3. LeMay, S.P., Batill, S.M. and Nelson, R.C., "Vortex Dynamics on a Pitching Delta Wing", *Journal of Aircraft*, vol. 27, no. 2, February 1990, pp. 131-138.
4. Gursul, I. and Yang, H. "Vortex Breakdown over a Pitching Delta Wing", AIAA Paper 94-0536, 32nd Aerospace Sciences Meeting and Exhibit, January 10-13, 1994, Reno, NV.
5. Gursul, I. and Ho, C-M. "Vortex Breakdown over Delta Wings in Unsteady Freestream", *ALAA Journal*, vol. 32, no. 2, February 1994, pp. 433-436.
6. Gursul, I. and Ho, C-M., "Vortex Breakdown over Delta Wings in Unsteady Free Stream", AIAA Paper 93-0555, January 1993.
7. Wood, N.J., Roberts, L. and Celik, Z., "Control of Asymmetric Vortical Flows over Delta Wings at High Angles of Attack", *Journal of Aircraft*, vol. 27, no. 5, pp. 429-435.
8. Gu, W., Robinson, O. and Rockwell, D., "Control of Vortices on a Delta Wing by Leading-Edge Injection", *AIAA Journal*, vol. 31, no. 7, July 1993, pp. 1177-1186.
9. Werle, H. "Sur l'eclatement des tourbillons d'apex d'une aile delta aux faibles vitesses", *La Recherche Aeronautique*, no. 74, January-February 1960, pp. 23-30.
10. Parmenter, K. and Rockwell, D., "Transient Response of Leading-Edge Vortices to Localized Suction", *AIAA Journal*, vol. 28, no. 6, June 1990, pp. 1131-1133.
11. Spedding, G.R., Maxworthy, T. and Rignot, E., "Unsteady Vortex Flows over Delta Wings", Proc. of 2nd AFOSR Workshop on Unsteady and Separated Flows, Colorado Springs, July 1987, pp. 283-287.

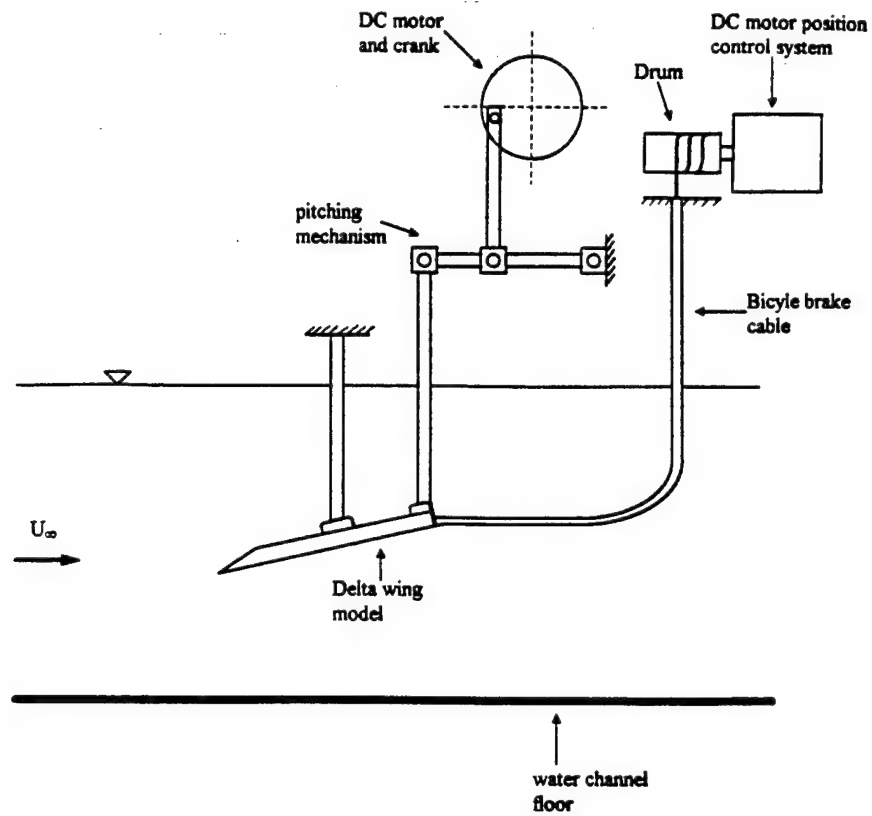


Figure 3: Schematic of experimental setup.

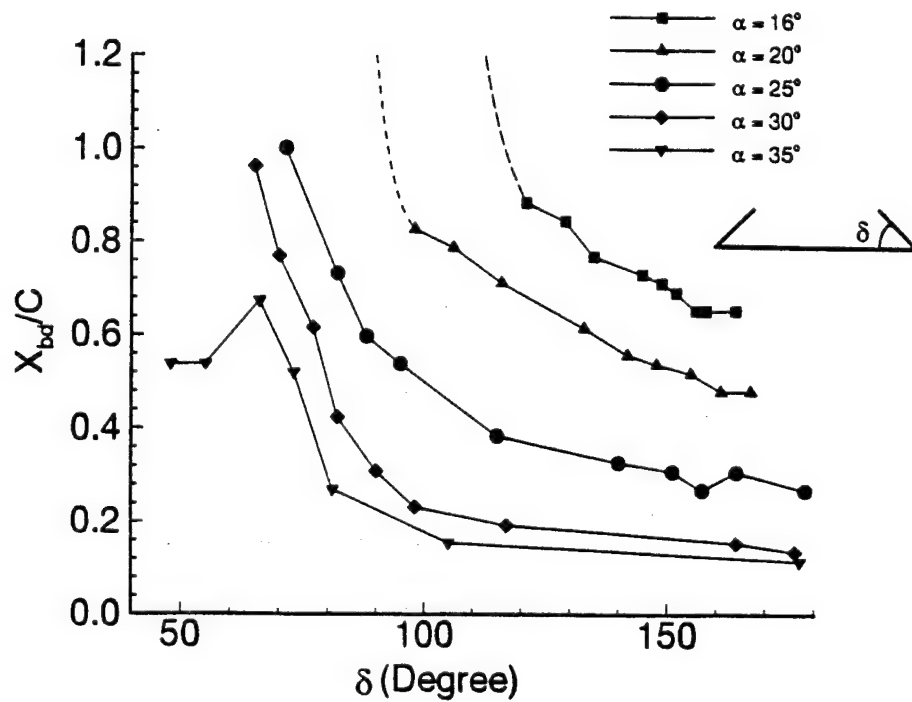


Figure 4: Variation of breakdown location as a function of flap angle for several values of angle of attack.

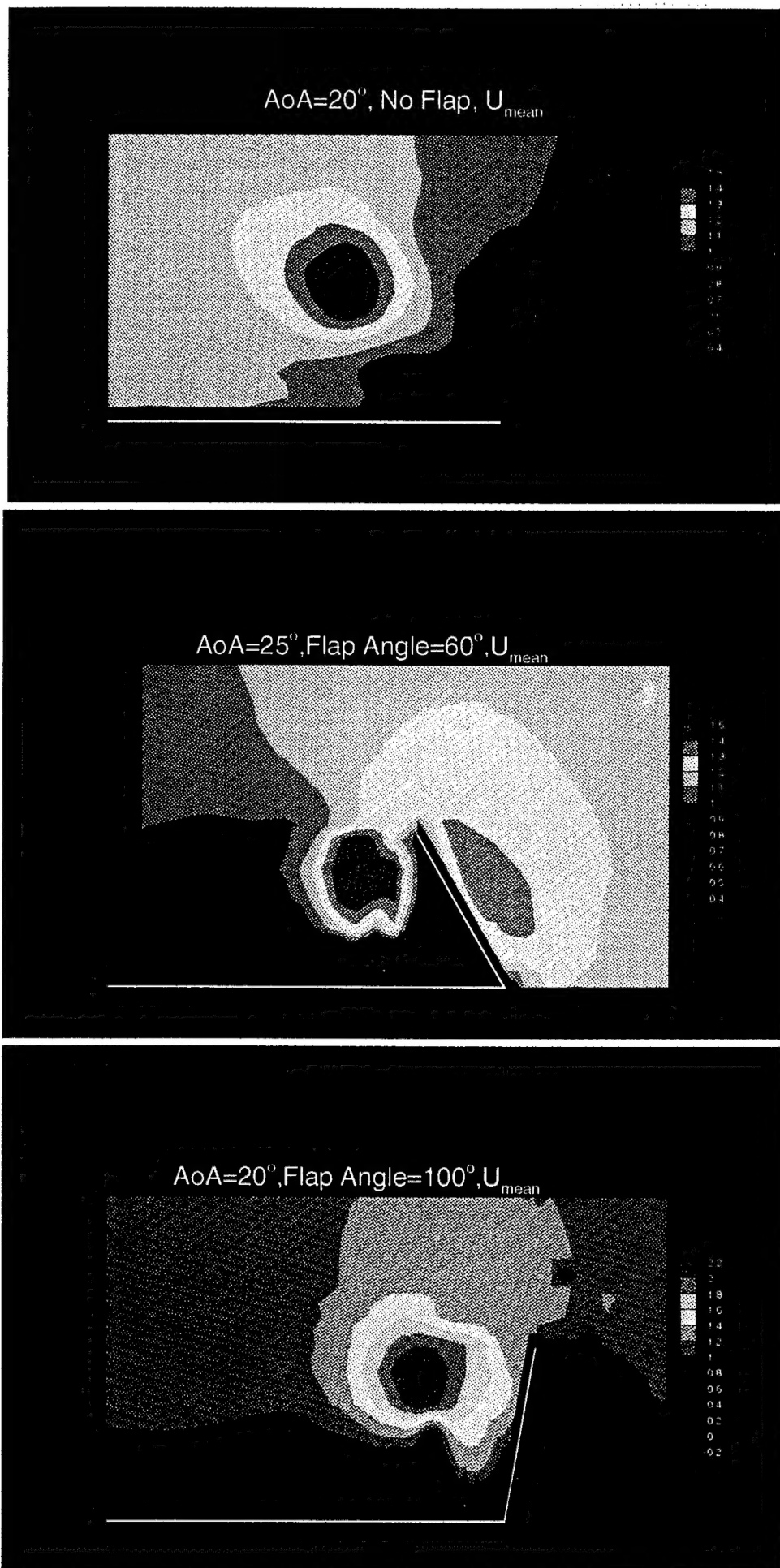


Figure 5: Constant contours of normalized mean axial velocity for $\delta=0^\circ$ (top, $\alpha=20^\circ$), $\delta=60^\circ$ (middle, $\alpha=25^\circ$), $\delta=100^\circ$ (bottom, $\alpha=20^\circ$).

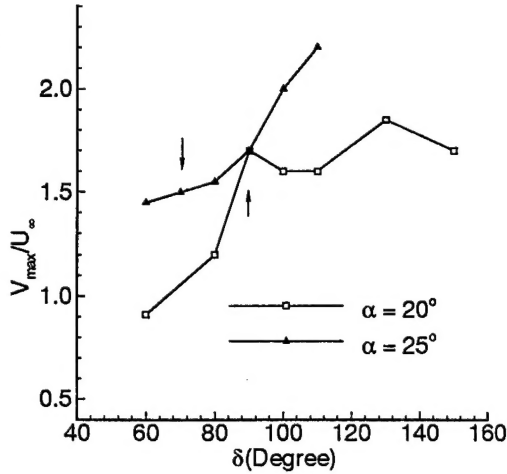


Figure 6: Variation of maximum swirl velocity as a function of flap angle for $\alpha=20^\circ$ and $\alpha=25^\circ$. The arrows indicate the flap angle at which breakdown is at the trailing-edge of the wing.

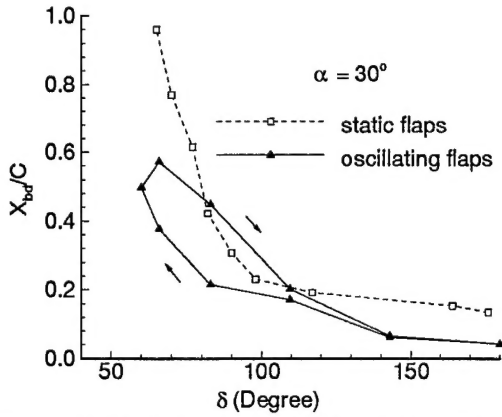


Figure 7: Variation of vortex breakdown location for harmonic variations of flap angle ($k=0.4$), and for static flaps ($\alpha=30^\circ$).

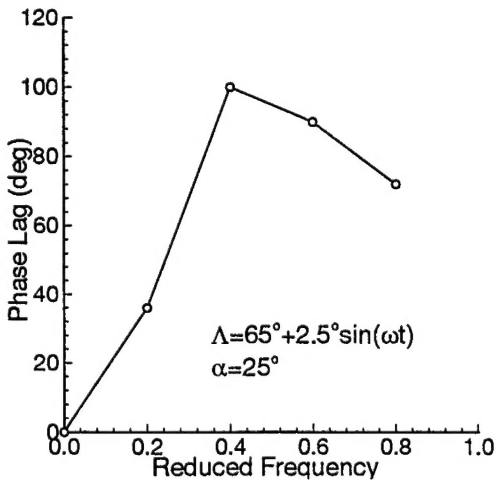


Figure 9: Variation of phase lag as a function of reduced frequency.

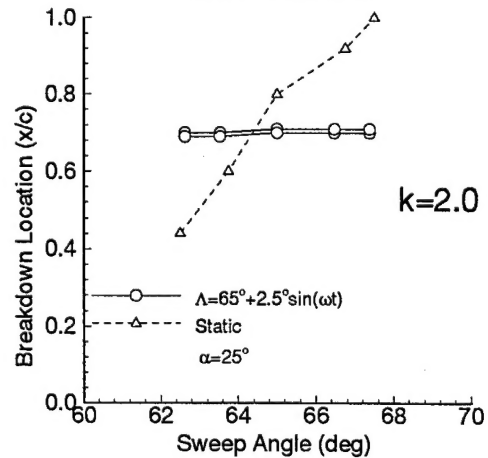
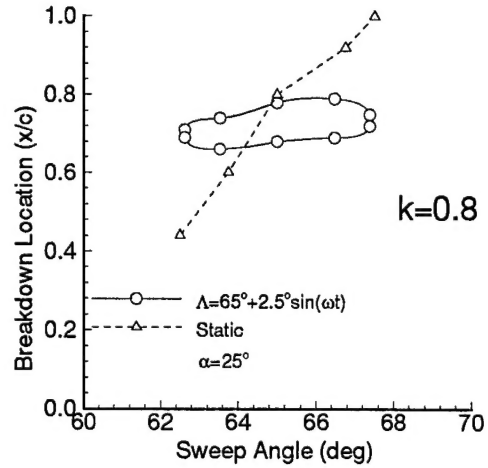
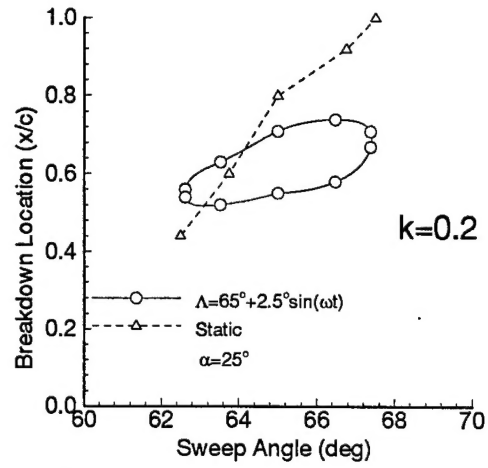
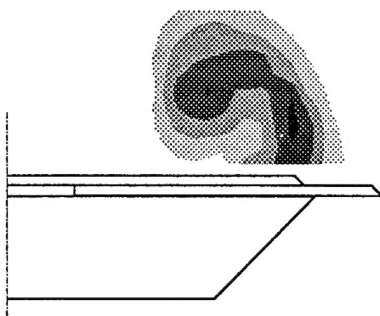
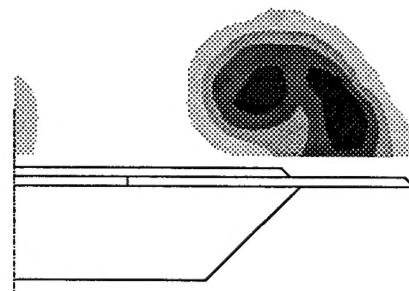
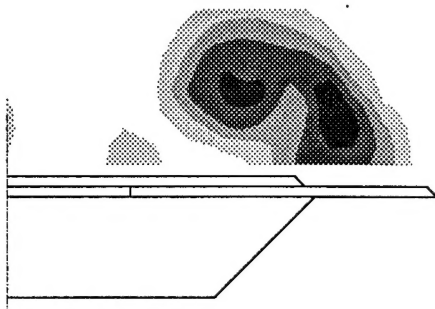


Figure 8: Variation of breakdown location for harmonic variations of sweep angle and for static case.

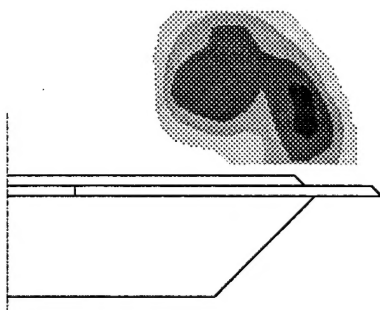
$\Lambda=66^\circ$



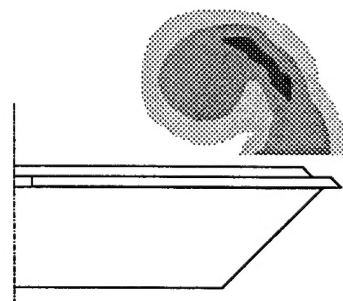
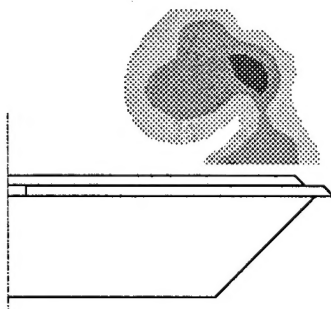
$\Lambda=63^\circ$



$\Lambda=66^\circ$



$\Lambda=69^\circ$



Dynamic

Static

Figure 11: Contours of standard deviation and rms velocity (in the static case).

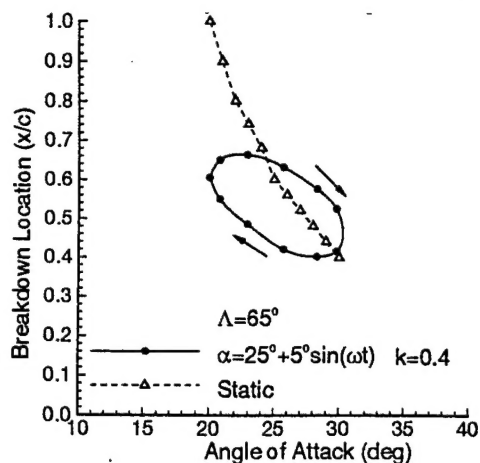


Figure 13: Variation of breakdown location for pitching motion and for static case.

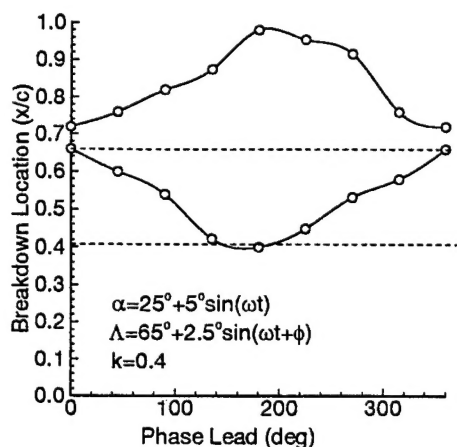


Figure 15: Maximum and minimum locations of breakdown as a function of phase angle. The dashed line is for pitching motion only for the average sweep angle.

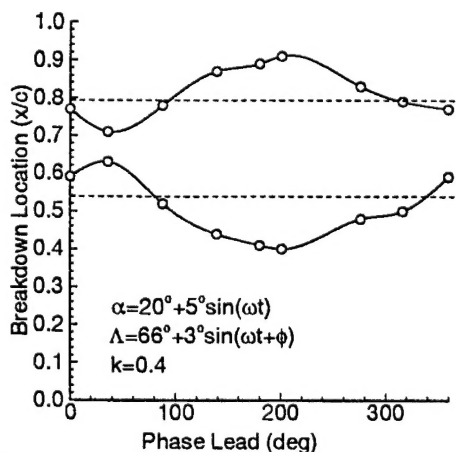


Figure 16: Maximum and minimum locations of breakdown as a function of phase angle. The dashed line is for pitching motion only for the average sweep angle.

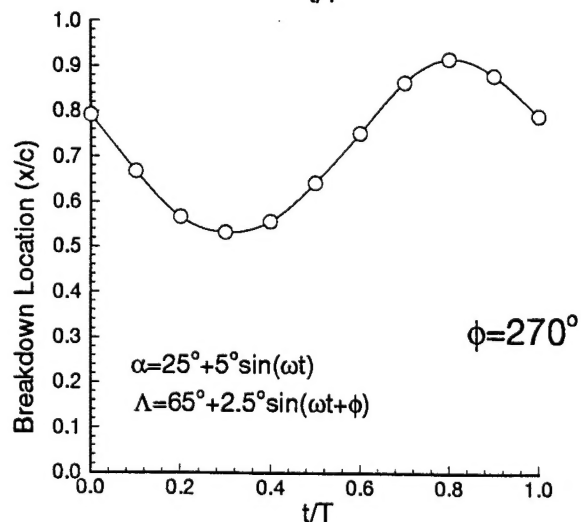
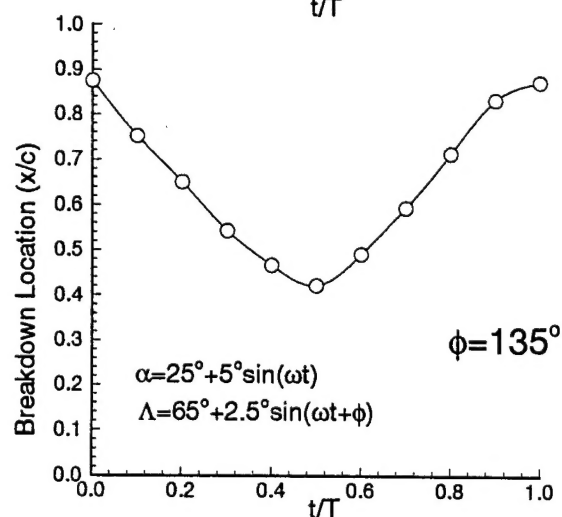
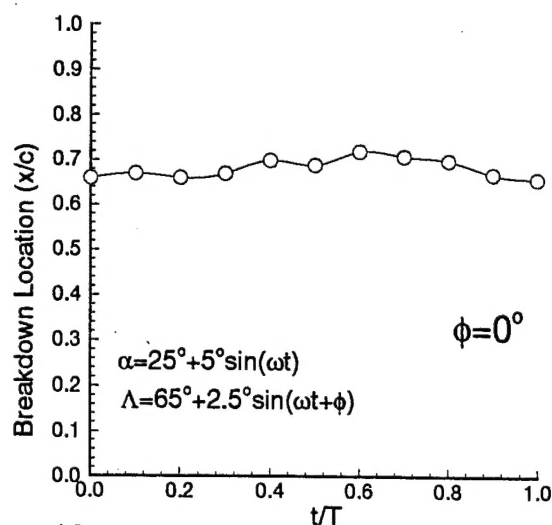


Figure 14: Variation of breakdown location for combined motion of pitching and variable sweep for different values of phase angle.